

2016

Microtubule plus-end binding protein CLASP2 in neural development

<https://hdl.handle.net/2144/14544>

"Downloaded from OpenBU. Boston University's institutional repository."

BOSTON UNIVERSITY
GRADUATE SCHOOL OF ARTS AND SCIENCES

Dissertation

**MICROTUBULE PLUS-END BINDING PROTEIN CLASP2
IN NEURAL DEVELOPMENT**

by

GREGORY MICHAEL DILLON

B.S., Tulane University, 2002
M.S., Tulane University, 2003

Submitted in partial fulfillment of the
requirements for the degree of
Doctor of Philosophy

2016

© 2016
Gregory Michael Dillon
All rights reserved

Approved by

First Reader

Angela Ho, Ph.D.
Assistant Professor of Biology

Second Reader

Hengye Man, Ph.D.
Associate Professor of Biology

ACKNOWLEDGMENTS

I would like to thank everyone in the Boston University Biology Department as this experience has been very humbling. I have needed help from so many of you along the way.

I would especially like to thank my mentor, Dr. Angela Ho. You have provided me with great guidance throughout this process and I can't thank you enough for always being there for me. You have made me a better scientist and I also think of you as a friend. I will always be grateful for your help.

I would like to thank Dr. Uwe Beffert, you have a passion for science and you are constantly pushing everyone in the lab to be better, even if we may not understand that at the time.

Lastly, I would like to thank my family for supporting me through this process. Having people in your life who are there for you regardless of the circumstances is important, especially since I am not always the easiest person to deal with.

Microtubule plus-end binding protein CLASP2 in neural development

Gregory Michael Dillon

Boston University Graduate School of Arts and Sciences, 2016

Major Professor: Angela Ho Assistant Professor of Biology

ABSTRACT

Normal brain function is dependent on the correct positioning and connectivity of neurons established during development. The Reelin signaling pathway plays a crucial role in cortical lamination. Reelin is a secreted glycoprotein that exerts its function by binding to lipoprotein receptors and inducing tyrosine phosphorylation of the intracellular adaptor protein Dab1. Mutations in genes of the Reelin signaling pathway lead to profound defects in neuronal positioning during brain development in both mice and humans. However, the molecular mechanisms by which Reelin controls neuronal morphology and migration are unknown. We have used a systems analysis approach to identify genes regulated through the Reelin signaling pathway and identified microtubule stabilizing CLIP-associated protein 2 (CLASP2) as a key cytoskeletal modifier of Reelin mutant phenotypes. Previously, little was known about the role of CLASP2 in the developing brain. We propose that CLASP2 is a key effector in the Reelin signaling pathway controlling basic aspects of cortical layering, neuronal morphology, and function.

CLASP2 is a plus-end tracking protein and this localization places CLASP2 in a strategic position to control neurite outgrowth, directionality, and responsiveness to extracellular cues. Our results demonstrate that CLASP2 expression correlates with

neurite length and synaptic activity in primary neuron cultures; however, the role of CLASP2 during brain development was unknown. In this dissertation, we have characterized the role of CLASP2 during cortical development by *in utero* electroporation of shRNA plasmids and found that silencing CLASP2 in migrating neurons leads to mislocalized cells at deeper cortical layers, abnormal positioning of the centrosome-Golgi complex, and aberrant length/orientation of the leading process. In addition, we found that GSK3 β -mediated phosphorylation of CLASP2 controls Dab1 binding and is required for regulating CLASP2 effects on neuron morphology and migration. This dissertation provides the first steps into gaining insight on how Reelin signaling affects cytoskeletal reorganization in order to regulate fundamental features of neuronal migration, positioning and morphogenesis.

TABLE OF CONTENTS

ACKNOWLEDGMENTS	iv
ABSTRACT.....	v
TABLE OF CONTENTS.....	vii
LIST OF TABLES	xi
LIST OF FIGURES	xii
LIST OF ABBREVIATIONS.....	xiv
CHAPTER 1: INTRODUCTION.....	1
1.1 Mammalian Cortex Development.....	1
1.2 Reelin Signaling in Brain Development	5
1.3 Role of Microtubules in Neural Development and Migration	6
1.4 Microtubule Organizing Centers (MTOCs).....	10
1.5 Microtubule Plus-End Binding Proteins (+TIPs).....	13
1.6 Overview of CLIP-170 Associated Protein (CLASP)	15
1.7 Thesis Rationale.....	20
CHAPTER 2: MATERIALS AND METHODS	26
2.1 Cloning and Plasmids	26
2.2 Primary Neuron Culture and Lentiviral Infection.....	27
2.3 Western Blotting	27
2.4 Immunocytochemistry and Electron Microscopy	28

2.5 Quantitative Protein Analysis	28
2.6 Electrophysiological Analysis	29
2.7 <i>In vitro</i> Migration Assay	29
2.8 <i>In Utero</i> Electroporation	30
2.9 Immunohistochemistry	31
2.10 Edu/Ki67 Cell-Labeling Experiment	31
2.11 Microarray and IPA Systems Analysis	32
2.12 Quantitative PCR	32
2.13 Immunoprecipitation	33
2.14 <i>In situ</i> hybridization	33
2.15 Image Analysis and Quantification	34
2.16 Statistical Analysis	36

CHAPTER 3: MICROTUBULE PLUS-END TRACKING PROTEIN CLASP2

REGULATES NEURONAL POLARITY AND SYNAPTIC FUNCTION	43
3.1 Introduction	44
3.2 Results	46
3.2.1 CLASP2 Expression During Neural Development	46
3.2.2 CLASP2 Regulates Polarization and Axon Growth	47
3.2.3 CLASP2 Regulates Dendritic Growth and Branching	48
3.2.4 CLASP2 Controls Neuronal Golgi Morphology	49
3.2.5 CLASP2-Mediated Golgi Morphology Correlates with Dendritogenesis	50
3.2.6 CLASP2 Regulates Spontaneous Excitatory Synaptic Transmission	51

3.2.7 CLASP2 Affects on Synapse Morphology and Protein Levels	52
3.2.8 CLASP2 is Required for PI3K-Induced Axon Elongation	54
3.3 Discussion	55
CHAPTER 4: PHOSPHORYLATION OF CLASP2 CONTROLS DAB1	
SIGNALING NECESSARY FOR PROPER NEURON MIGRATION	77
4.1 Introduction.....	78
4.2 Results.....	80
4.2.1 CLASP2 Expression is Developmentally Regulated and Associated with the Reelin Signaling Pathway.	80
4.2.2 Differential Expression of CLASP2 Isoforms During Mouse Cortical Development.	81
4.2.3 CLASP2 is Necessary for Proper Neuron Migration During Corticogenesis.....	82
4.2.4 CLASP2 is Required for the Extension and Orientation of the Leading Process of Migrating Neurons.....	84
4.2.5 CLASP2 Controls the Spatial Positioning of the Centrosome and Golgi Complex.....	85
4.2.6 CLASP2 is Necessary for Regulating Proliferative Cells in the Ventricular Zone	86
4.2.7 CLASP2 Regulates Progenitor Cell Cycle Dynamics.	87
4.2.8 CLASP2 Knockdown Delays Differentiation.....	88
4.2.9 GSK3 β Phosphorylation of CLASP2 Regulates Binding to Dab1.	89

4.2.10 GSK3 β Phosphorylation of CLASP2 Controls Cell Motility and Neurite Extension.....	91
4.3 Discussion.....	92
CHAPTER 5: GENERAL DISCUSSION	124
5.1: Major Findings.....	124
5.2: The Effects of CLASP2 on Cortical Circuits.....	126
5.3: The Effects of CLASP2 on Mitosis versus Migration	129
5.4: CLASP2 Regulation of the Golgi Complex	130
5.5: Conclusions and Significance	131
BIBLIOGRAPHY	132
CURRICULUM VITAE.....	151

LIST OF TABLES

Table 2.1: Antibodies.....	37
Table 2.2: Plasmids.....	40
Table 3.1: Quantitative Ultrastructural Analysis of Asymmetric Neuronal Synapses	76

LIST OF FIGURES

Figure 1.1: Mammalian Cortex Development	21
Figure 1.2: Reelin Signaling Pathway	22
Figure 1.3: The Role of Microtubules and the Golgi/Centrosome Complex in Cell Movement	23
Figure 1.4: Mechanisms of Microtubule Plus-End Tracking.....	24
Figure 1.5: CLASP2 Protein Binding Domains.....	25
Figure 3.1: Localization and Expression of CLASP2 in the Developing Neuron	63
Figure 3.2: CLASP2 Increases Axon Length and Induces the Formation of Multiple Axons	65
Figure 3.3: CLASP2 Regulates Dendritic Growth and Branching	67
Figure 3.4: CLASP2 Regulates Golgi Morphology in Neurons	69
Figure 3.5: CLASP2 Increases Dendritic Branching in Neurons with Stacked but Not Ribbon Golgi Phenotypes	70
Figure 3.6: CLASP2 Increases Spontaneous Synaptic Activity at Excitatory but Not Inhibitory Synapses.....	72
Figure 3.7: CLASP2 Regulates Synaptic Structure and Synaptic Protein Levels	74
Figure 3.8: CLASP2 is Required for PI3K-Induced Axon Elongation	75
Figure 4.1: CLASP2 Expression is Regulated by the Reelin Signaling Pathway	100
Figure 4.2: Differential Expression of CLASP2 Isoforms during Mouse Cortical Development	102

Figure 4.3: CLASP2 is Necessary for Radial Migration of Cortical Projection Neurons	104
Figure 4.4: CLASP2 Knockdown Affects Neuron Morphology But Not Cell Fate	106
Figure 4.5: Overexpression of CLASP2 α Perturbs Neuron Migration.....	107
Figure 4.6: CLASP2 Affects Leading Process Extension and Orientation.	108
Figure 4.7: CLASP2 Knockdown Leads to Aberrant Localization of the Golgi/Centrosome Complex.	110
Figure 4.8: CLASP2 Expression Does Not Alter the Radial Glia Scaffold.....	112
Figure 4.9: CLASP2 Regulates the Percentage of Proliferative Cells.....	113
Figure 4.10: CLASP2 may Regulate Progenitor Cell Differentiation by Altering the Angle of the Cleavage Plane.....	115
Figure 4.11: CLASP2 Knockdown Delays Differentiation of Progenitors	117
Figure 4.12: CLASP2 Binds to Dab1 at the S/R Domain of CLASP2.....	118
Figure 4.13: GSK3 β Phosphorylation of CLASP2 Regulates its Binding to Dab1	119
Figure 4.14: GSK3 β Phosphorylation of CLASP2 Regulates Cell Motility.	121
Figure 4.15: GSK3 β Phosphorylation of CLASP2 Regulates Neurite Extension.	122
Figure 4.16: The GSK3 β -mediated phosphorylation of CLASP2 controls Dab1 binding and is required for regulating CLASP2 effects on neuron morphology and migration	123

LIST OF ABBREVIATIONS

+TIP	Plus-End Binding Protein
α	Alpha-
AKAP450.....	A Kinase Anchor Protein 450
Akt.....	Protein Kinase B
APC.....	Adenomatous Polyposis Coli
aPKC.....	Atypical Protein Kinase C
ApoER2.....	Apolipoprotein E receptor 2
Aspm.....	Abnormal Spindle-like, Microcephaly-associated
β	Beta-
BU.....	Boston University
$^{\circ}\text{C}$	Degrees Celsius
C-Terminal.....	Carboxy Terminal
Cdc42	Cell Division Control Protein 42
CDK	Cyclin Dependent Kinase
CDP.....	CCAAT displacement protein
Cdk5rap2.....	Cdk5 Regulatory Subunit Associated Protein 2
cDNA	Copy Deoxyribonucleic Acid
CENP-E.....	Centrosome Associated Protein E
CLASP	CLIP-170 Associated Protein
CLIP	Cytoplasmic Linker Protein
DAPI.....	4',6-diamidino-2-phenylindole

DAB1	Disabled-1
DCX	Doublecortin
ddCt.....	Delta Cycle Threshold
DIV	<i>Days In Vitro</i>
DNA.....	Deoxyribonucleic Acid
E.....	Embryonic Day
EB1	End-Binding Protein-1
EDTA.....	Ethylenediaminetetraacetic acid
EdU	5-ethynyl-2'-deoxyuridine
EGFP.....	Enhanced Green Fluorescent Protein
ELM	Eukaryotic Linear Motif
<i>g</i>	Gravitational Force
GAPDH.....	Glyceraldehyde 3-Phosphate Dehydrogenase
GDP.....	Guanosine Diphosphate
GFP	Green Fluorescent Protein
GluA1.....	Glutamate Receptor Subunit A1
GSK3 β	Glycogen Synthase Kinase 3 β
GTP.....	Guanosine Triphosphate
HEK293T.....	Human Embryonic Kidney
ICC.....	Immunocytochemistry
IHC.....	Immunohistochemistry
IP	Immunoprecipitation

IUE.....	<i>In Utero</i> Electroporation
IZ.....	Intermediate Zone
LIS1.....	Lissencephaly 1
loCP.....	Lower Cortical Plate
M.....	Molar
m.....	Milli-
MAP.....	Microtubule Associated Protein
MCPH1.....	Microcephalin
mEPSC.....	Miniature Excitatory Post-Synaptic Current
min.....	Minute
mIPSC.....	Miniature Inhibitory Post-Synaptic Current
mRNA.....	Messenger Ribonucleic Acid
MTOC.....	Microtubule Organizing Center
n.....	Nano-
NBF.....	Neutral Buffered Formalin
NHS-LC-Biotin.....	Succinimidyl-6-(Biotinamido) Hexanoate
N-Terminal.....	Amino Terminal
P.....	Post-Natal Day
PAR.....	Partitioning-Defective Proteins
PBS.....	Phosphate Buffered Saline
PCR.....	Polymerase Chain Reaction
PH3.....	Phosphorylation of Histone 3

PI3K	Phosphoinositide 3-Kinase
PLK1	Polo-Like Kinase 1
PKC.....	Protein Kinase C
PRC1	Protein Regulator of Cytokinesis 1
PSD-95	Postsynaptic Density Protein 95
qPCR.....	Quantitative Polymerase Chain Reaction
RIPA	Radio-Immunoprecipitation Assay
RRE.....	Rev Response Element
RSV.....	Rous Sarcoma Virus
SDS-PAGE	Sodium Dodecyl Sulfate Polyacrylamide Gel Electrophoresis
SEM	Standard Error of the Mean
shRNA.....	Short Hairpin Ribonucleic Acid
SMI-312	Anti-Neurofilament Antibody
SNARE	Soluble NSF Attachment Protein Receptor Family
S/R.....	Serine Rich
Src	Proto-oncogene Tyrosine-Protein Kinase
SVZ.....	Subventricular Zone
SXIP	Serine-(Any Amino Acid)-Isoleucine-Proline
Tau	Microtubule Associated Protein Tau
TOG	Tumor Overexpressing Gene
TUB1A.....	Tubulin 1A
μ	Micro-

upCP.....	Upper Cortical Plate
UTR.....	Untranslated Region
VLDLR.....	Very-Low-Density-Lipoprotein Receptor
VSVG.....	Envelope Protein Env
VZ.....	Ventricular Zone
WB.....	Western Blotting
γ	Gamma-

CHAPTER 1: INTRODUCTION

1.1 Mammalian Cortex Development

The mammalian cortex is distinguished by its six horizontal cell layers, each layer comprised of neurons with distinct morphological and functional identities. Excitatory, projection (pyramidal) neurons exhibit layer specific differences in their molecular expression and subsequent connectivity (Angevine and Sidman, 1961; Wise and Jones, 1977; Rakic, 1988; Lai et al., 2008; Belgard et al., 2011). Projection neurons which occupy deeper layers (V and VI) extend corticofugal axons targeting subcortical structures like the thalamus and spinal cord, whereas upper-layer (II and III) neurons project within the cortex, either in the same hemisphere or contralaterally *via* the corpus callosum. In contrast, layer IV serves as the main input layer, receiving sensory information from thalamocortical axons (DeFelipe and Farinas, 1992). Therefore, the ability of the neocortex to mediate complex cognitive and motor tasks depends on the positioning and connections of these neurons during development.

During development, the ventricular zone of the dorsal telencephalon contains progenitor cells which give rise to the incredible heterogeneity of excitatory neurons present in the mature neocortex (Noctor et al., 2001; Miyata et al., 2001; Noctor et al., 2002; Fishell and Kriegstein, 2003; Anthony et al., 2004; Gal et al., 2006; Stancik et al., 2010). Neurogenesis within the ventricular zone relies on a delicate balance between maintenance of a progenitor pool and production of new, post-mitotic neurons. During this process, neural progenitors initially divide symmetrically to increase the pool of

proliferative cells. As development progresses, neuroepithelial cells differentiate into radial glia cells and begin to undergo increasing numbers of asymmetric divisions in an effort to promote both self-renewal and the production of post-mitotic neurons (Figure 1.1; Iacopetti et al., 1999; Sahara and O'Leary, 2009; Siegenthaler et al., 2009; reviewed in Matsuzaki and Shitamukai 2015). This shift in the mode of division from proliferative to neurogenic does not occur as a single event but rather as a gradual process and subsequently determines neuron number and brain size (Gotz and Huttner 2005).

During asymmetric divisions, the unequal distribution of cell-fate determinants between the mother and daughter cell has been shown to control differentiation and cell fate (Zhong et al., 1996; Bultje et al., 2009; Wang et al., 2009; Dong et al., 2012; reviewed in Morin and Bellaiche, 2011). In order to accomplish this goal, the mitotic spindle acts as a cellular scaffold to organize and segregate both genetic material and fate determining factors. The mitotic spindle is a microtubule based structure that originates from the two centrosomes and works to segregate the chromatids during mitosis. Formation and orientation of the mitotic spindle depends on microtubule length, stability, and capture at the cell cortex (Kirschner and Mitchison, 1986; Aist et al., 1991; Carminati and Stearns, 1997; reviewed in Wynshaw-Boris et al., 2010). Previous experiments suggest that changes in the orientation of the mitotic spindle may regulate the switch from symmetric to asymmetric cell divisions in both vertebrate and invertebrate progenitors (Das et al., 2003; Sun et al., 2005; Das and Storey, 2012; Lancaster and Knoblich, 2012); however, experiments examining time-lapse videos of progenitor divisions in brain slices have demonstrated that orientation of the cleavage plane does not

accurately predict cell fate (Haydar et al., 2003; Gotz and Huttner, 2005; Iacopetti et al., 1999). Spindle orientation is tightly regulated by mechanisms involving the centrosomes, astral microtubules, and interactions between proteins adherent to the cell cortex (Carminati and Stearns, 1997; Feng and Walsh, 2004; Kosodo et al., 2004) and in humans mutations in genes regulating spindle orientation have been shown to cause brain disorders such as lissencephaly (smooth brain characterized by the absence of gyri) and microcephaly (deficits in brain size) (Moon et al., 2014; Chen et al., 2014; Gilmore and Walsh 2013). Interestingly, the majority of known microcephaly genes encode centrosomal proteins (such as *Aspm*, *Cdk5rap2*, and *MCPH1*) regulating a wide range of processes including centriole duplication, centrosome maturation, and entry into mitosis. Therefore, the molecular mechanisms controlling progenitor cell populations and their mode of division are critical in determining brain size, neuron heterogeneity, and eventual physiology.

During development, cortical layers form in an “inside-out” pattern with early-born neurons occupying deeper layers and later-born neurons migrating past them to form the superficial/outer layers. Therefore, the birth-date of projection neurons is intimately associated with laminar identity, connectivity, and physiological function (Angevine and Sidman, 1961; Wise and Jones, 1977; Rakic, 1988; reviewed in McConnell, 1988). Excitatory-projection neurons of the cortex are generated by apical and basal progenitor cells located within the ventricular and subventricular zones, respectively. Following terminal division, neurons generated in these proliferative zones move upwards into the intermediate zone, briefly adopting a multipolar morphology, before continuing their

migration into the cortical plate. Several studies have revealed that the transition out of the multipolar stage requires stabilization of a leading neurite and depends on cytoskeletal associated proteins including filamin A, lissencephaly-1 (LIS1), and doublecortin (DCX) (Bai et al., 2003; Nagano et al., 2004; Tsai et al., 2005; reviewed in LoTurco and Bai 2006). Before entering the cortical plate, the morphology of migrating neurons again changes from multipolar to bipolar as these cells begin to move along radial glial fibers towards their final location (Figure 1.1). Consequently, for neurons destined for upper cortical layers, radial glia serve as both the main progenitor cell and the scaffolding which subsequently guides migration (Kriegstein and Alvarez-Buylla, 2009).

Formation of the mature cortex requires the movement of neurons over great distances from the site of birth to their final laminar position. Time-lapse imaging has demonstrated that migrating neurons use two distinct forms of cell movement termed locomotion and somal translocation (Nadarajah et al., 2001). These modes of cell movement have been dissociated based on differences in microtubule dynamics, cell morphology, and reliance on radial glia fibers. Generally, projection neurons migrate into the cortical plate using somal translocation during the initial stages of corticogenesis and then switch to radial glial guided locomotion at later embryonic stages as the distance needed to travel increases (Miyata et al., 2001; Nadarajah et al., 2001; Tabata and Nakajima, 2003; Noctor et al., 2004). Once neurons reach their final destination, they further differentiate by extending their axons to form connections with target cells and create extensive dendritic branching to establish functional connectivity.

1.2 Reelin Signaling in Brain Development

The Reelin signaling pathway is one of the most well studied signaling cascades involved in the cytoarchitecture of the cerebral cortex (Figure 1.2). In humans, mutations in reelin signaling cause lissencephaly and cerebellar hypoplasia (Hong et al., 2000). Mice with mutations in reelin or its receptors have severe developmental abnormalities, including the inability of migrating neurons to split the developing preplate and an inversion of the normal inside-out pattern of cortex development (D'Arcangelo et al., 1995; Howell et al., 1997; Trommsdorff et al., 1999; Rice and Curran, 2001). Reelin is a large secreted glycoprotein and during corticogenesis Reelin is primarily expressed in Cajal Retzius cells located within the uppermost, marginal zone. Reelin exerts its function by binding to the lipoprotein receptors apolipoprotein E receptor 2 (ApoER2) and very-low-density-lipoprotein receptor (VLDLR) and inducing tyrosine phosphorylation of the intracellular adaptor protein disabled-1 (Dab1) (Howell et al., 2000; Bock and Herz, 2003). Phosphorylation of Dab1 by Src-family kinases recruits downstream signaling molecules in order to promote cytoskeletal changes necessary for neuron migration, radial glia detachment, and neurite morphology (Figure 1.3; D'Arcangelo 2005). Previous studies have demonstrated that Reelin signaling can induce opposing effects on the phosphorylation of cytoskeletal proteins such as MAP1B and Tau (Beffert et al., 2004; Gonzalez-Billault et al., 2005). For example, Reelin can stabilize the leading process of migrating neurons by inducing cofilin phosphorylation at Ser3, which regulates actin dynamics (Chai et al., 2009). In addition, Reelin can induce MAP1B phosphorylation through glycogen-GSK-3 β activation which has been shown to be

necessary for correct cortical lamination (Gonzalez-Billault et al., 2005). A number of mutations in cytoskeletal-encoded genes also produce deficits in neuron migration and cortical lamination phenotypically similar to Reelin mutants. For example, human mutations in LIS-1, DCX, and tubulin-1A (TUB1A), integral components of the microtubule cytoskeleton, cause severe cortical lamination defects with later born neurons failing to migrate past previously born neurons (Gleeson et al., 1998; Romaniello et al., 2015). The culmination of these genetic studies indicates that several signaling pathways, including the Reelin pathway, must converge on downstream cytoskeletal proteins to affect proper neuronal migration and brain development.

1.3 Role of Microtubules in Neural Development and Migration

Dynamic changes to the cytoskeleton are necessary to regulate neuron proliferation, differentiation, and migration. In particular, microtubules provide tracks for intracellular transport, set up local cues to position organelles, and work to generate contractile forces for both adhesion and/or cell movement (Kapitein and Hoogenraad, 2015). Microtubules are constructed from α - and β -tubulin dimers, which bind in a head to tail fashion to form polarized filaments (Akhmanova and Steinmetz, 2008). In neurons, polarized microtubules are nucleated with their minus-ends orientated towards the centrosome/Golgi complex in the cell body, and the plus-ends projecting towards the tips of extending axons. At the dynamic plus-ends, frequent transitions between periods of growth and shortening permits the extension or retraction of neurites in response to guidance cues and is necessary to maintain directional growth towards synaptic targets. In neurons, microtubule diversity can be generated by many cellular processes including

the expression of different α - and β -tubulin genes, the generation of post-translational modifications, and the regulation of protofilament numbers (Brouhard and Rice, 2014). Clinically, mutations in various α/β -tubulin isotypes have been linked to several human neurodevelopmental and degenerative disorders (Tischfield et al., 2011) and these mutations are associated with a wide range of microtubule functions including tubulin stability, polymerization, and motor protein or microtubule associated protein (MAP) binding (Kapitein and Hoogenraad, 2015).

During cell division, correct positioning of the mitotic spindle relies on the capture and stability of astral microtubules. Astral microtubules are nucleated at the spindle poles and engage the cell cortex to generate the traction forces necessary to maintain or alter spindle position. The dynamic lengthening and shortening of spindle microtubules determines the shape of the mitotic spindle and promotes proper alignment of chromosomes at the spindle midzone. Identifying components of the cortical-spindle machinery and determining molecular mechanisms that control their activity is essential to understand how cell division kinetics and cell fate can be determined.

Migrating neurons are highly polarized in the direction of their movement and this is achieved through the generation, maintenance, and constant remodeling of microtubules in response to extracellular cues and intracellular polarity signals (Figure 1.3). During migration, the cell first extends a leading neurite preceded by a growth cone that expands and collapses as it explores the microenvironment. Previous research has shown that the local stabilization of a single neurite is required for newly generated neurons to exit the multipolar stage and enter the cortical plate. This stabilization

ultimately results in formation of the leading process while the trailing process eventually develops into the future axon (Shim et al., 2008; Witte et al., 2008). Next, in order to move forward, the cell undergoes a translocation of the nucleus into the stabilized leading neurite. During this process termed nucleokinesis, the attachment of microtubules from the centrosome to the nuclear envelope exerts a traction force, pulling the nucleus into the leading neurite and along the radial glia process (Bellion et al., 2008). Therefore, microtubules are required for each step in cell movement including: leading process stabilization, rapid elongation, and finally nuclear translocation through actions of centrosome.

MAPs can function to stabilize the cytoskeleton through polymerization at the growing tip or by rescuing catastrophe events along the neurite shaft. Stable microtubules acquire several post-translational modifications such as acetylation of α -tubulin, or proteolytic removal (detyrosination) of the C-terminal tyrosine (Westermann and Weber, 2003). Acetylation of microtubules has been shown to enhance the binding of motor proteins that are crucial for the transport of key cargo to and from the future axon. For example, the molecular motor protein kinesin-1 demonstrates increased binding to acetylated microtubules and functions to set the asymmetric distribution of polarity determinants such as APC and PAR-3 (Reed et al., 2006). The creation of several mutant mouse lines indicates that deletion or knockdown of proteins which destabilize microtubules (including MAP1B, Tau, and Lis1) leads to consistent defects in neuron migration, axon elongation, and dendritic arborization (Dehmelt and Halpain, 2004). For example, the protein Elongator functions as a multi-subunit histone acetyltransferase and

silencing of its catalytic subunit causes a global reduction in acetylated α -tubulin. Knockout of Elongator in mice causes a significant reduction in microtubule stabilization, delaying migration of cortical projection neurons, and impairing dendritic branching (Creppe et al., 2009).

Clinically, the characterization of genes involved in neuronal migration disorders has also emphasized the importance of microtubule function in human neural development. Lissencephaly (smooth brain), pachygyria (few gyri), and subcortical band heterotopias are each pediatric brain malformations caused by disruptions in neuronal migration with known mutations present on cytoskeleton-related genes (Liu, 2011). For example, hemizygous mutations in *Lis1* cause type-1 lissencephaly, a disorder of neuronal migration resulting in cortical lamination defects and functional impairments of cognitive and motor skills. *Lis1* has been shown to bind to microtubules and increase their stability, as well as functioning to couple the centrosome with the nuclear envelope (McKenney et al., 2010). Many additional microtubule stabilizing proteins have also been shown to be essential during neuron development. For example the loss of *MAP1B* or *DCX* results in an increase in axon/leading process branching as neurons move through the cortical plate (Bouquet et al., 2004; Kappeler et al., 2006). In addition, *DCX* knockout mice demonstrate an accumulation of multipolar neurons in the intermediate zone of the cortex which resembles the formation of subcortical laminar heterotopias observed in human patients (Bai et al., 2003; Gleeson et al., 1998). The appropriate positioning of neurons to the correct cortical layer is essential for connectivity and neocortical function. Experimental or genetic disruptions that alter cortex lamination

often create neocortical circuits that have aberrant, enhanced excitability which has been shown to lead to enhanced susceptibility of patients to epilepsy (LoTurco and Bai, 2006). Therefore, it is clear that a further understanding of the molecular mechanisms controlling migration through microtubule remodeling is of important clinical value.

1.4 Microtubule Organizing Centers (MTOCs)

Nucleation is the process by which several tubulin molecules interact to form a microtubule seed and initiate the *de novo* formation of microtubule filaments (Job et al., 2003). Microtubules are organized into arrays that serve as tracks for directed vesicular transport and are essential for the establishment of cell polarity and maintenance of neuronal architecture. Therefore, the nucleation of microtubules must be highly regulated in order to regulate the cytoskeleton during development. Microtubule organizing centers (MTOCs) function as the site where microtubules emerge and gamma (γ)-tubulin represents the core component of MTOCs implicated in nucleating microtubules at both the mitotic spindle and cytoplasm (Oakley, 2000). In mammals, γ -tubulin ring complexes form a template which binds the α -tubulin subunit at the microtubule minus-end. Microtubules then grow with a defined polarity from this complex with minus-ends anchored on the γ -tubulin ring and plus-ends extending into the cytoplasm (Petry and Vale 2015). Previous studies have proposed that in mammalian neurons, microtubules are primarily nucleated by γ -tubulin at the centrosome, released by the microtubule severing protein katanin, and then transported into developing neurites (Ahmad et al., 1998, Baas et al., 2005). However, recent results demonstrate that although the centrosome acts as an active MTOC in polarizing neurons, as development progresses, γ -tubulin is depleted

from the centrosome and the majority of microtubules originate from acentrosomal sites (Stiess et al., 2010). Therefore, the mechanisms which control the shift and development of additional MTOCs must have important consequences on cell morphology and function.

In general, microtubule arrays originating from the centrosome are organized in a radial fashion while non-centrosomal arrays appear to have a significantly more polarized distribution (Efimov et al., 2007). Within neurons, one potential site of acentrosomal, microtubule nucleation is the Golgi complex and γ -tubulin has been shown to be recruited to the cis-Golgi membrane through interactions with AKAP450 and subsequent binding to the Golgin, GM130 (Rivero et al., 2009). A number of studies have shown that the Golgi complex can nucleate microtubules and that microtubules nucleated at the Golgi are preferentially oriented towards the leading edge in motile cells (Efimov et al., 2007). The Golgi apparatus is integral to the sorting and delivery of newly synthesized proteins and this function is conserved across animals, plants, and fungi. In neurons, Golgi stacks are connected by tubules to form a ribbon-like structure adjacent to the centrosome within the cell body. The polarized shape of the Golgi ribbon is necessary for both directed secretory trafficking as well as axon specification and extension (De Zio et al., 2015). Recent studies indicate that as neurons mature, the increasing complexity and length of dendritic arbors requires microtubule nucleating centers located away from the cell body. In particular, Golgi outposts have been found to be enriched at dendritic branchpoints and have the ability to seed and nucleate new microtubules (Ori-McKenney et al., 2012). The appearance of these outpost was shown to correlate with the formation

of new End-Binding protein-1 (EB1) comets and confer polarity by maintaining directed vesicle trafficking within the neurite (Ori-McKenney et al., 2012; Horton et al., 2005). Disruption of Golgi polarity produces neurons with symmetric dendritic arbors, lacking a single longest principal dendrite (Horton et al., 2005). Therefore, it is clear that Golgi-derived microtubules contribute to the asymmetric networks of polarized neurons and support cargo delivery to the leading edge.

Cell migration requires the regulated transport of vesicles and the addition of new plasma membrane to supplement extending neurites (Jaffe and Hall, 2005). Therefore, it is not surprising that in migrating cells both the Golgi and centrosome re-orient to face the leading edge in response to a variety of external cues including trophic factors, electrical fields, and/or chemotaxic gradients (Bisel et al., 2008). Polarization cues initiated at the leading edge have been shown to activate the GTPase Cdc42, which establishes the Par6-Par3-PKC polarity complex. This complex can then recruit and anchor the motor protein dynein, which pulls on microtubules creating tension to move the centrosome/Golgi complex towards the leading edge (Palazzo et al., 2001). Migrating neurons are highly polarized in the direction of their movement and this is achieved through the correct orientation and remodeling of a leading neurite. During the radial migration of neurons in the developing cortex, somal translocation occurs following movement of the centrosome into the leading process which creates traction forces pulling the nucleus forward (Figure 1.3; Sakakibara et al., 2013). In addition, previous experiments indicate that during the tangential migration of cortical interneurons movement of the Golgi/centrosome complex into an extending neurite is the key step for

selecting directionality (Yanagida et al., 2012). This movement is achieved through regulation of the microtubule associated protein Lis1 stimulating dynein motor activity to pull the centrosome into the leading process (Levy and Holzbauer 2008; Tsai et al., 2007). Knockdown of either dynein or Lis1 results in a loss of centrosome motility and significant impairments in somal translocation (Tsai et al., 2007). Therefore, it is clear that directed cell migration requires orientation of the MTOCs towards the leading edge.

1.5 Microtubule Plus-End Binding Proteins (+TIPs)

Growing microtubules serve as transient binding platforms for proteins that can both regulate microtubule dynamics and affect their interactions with extracellular cues. A subgroup of the MAPs, the plus-end-tracking proteins (+TIPs), specifically accumulate at the growing ends of microtubules. Therefore, +TIPs are in a strategic position to regulate interactions between the cytoskeleton and other intracellular structures. (Akhmanova and Steinmetz, 2010 and Galjart, 2010).

Microtubule dynamics are regulated at the polarized plus-ends, which undergo successive episodes of growth and shrinkage (Figure 1.4; Akhmanova and Steinmetz 2008). This process, called dynamic instability, involves alternations between catastrophes (transitions from microtubule growth to shrinkage) and rescues (shrinkage to growth). Dynamic instability creates fractions of growing, shrinking, and stable (pausing) tubulin polymers and this enables the cell to constantly probe the cytoplasm and adapt quickly to a changing environment. In addition, microtubule dynamics can generate traction forces which can be used to transport vesicles, pull chromosomes apart during mitosis, and position organelles within the cell (Galjart, 2010).

The polymerization of microtubules begins with the addition of GTP bound tubulin dimers at the plus-end. Electron microscopy experiments have demonstrated that GTP-bound tubulin is relatively straight allowing for microtubule polymerization, while GDP-bound tubulin favors a more curved conformation. +TIPs bind with varying affinities to microtubules grown in the presence of different GTP analogs (notably with enhanced affinity for GTP γ compared to GDP microtubules) suggesting that +TIPs sense a tubulin conformation that is linked to the GTPase cycle at the leading edge (Maurer et al., 2011). Therefore, by binding close to the GTP-binding site, +TIPs are able to recognize the nucleotide state of microtubules and provide a stabilized structural cap protecting extending neurites from depolymerization (Figure 1.4; Maurer et al., 2012).

The growth cone represents the specialized, highly motile tip of extending neurites. Intrinsic polarity signals and extracellular guidance cues are responsible for directing growth cone navigation through the regulation of microtubule dynamics. Previous experiments have demonstrated that microtubule stability can induce growth cone attraction and neurite outgrowth both *in vitro* and *in vivo* (Buck and Zheng, 2002). In addition, the selective stabilization and extension of microtubules at the leading edge has been shown to be essential for cell migration (Wantanabe et al., 2005). Therefore, +TIPs can operate as regulatory factors involved in neuron migration and cortex development. Accumulating evidence demonstrates a role for +TIP proteins in a range of developmental phenotypes including: neuron differentiation, conversion of multipolar cells to their bipolar migratory state, and the migration of neurons through the cortical plate (de Anda et al., 2012; Purro et al., 2008; Koester et al., 2007; Eom et al., 2014).

During cell division chromosome segregation is governed by the interaction of spindle microtubules with the kinetochore and following nuclear envelope breakdown, the plus-ends of dynamic microtubules probe the cytoplasm in an effort to capture and initiate chromosome alignment (Kirschner and Mitchison, 1986; Hill, 1985; Holy and Leibler, 1994). Microtubules that encounter a kinetochore become stabilized, whereas those that do not depolymerize and are broken down (Hayden et al., 1990). Knockdown of +TIP proteins such as Adenomatous Polyposis Coli (APC) and EB1 has been shown to cause deficits in chromosome segregation and spindle positioning (Fodde et al., 2001; Kaplan et al., 2001; Tirnauer et al., 2002; Rogers et al., 2002) and these phenotypes could be the result of reduced astral microtubule numbers or by preventing microtubule plus-ends from interacting with specific depolymerases. In mammalian cells, loss of spindle pole integrity during mitosis can lead to incorrect chromosome segregation and deficits in daughter cell viability (Silkworth et al., 2009). Therefore, the localization and specialized nature of +TIPs allows for them to affect all aspects of neuron development from cell division, to polarization, and migration.

1.6 Overview of CLIP-170 Associated Protein (CLASP)

CLASPs belong to a heterogeneous family of +TIPs which regulate microtubule stability during both interphase and mitosis. Previous evidence demonstrates that CLASPs can stabilize microtubules through direct interactions with tubulin by promoting pausing events and preventing catastrophe during polymerization (Drabek et al., 2006; Mimori-Kiyosue et al., 2005; Al-Bassam and Chang, 2011; Slep, 2009; Ortiz et al., 2009). Initially, CLASPs were identified as binding partners of CLIP-associated proteins and

were shown to track microtubule plus-ends through binding with other +TIP proteins including CLIP-170 and EB1 (Akhmanova et al., 2001). Several mammalian CLASP proteins have been characterized including CLASP1 and two isoforms, CLASP2 α and CLASP2 γ , which are transcribed from a second gene expressed predominantly in the nervous system (Akhmanova et al., 2001). CLASP2 α and CLASP2 γ are highly conserved isoforms that share all known CLASP2 protein interaction domains, differing only at the N-terminus where CLASP2 α contains a 233 amino acid dis1/TOG domain insertion. Therefore, determining how the localization of CLASP is regulated will provide a better understanding of its function.

Mapping analysis of the CLASP2 protein reveals three main binding domains of interest: 1) N-terminal tumor overexpressed gene (TOG) domains 2) a repetitive middle region rich in serine, arginine, and proline residues and 3) a C-terminal region responsible for interactions with CLIP-170, LL5 β , the mitotic spindle, and the Golgi apparatus (Mimori-Kiyosue et al., 2005; Maia et al., 2012; Lansbergen et al., 2006). The N-terminal region of CLASP contains a total of three TOG domains with sequence similarity to HEAT repeats found in the microtubule polymerase, XMAP215 (Bratman and Chang, 2007). These domains within CLASP have been shown to bind free tubulin dimers and aid in microtubule polymerization (Al-Bassam et al., 2010). The central region of the CLASP protein is highly conserved across species and contain two SXIP (Serine -any amino acid- Isoleucine -Proline), EB1 binding motifs required for CLASP, plus-end tracking *in vitro* (Kumar et al., 2012). These SXIP binding motifs are flanked by positively charged arginine residues which form electrostatic interactions between

CLASP and the acidic C-terminal regions of EB1 and α/β tubulin isoforms (Komarova et al., 2005). These results suggest that CLASP localization in the cell can be dependent on the shuttling of binding partners or changes in protein charge following post-translational modifications.

In mitotic cells, CLASPs localize to both kinetochores and the central spindle through associations with the centromere associated protein E (CENP-E) and bundling protein regulator of cytokinesis 1 (PRC1), respectively (Hannak and Heald, 2006; Liu et al., 2009). Previous studies demonstrate that CLASPs play important roles in kinetochore-microtubule attachment and chromosome alignment/segregation (Logarinho et al., 2012; Mathe et al., 2003; Cheeseman et al., 2005; Maiato et al., 2003, 2005; Hannak and Heald, 2006). During mitosis, chromosome segregation relies on dynamic kinetochore to microtubule attachments that switch from dynamic to stable in order to generate the forces necessary for cytokinesis. In dividing cells, knockdown of CLASPs have been shown to cause depolymerization of astral microtubules, mispositioning of the mitotic spindle, and mitotic delays (Maia et al., 2012; Samora et al., 2011). CLASP2 stabilization of kinetochore-microtubule attachments is regulated by phosphorylation of the CLASP2 C-terminal domain by Cdk1 and Plk1 kinases (Maia et al., 2012) and Cdk1 and GSK3 β dependent phosphorylation was previously shown to switch off CLASP2 plus-end tracking (Kumar et al., 2012). Therefore, CLASP phosphorylation can temporally regulate microtubule dynamics in order to satisfy the spindle assembly checkpoint during cell division, and microtubule stabilization by CLASPs establishes

chromatid segregation by organizing kinetochore-microtubule attachments to the cell cortex.

Cell polarity requires the asymmetric distribution of proteins and the Golgi apparatus acts as a sorting center, helping to direct newly synthesized proteins to functionally specialized domains such as the leading edge. CLASPs have been shown to localize to the trans-Golgi network through binding of its C-terminal portion with the Golgin protein, GCC-185 (Mimori-Kiyosue et al., 2005; Efimov et al., 2007; Hayes et al., 2009; Lin et al., 2011). The binding of CLASP2 and GCC-185 is controlled by a direct interaction with members of the polarity complex PAR3 and subsequent phosphorylation by aPKC (Matsui et al., 2015). CLASP localization at the Golgi is required for the nucleation of Golgi-derived microtubules, most of which are directed towards the leading edge and are biochemically dissimilar from the centrosomal microtubule array (Efimov et al., 2007). Knockdown of CLASPs has no effect on centrosomal microtubule nucleation, but dramatically decreases the number of microtubules emanating from the Golgi and abolishes directional trafficking of intracellular cargo (Efimov 2007; Miller et al., 2009). In addition, CLASP-dependent microtubules have been shown to be necessary for the formation of the polarized Golgi ribbon (Miller et al., 2009). These studies indicate that CLASPs regulate directional trafficking from the Golgi apparatus by establishing asymmetry in the microtubule network and affecting Golgi morphology.

+TIPs are enriched at the growth cone and this localization strategically places them in a position to control neurite stability, pathfinding, and interactions between actin and the microtubule cytoskeleton. Previous studies have determined that a conserved,

serine-rich sequence in CLASP2 α (amino acids 677-813) is required for microtubule plus-end tracking whereas a neighboring domain (amino acids 1031-1240) is necessary for association with the microtubule lattice (Mimori-Kiyosue et al., 2005; Wittmann and Waterman-Storer, 2005). Interestingly, recent studies indicate that CLASP microtubule binding can redistribute other +TIP proteins (including EB1 and CLIP-170) away from the leading edge (Grimaldi et al., 2014) possibly by altering GTP-tubulin content. CLASPs accumulate asymmetrically toward the leading edges of migrating fibroblasts (Akhmanova et al., 2005; Wittmann and Waterman-Storer, 2005) and this localization is required for directional cell movement and contact repulsion (Wittmann and Waterman-Storer, 2005; Stramer et al., 2010). CLASP2 has also been shown to bind directly to actin filaments (Tsvetkov et al., 2007). and CLASP knockdown in *Xenopus* spinal cord axons results in abnormalities in F-actin structure (Marx et al., 2013). In summary, CLASP localization at the leading edge has been shown to promote neurite extension, cross-talk between actin and microtubules, and directional migration.

CLASP plus-end tracking is conferred by two SXIP, EB1 binding motifs and each of these domains is flanked by conserved GSK3 β phosphorylation sites. Multisite phosphorylation of CLASP by GSK3 β can disrupt electrostatic hydrogen bonds between the arginine residues of CLASP and the C-terminal tail of tubulin. Therefore, GSK3 β phosphorylation of CLASP negatively regulates its affinity for microtubules and plus-end tracking (Kumar and Wittmann 2012). In contrast to most other kinases, GSK3 β activity is high in non-stimulated cells and is inhibited at the leading edge of migrating astrocytes and in the growth cone of extending neurites (Etienne-Manneville and Hall, 2003; Zhou

et al., 2004). Previous experiments have demonstrated that activated GSK3 β can cause cortical migration defects, abnormal centrosome positioning, and destabilization of microtubules at the leading process (Asada and Sanada, 2010). Therefore, it is likely that cytoskeletal proteins downstream of GSK3 β regulate its affect on cell motility and polarization.

1.7 Thesis Rationale

Microtubule dynamics are essential during many developmental processes including neuron differentiation, polarization, and migration. In particular, microtubule plus-end tracking proteins (+TIPs) are enriched at the growth cone and this localization strategically places them in a position to control neurite directionality, stability, and the crosstalk between microtubules and the actin cytoskeleton. Previous results demonstrate that CLASP2, a +TIP can regulate polarity and motility in non-neuronal cells; however, the function of CLASP2 during brain development is unknown. Therefore, **the goal of my thesis is to understand how CLASP2 regulates neuron migration, morphology, and function in the developing brain.** In the cerebral cortex, defects in cortical lamination can lead to mental retardation, autism spectrum disorders, and epilepsy (Kerjan and Gleeson, 2007; Walsh and Engle, 2010). Therefore, results from this study will offer invaluable insights into the mechanisms by which microtubule dynamics affect mammalian brain development and elucidate the pathways which integrate extracellular cues with cytoskeleton reorganization.

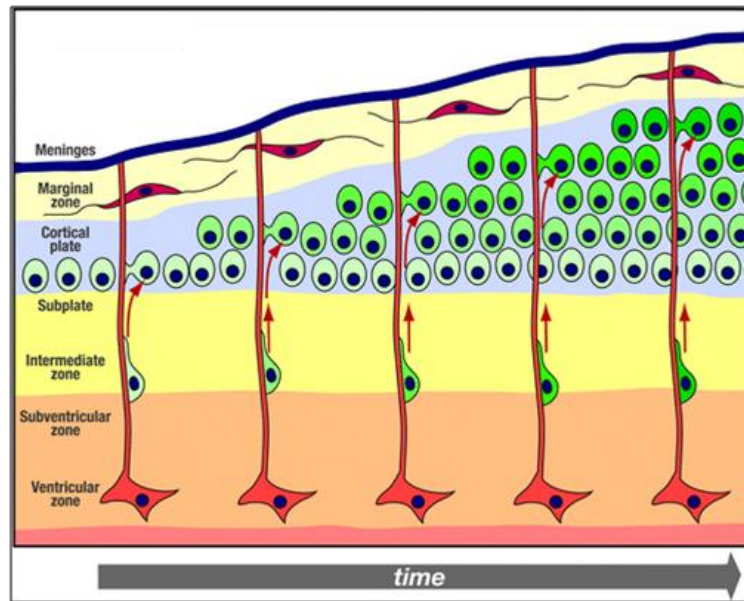


Figure 1.1: Mammalian Cortex Development

Schematic diagram of radial-directed neuronal migration in the cortex. Radial glia cells (orange) lie in the ventricular zone and send long basal process to the pial surface.

Neurons (green) are generated in the ventricular zone directly or indirectly from radial glia divisions and migrate along radial glia fibers through the subventricular zone, intermediate zone, and cortical plate. The cortical plate is established in an inside-out pattern so that later-generated neurons destined for more superficial layers bypass earlier-generated neurons in deeper layers (progressively darker green shading). The marginal zone includes horizontally oriented Cajal-Retzius which release the extracellular signaling glycoprotein Reelin (red). *Adapted from Bielas et al., 2004.*

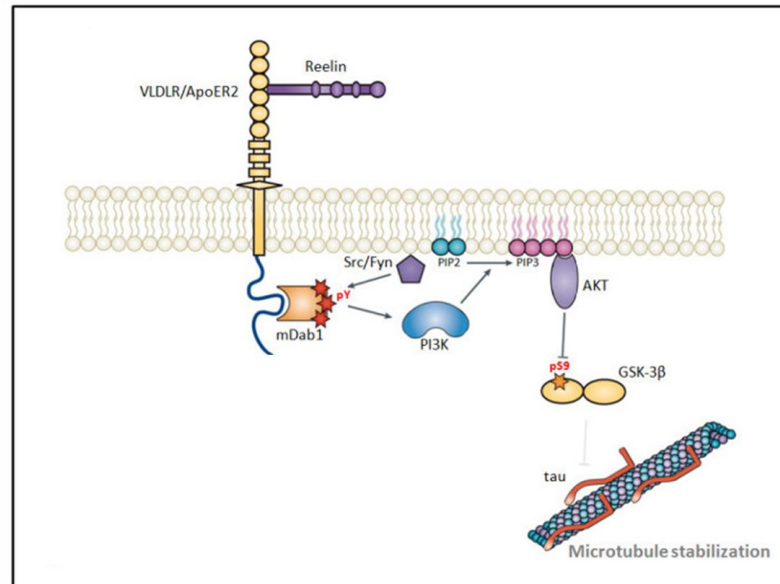


Figure 1.2: Reelin Signaling Pathway

Intracellular signaling events triggered by the binding of Reelin to its two main receptors, the very-low density lipoprotein receptor (VLDLR) and the Apolipoprotein E receptor 2 (ApoER2). The binding of Reelin to its receptor induces the phosphorylation of the adapter protein Dab1 on tyrosine residues and Dab1 phosphorylation eventually leads to the modulation of cytoskeleton effectors molecules such as MAP1B and Tau. *Adapted from Bórquez et al., 2013.*

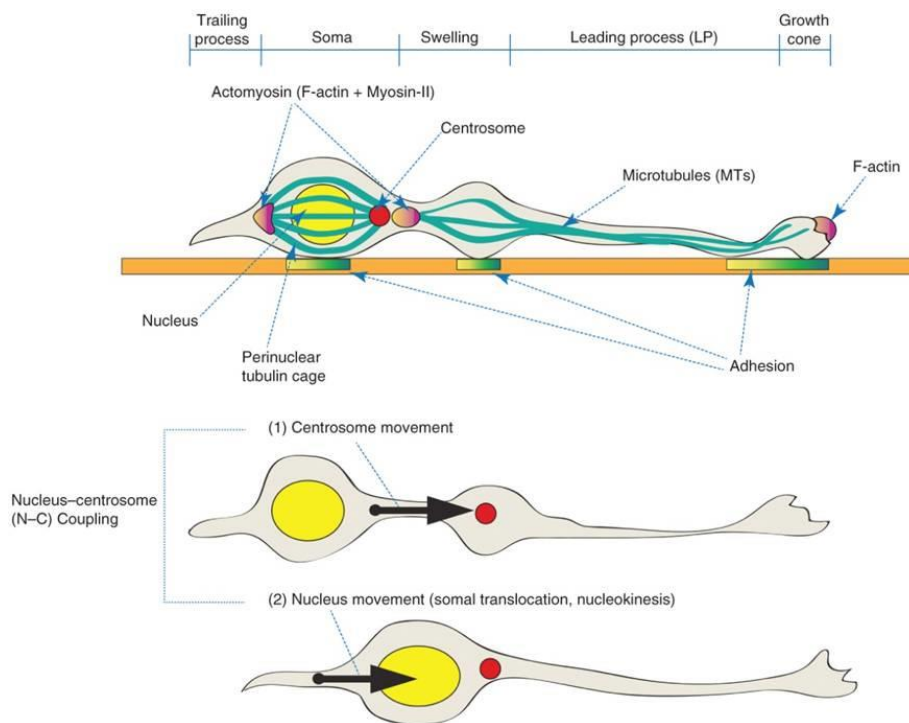


Figure 1.3: The Role of Microtubules and the Golgi/Centrosome Complex in Cell Movement

Migrating neurons are highly polarized in the direction of their movement and this is achieved through the generation, maintenance, and constant remodeling of microtubules in response to extracellular cues and intracellular polarity signals. During migration, the cell first extends a leading process preceded by a growth cone that expands and collapses as it explores the microenvironment. The centrosome then moves into a swelling in the leading process and the nucleus follows (nucleokinesis) due to a pulling force from microtubules and dynein motors located at the centrosome. *Adapted from Moon and Wynshaw-Boris, 2012.*

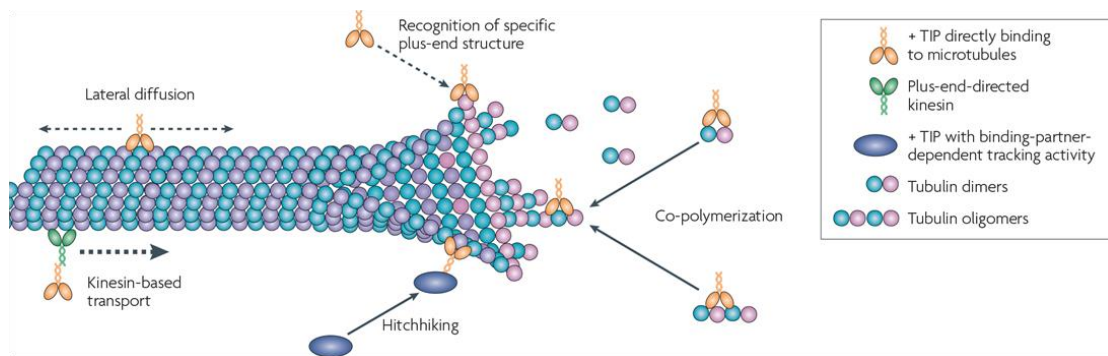


Figure 1.4: Mechanisms of Microtubule Plus-End Tracking

Microtubule dynamics are regulated at the polarized plus-ends, which undergo successive episodes of growth and shrinkage called dynamic instability. Plus-end tracking proteins (+TIPs) arrive at the microtubule tip by diffusion along the microtubule lattice or by kinesin motor protein transportation. +TIP localization is likely the result of their preference for tubulin conformations linked to the GTPase cycle or from their affinity for specific binding partners (this is known as hitchhiking). +TIPs function to stabilize microtubules thereby protecting extending neurites from catastrophe events and depolymerization. *Adapted from Akhmanova and Steinmetz 2008.*



Figure 1.5: CLASP2 Protein Binding Domains

CLASP2 α and CLASP2 γ are highly conserved isoforms that share all known CLASP2 protein interaction domains, differing only at the N-terminus where CLASP2 α contains a 233 amino acid dis1/TOG domain insertion. Mapping analysis of the CLASP2 protein reveals three main binding domains of interest: 1) N-terminal TOG domains with the ability to bind free tubulin dimers and aid in microtubule polymerization 2) a repetitive middle region rich in serine, arginine, and proline residues which is required for plus-end tracking and 3) a C-terminal region responsible for interactions with CLIP-170, the mitotic spindle, and the Golgi apparatus.

CHAPTER 2: MATERIALS AND METHODS

2.1 Cloning and Plasmids

Full-length human CLASP2 (National Center for Biotechnology Information reference sequence NM_015097.2) was PCR amplified from a full-length cDNA clone (ImaGenes) and subcloned into pEGFP-C1 (Clontech) to create an N-terminal enhanced green fluorescence protein (EGFP) tag. EGFP-CLASP2 and EGFP control were then subcloned into the lentiviral vector pFUW and sequence verified. The shRNA constructs for mouse CLASP2 include GCATCAGTCCTTTCAACAAGT and GAACTTGAAGAGACGTAAAT, and control, scrambled shRNA CCGCAGGTATGCACGCGT. Each shRNA was cloned into the pLKO.1 (Addgene plasmid 10879) and pCGLH (generous gift from the Haydar lab) vectors for lentivirus and *in utero* electroporation experiments, respectively.

To generate truncated GFP-CLASP2 variants that isolate individual domains of the protein, we first examined protein hydrophobicity using the Eukaryotic Linear Motif (ELM; elm.eu.org) to identify globular domain regions and regions of low complexity or disorder. Using full-length human CLASP2 α (IMAGE clone 9021646; BC140778) as template, we designed PCR primers at the regions of lowest complexity in order to optimally preserve domain structure. We divided the CLASP2 α cDNA in to 5 distinct domains and amplified regions of 738 to 1137 bp by PCR and inserted them in to pEGFP-C3 (Invitrogen).

CLASP2 α and the phospho-mutant plasmids CLASP2 α 8S/D and CLASP2 α 9S/A were generous gifts from the Torsten Wittmann Lab, University of California, San Francisco.

All additional plasmids are listed in Table 2.2.

2.2 Primary Neuron Culture and Lentiviral Infection

Primary neuronal cultures were prepared from newborn mice of either sex and infected with lentivirus on the day of plating as previously described (Beffert et al., 2012; Ho et al., 2006, 2008). Briefly, neurons were dissociated with trypsin for 5 min at 37°C, triturated, and plated onto coverslips coated with Matrigel. Neurons were maintained in culture at 37°C in a humidified incubator with 95% air and 5% CO₂.

Recombinant lentivirus was produced by transfecting HEK293T cells using the FuGENE6 reagent (Roche) with a shuttle vector encoding the gene of interest in addition to plasmids for viral enzymes and envelope proteins (RSV/REV, MDLg/RRE, and VSVG). Conditioned medium containing lentivirus was harvested 48 hours following transfection and centrifuged at 1000 x g for 10 minutes to remove cellular debris.

2.3 Western Blotting

SDS-PAGE was performed to separate proteins of interest using standard procedures. Proteins were transferred to nitrocellulose membranes and then blocked for one hour in Odyssey Blocking Buffer prepared in Phosphate Buffered Saline (PBS) with 0.02% Tween 20. Following block, membranes were probed with the appropriate primary antibody overnight at 4°C. Membranes were washed thoroughly in PBS before incubation with appropriate secondary antibody for LICOR detection.

2.4 Immunocytochemistry and Electron Microscopy

Primary hippocampal neurons were fixed on coverslips in 4% paraformaldehyde at room temperature for 8 min, permeabilized with 0.3% triton for 10 minutes, and then blocked with 5% goat serum for 1 hour. Primary antibody incubation was performed with 5% goat serum in PBS overnight at 4°C. After washing with PBS, cells were incubated with goat anti-rabbit or goat anti-mouse secondary antibodies conjugated to Alexa Fluor-488, 546, or 647 (Invitrogen). Labeled coverslips were washed in PBS, mounted in ProLong Gold with DAPI (Invitrogen), and imaged with a Carl Zeiss LSM 700 laser scanning confocal microscope.

For electron microscopy, coverslips were fixed in 2.5% glutaraldehyde and 0.1 M sodium cacodylate buffer, pH 7.2, and examined by standard procedures (Rosahl et al., 1995).

2.5 Quantitative Protein Analysis

For protein quantifications, brain tissue from mice at various postnatal stages was isolated and homogenized in PBS containing 10 mM EDTA and protease inhibitors. Brain lysates (25–40 µg) were separated by SDS-PAGE, and immunoblotting was performed as described previously. For protein quantifications in neuronal cultures, high-density neocortical cultures at various timepoints were harvested by washing neurons with cold PBS, followed by the addition of reducing sample buffer.

For GluA1 surface expression, neuronal cultures were incubated with 1 mg/ml sulfo-NHS-LC-Biotin (Thermo Fisher Scientific) in PBS for 20 min on ice, quenched with Tris-buffered saline (150 mM NaCl and 50 mM Tris, pH 7.5), and lysed with RIPA

buffer (65 mM Tris, pH 7.4, 150 mM NaCl, 1% Triton X-100, 0.1% SDS, 0.5% Na-deoxycholate, 1 mM EDTA, pH 8.0, 50 mM NaH₂PO₄, 50 mM NaF, 10 mM Na₄P₂O₇, 1 mM Na₃VO₄, and protease inhibitor cocktail). Lysates were clarified by centrifugation at 14,000 × *g* for 20 min at 4°C. Supernatants containing 100 µg of protein were incubated with RIPA-equilibrated NeutrAvidin beads (50% slurry; Thermo Fisher Scientific) overnight at 4°C with gentle rocking to precipitate biotinylated proteins. Beads were washed several times with RIPA buffer and spun at 800 × *g* for 1 min. Proteins were eluted from the NeutrAvidin beads by boiling for 10 min in reducing sample buffer, resolved by SDS-PAGE, and immunoblotted for GluA1.

2.6 Electrophysiological Analysis

Synaptic transmission was recorded from neurons cultured at 14-17 days *in vitro* (DIV) using whole-cell voltage-clamp techniques. Recordings were obtained with an Axopatch 200A amplifier and Clampex 10.0 software (Molecular Devices). Synaptic recordings were filtered at 1 kHz and sampled at 10 kHz. Electrode solution for the pipette contained the following (in mM): 105 Cs-MeSO₃, 10 CsCl, 5 NaCl, 10 HEPES, 0.2 EGTA, 4 Mg-ATP, and 0.3 Na₂GTP, pH 7.4 (300 mOsm). Spontaneous event recordings were performed in the presence of 1M tetrodotoxin and 50M D-2-amino-5-phosphonovaleric acid. For recording miniature EPSCs (mEPSCs), 20 M bicuculline was added to the bath. For mIPSCs, 20 M 6-cyano-7-nitroquinoxaline-2,3-dione was added.

2.7 *In vitro* Migration Assay

Primary neurons were harvested from the cortex of newborn mice of either sex and dissociated to form a single cell suspension. Cell suspensions were allowed to stand

overnight in polypropylene tubes causing them to re-aggregate before being plated into 24-well dishes coated with Matrigel. Four hours after plating, cell aggregates were adherent to the substrate and initial pictures were taken using a Carl Zeiss LSM 700 laser scanning confocal microscope. Cell aggregates were photographed at 2 hour intervals using 10x phase-contrast optics. Quantification of the migration area was calculated using ImageJ software. Lines were drawn in freehand connecting the outermost cells recognizable to the initial aggregate. All observations were recorded blind to the treatment group and migration area was calculated as a percentage with respect to the size of the initial aggregate.

2.8 *In Utero* Electroporation

In utero electroporation (IUE) was performed on timed-pregnant, CD-1 dams (Charles River Laboratories) at embryonic day 14.5 (E14.5) as described previously (Gal et al., 2006). Dams were anesthetized via intraperitoneal injection of a ketamine/xylazine mixture and the uterine horns were exposed by midline laparotomy. One to two microliters of plasmid DNA (final concentration of 3 μ g/ μ l) mixed with 0.1% fast green dye (Sigma Aldrich) was injected intercerebrally *via* a pulled glass micropipette. For electroporation, the anode of a Tweezertrode (Harvard Apparatus) was placed over the dorsal telencephalon above the uterine muscle and four, 35 volt pulses (50 ms duration separated by a 950 ms interval) were applied with a BioTechnology-eXperimental-Research, ECM830 pulse generator (Harvard Apparatus). Following electroporation, the uterine horns were returned to the abdomen and the cavity was filled with a warm 0.9% saline solution. Incisions were closed with silk sutures and dams were returned to a clean

cage and monitored closely during recovery. These procedures were reviewed and approved by the Institutional Animal Care and Use Committee at the Boston University School of Medicine.

2.9 Immunohistochemistry

Electroporated mice underwent transcardial perfusion with ice cold PBS at postnatal day 14. For embryonic day 16 and post-natal day 0, brains were left in the skull for fixation and slicing. Brains were fixed in 4% paraformaldehyde for 4-6 hours and cryoprotected in 30% sucrose/PBS. The tissue was then frozen in OCT compound and cut into 12 μ m sections using a LEICA CM1850 cryostat (LEICA Biosystems). Sections were immediately mounted onto SuperFrost microscope slides (Fisher Scientific) and kept at -80°C for storage. Prior to immunostaining, sections were rinsed with PBS for a minimum of 2 hours and treated with 0.3% methanol peroxidase for 10 min to quench endogenous peroxidase activity. Antigen retrieval was performed by microwaving brain sections in sodium citrate buffer (10 mM, pH 6) at 800 watts for 1 min followed by 80 watts for 10 minutes. Sections were then blocked in 5% goat serum, 0.2% Triton X-100/PBS for 1 hour followed by incubation with primary antibodies overnight at room temperature. The following day, sections were washed with PBS and incubated with the appropriate Alexa-conjugated secondary antibodies. Sections were mounted with ProLong-Gold mounting medium containing DAPI (Invitrogen).

2.10 Edu/Ki67 Cell-Labeling Experiment

IUE was performed on timed pregnant CD-1 dams (Charles River Laboratories) at embryonic day 14.5 (E14.5). 16 and 20 hours following electroporation surgery, pregnant

dams were given two intraperitoneal injections of 5-ethynyl-2'-deoxyuridine (Edu; 50 μ g of Edu per gram of mouse body weight). 24 hours following Edu injections mice were sacrificed and the embryos were harvested for immunohistochemical staining.

2.11 Microarray and IPA Systems Analysis

Total RNA from control, C57Bl/6 (n = 6), ApoER2/VLDL double knockout, Dab1 knockout and *Reeler* mice was prepared by TRIzol® isolation (Invitrogen). A total of 3 cortex samples were taken at 21 days of age and pooled per condition. Samples were hybridized to the GeneChip® Mouse Genome 430 2.0 Array (3'IVT, Affymetrix) at the University of Texas Southwestern Microarray Facility.

Ingenuity Pathway Analysis® (Ingenuity Systems) was used to determine downstream effects most likely associated with knockout of Reelin signaling. Core analysis was run for each mouse model with a cut-off of 1.5x fold change compared to age-matched controls. A comparison analysis was run between mouse models and relevant disease profiles were pulled out based on *p*-value rank.

2.12 Quantitative PCR

Embryonic and newborn cortex was homogenized with a pestle (Thomas) and total RNA was purified using the RNeasy Mini Kit (Qiagen). Total RNA from the adult cortex samples were processed with Trizol (Invitrogen). At least five independent cortex samples were isolated for each developmental timepoint. cDNA was synthesized using Superscript III Reverse Transcriptase (Invitrogen). Reverse transcription quantitative PCR was performed on a 7900HT Fast Real-Time PCR System (Applied Biosystems) using the Power SYBR Green PCR Mastermix (Applied Biosystems) with a two-step

cycling protocol and an annealing/extension temperature of 60°C. The experiment was performed in duplicate with at least two biological replicates and three technical replicates each. The relative amount for each target was normalized using GAPDH as a reference gene and the fold change in gene expression was calculated using the ddCt method with the adult cortex samples as the control group.

2.13 Immunoprecipitation

Human Embryonic Kidney (HEK) 293T cells were lysed 48-72 hours following transfection in buffer containing, 20 mM Tris HCL, 100 mM NaCl, 1 mM EDTA pH 8, and 1% NP-40, supplemented with protease/phosphatase inhibitors (Biotool). Protein extracts were incubated for 2 hours with rotation at 4°C with the precipitating antibody (rabbit anti-GFP 1:500) followed by overnight incubation with 25 µl of protein A Ultralink resin (Thermo Scientific). The following day the resin was washed 5 times with immunoprecipitation buffer. Precipitated proteins were eluted from the resin by boiling for 5 minutes in SDS sample buffer and analyzed by electrophoresis.

2.14 *In situ* hybridization

Tissue samples were harvested from CD1 mice and fixed in 10% Neutral Buffered Formalin (NBF). Fixed samples were processed into paraffin wax, embedded, and sectioned at 4 µm onto positively charged slides. Prior to staining, paraffin was removed by heating slides to 90-95°C for 10 min in aqueous buffered solution before protease digestion. Slides were then fixed in 10% NBF for 5 min before target probe set hybridization at 40°C for 2 hours. Probes were labeled with an alkaline phosphatase-

conjugated oligonucleotide for 15 min before addition of fast blue or fast red substrates for fluorescent imaging.

2.15 Image Analysis and Quantification

To determine axon length, hippocampal neurons were infected at the day of plating and fixed 48-72 hours later. Images were stained for the pan-axonal neurofilament marker SMI-312 or Tau-1. Quantitative immunofluorescence to determine the length of each individual axon was performed using ImageJ software (<http://imagej.nih.gov/ij/>). For axon polarization, the number of axons per neuron was determined using SMI-312 immunostaining at 4 and 9 days *in vitro* (DIV).

To measure neuronal branching, neurons were infected at the day of plating, fixed at 4 and 5 DIV, and processed for microtubule-associated protein 2 (MAP2) immunostaining. The number and length of all neuronal processes was measured using NIH ImageJ software with the Sholl plug-in (<http://imagej.nih.gov/ij/>).

To assess Golgi morphology, immunocytochemistry for the cis-Golgi marker GM130 in combination with MAP2 at 5 DIV. Golgi morphology was defined as “stacked” when the Golgi appeared condensed and nearly circular in shape and “ribbon” when extended so that the length exceeded the width by more than fourfold. Golgi with intermediate phenotypes (representing <5%) were excluded from the analysis.

To assess synapse area and density, primary neurons were infected at 1 DIV were processed at 14 DIV for immunocytochemistry with the presynaptic marker synapsin and the postsynaptic protein postsynaptic density 95 (PSD95). An equal number of

comparable processes in each condition were assessed using the colocalization plug-in NIH ImageJ (<http://imagej.nih.gov/ij/>).

Synaptic parameters on digital electron micrographs were quantified based on the following criteria: total number of synaptic vesicles, number of docked vesicles, number of docked vesicles within 150 nm of the active zone, presynaptic terminal circumference and area, and length of the PSD.

To analyze *in situ* hybridization images, puncta were counted using NIH Image J software. Briefly, particles were analyzed with a size exclusion threshold of 0-25 pixels² in 100µm bins spanning from the ventricle to the pial surface.

For all IUE experiments, coronal sections of the somatosensory cortex were visualized for transfected neurons (green) and cell nuclei (Hoechst 33342, blue). Different cortical areas (VZ=Ventricular Zone, IZ = Intermediate Zone, loCP = lower cortical plate, upCP = upper cortical plate) were determined qualitatively by the density of cell nuclei. The percentage of total transfected cells in each zone are expressed as the mean \pm SEM.

To determine the angle of the leading process, the longest, GFP-containing neurite was traced and the angle of this line was compared to a line from the cell soma to the pial surface. An angle of 0 degrees is equivalent to a line indicating the shortest possible distance from the transfected cell soma to the pia.

To determine the percentage of transfected cells co-expressing various transcription factors and cell-cycle markers. Five, 20 µm bins were created from the

ventricle to the pia. Co-localization was determined qualitatively by examining Z-stacks at 40x objective.

For the *in vitro* migration assay, primary neuron cultures were infected with lentivirus constructs at the day of plating. Cells were allowed to aggregate overnight and then plated on glass bottom wells coated with Matrigel. Cell migration was assessed by measuring the area of migration away from the initial aggregates over a 48 hour period.

2.16 Statistical Analysis

Statistical analyses were performed using Sigma Plot statistical analysis software. For experiments comparing two treatment groups, an unpaired *t* test was performed to assess statistical significance. For experiments in which multiple treatment groups or time points were examined, a one-way ANOVA was performed between groups.

Table 2.1: Antibodies

Name	Product Number	Dilution	Host	Source
<i>Primary Antibodies</i>				
α -Tubulin	3873	ICC 1:1000	Mouse	Cell Signaling
β -Tubulin	PRB-435P	WB 1:5000 ICC 1:1000	Rabbit	Biologend
CDP	SC-13024	IHC 1:250	Rabbit	Santa Cruz
CLASP1	MAB9736	WB 1:1000	Rat	Abnova
CLASP2	MAB9738	WB 1:1000 ICC 1:1000	Rat	Abnova
CLASP2	A302 155A	WB 1:1000	Rabbit	Bethyl
Dab1	27210	WB 1:500	Rabbit	Joachim Herz Lab
GFP	75-131	WB 1:1000 IHC 1:250	Mouse	Neuromab
GFP	132 002	WB 1:1000 IHC 1:250	Rabbit	Synaptic Systems
GluA1	P42261	WB 1:500	Rabbit	Millipore

GM-130	610822	ICC 1:1000 IHC 1:250	Mouse	BD Biosciences
Ki-67	12202	IHC 1:250	Mouse	Cell Signaling
MAP2	Ab5622	WB 1:5000 ICC 1:1000	Rabbit	Millipore
Nestin	611658	IHC 1:250	Mouse	BD Biosciences
Pericentrin	611814	IHC 1:250	Mouse	BD Biosciences
PH3	9701	IHC 1:250	Rabbit	Cell Signaling
PSD-95	75-028	WB 1:1000 ICC 1:1000	Mouse	Neuromab
SMI-312	SMI-312R	WB 1:1000 ICC 1:1000	Mouse	Biolegend
SNAP-25	SMI-81R	WB 1:1000	Mouse	Biolegend
SOX2	SC-17320	IHC 1:250	Goat	Santa Cruz

Synapsin	E018	WB 1:1000 ICC 1:500	Rabbit	Thomas Sudhof Lab
Synaptobrevin	104 211	WB 1:1000	Mouse	Synaptic Systems
Tau-1	Mab3420	ICC 1:3000	Mouse	Millipore
Tbr2	Ab23345	IHC 1:100	Rabbit	Abcam

Table 2.2: Plasmids

Description	Vector Backbone	Size (kbp)	Bacterial Resistance	Source	Experiment
GFP-CLASP2 γ	pFUW	14	Ampicillin	Cloned in-house	Chapter 3 Lentivirus
GFP-CLASP2 α	pFUW	14	Ampicillin	Cloned in-house	Chapter 3 and 4 Lentivirus
GFP-CLASP2 α 8S/D	pFUW	14	Ampicillin	Cloned in-house	Chapter 3 and 4 Lentivirus
GFP-CLASP2 α 9S/A	pFUW	14	Ampicillin	Cloned in-house	Chapter 3 and 4 Lentivirus
pLKO.1 CLASP2 shRNA B	pLKO.1	7	Ampicillin	Cloned in-house	Chapter 3 and 4 Lentivirus
pLKO.1 CLASP2 shRNA C	pLKO.1	7	Ampicillin	Cloned in-house	Chapter 3 and 4 Lentivirus
pCGLH CLASP2 shRNA B	pCGLH	7.9	Ampicillin	Cloned in-house	Chapter 4; <i>in utero</i> electroporation
pCGLH- CLASP2 shRNA C	pCGLH	7.9	Ampicillin	Cloned in-house	Chapter 4; <i>in utero</i> electroporation

pCAG GFP-CLASP2 α	pCAG	10.35	Ampicillin	Cloned in-house	Chapter 4; <i>in utero</i> electroporation
GFP-CLASP1 α	pEGFP-C1	10	Kanamycin	Cloned in-house	Chapter 4 IP
GFP-CLASP2 Domains 1-5	pEGFP-C3	9.27	Kanamycin	Cloned in-house	Chapter 4 IP
GFP-CLASP2 Domains 1-3	pEGFP-C3	7.19	Kanamycin	Cloned in-house	Chapter 4 IP
GFP-CLASP2 Domains 4-5	pEGFP-C3	6.81	Kanamycin	Cloned in-house	Chapter 4 IP
GFP-CLASP2 Domain 1	pEGFP-C3	5.5	Kanamycin	Cloned in-house	Chapter 4 IP
GFP-CLASP2 Domain 2	pEGFP-C3	5.6	Kanamycin	Cloned in-house	Chapter 4 IP
GFP-CLASP2 Domain 3	pEGFP-C3	5.5	Kanamycin	Cloned in-house	Chapter 4 IP
GFP-CLASP2 Domain 4	pEGFP-C3	5.9	Kanamycin	Cloned in-house	Chapter 4 IP
GFP-CLASP2 Domain 5	pEGFP-C3	5.7	Kanamycin	Cloned in-house	Chapter 4 IP
GSK3 β -S9A			Ampicillin	Geoff Cooper	Chapter 4 IP
pCMV5-c-src	pCMV5	6.5	Ampicillin	Tom Sudolf	Chapter 4 IP

pSrc KD (K295M)	pCMV5	7.1	Ampicillin	Yun Qiu U Minn	Chapter 4 IP
Dab1	pFUW	11.5	Ampicillin	Cloned in-house	Chapter 4 IP
EGFP- CLASP2 α Wild-type	pCAG	10.4	Ampicillin	Cloned in-house	Chapter 4 IP
EGFP- CLASP2 α 9S/A	pCAG	10.4	Ampicillin	Cloned in-house	Chapter 4 IP
EGFP- CLASP2 α 8S/D	pCAG	10.4	Ampicillin	Cloned in-house	Chapter 4 IP

CHAPTER 3:
MICROTUBULE PLUS-END TRACKING PROTEIN CLASP2 REGULATES
NEURONAL POLARITY AND SYNAPTIC FUNCTION

The studies presented in this chapter include contributions from additional graduate and undergraduate students. Dr. Uwe Beffert was instrumental in designing most of the experiments and performed data analysis. Undergraduates Josefa M. Sullivan, Christine E. Stuart, John A. Kambouris and myself performed immunocytochemistry, acquired fluorescent microscope images, and analyzed the data which has been incorporated into Figures 3.2, 3.3, 3.4, and 3.5. James P. Gilbert and I collaborated to run the electrophysiology experiments shown in Figure 3.6 and Dr. Angela Ho ran the biotinylation experiment presented in Figure 3.7F. This work was published in the *Journal of Neuroscience* as: Beffert U, **Dillon GM**, Sullivan JM, Stuart CE, Gilbert JP, Kambouris JA, Ho A. (2012). "Microtubule plus-end tracking protein CLASP2 regulates neuronal polarity and synaptic function." *Journal of Neuroscience* 32(40):13906-16.

3.1 Introduction

Neurons are highly polarized cells that are composed of two structurally and functionally distinct cell processes, axons and dendrites (Craig and Banker, 1994). Neuron polarization is initiated by the stabilization and growth of single immature neurite which eventually differentiates into an axon (Bradke and Dotti, 2000). In developing neurons, the actin and microtubule cytoskeleton work together to guide and support the growth and targeting of both axons and dendrites (Dent and Gertler, 2003). Extending axons navigate with the ultimate goal of making functional synaptic connections and synapses represent highly specialized intercellular junctions mediating the transmission of information between axons and their targets. Previous research has demonstrated that dynamic changes in the cytoskeleton are necessary for the establishment of synaptic connections and that the presence of microtubules in the synapse is correlated with synaptic stability and increased neuronal activity (Jaworski et al., 2009). Therefore, intracellular mechanisms that regulate dynamic microtubules have profound effects on a range of developmental processes including polarization, dendritic arborization and synaptogenesis.

The heterogeneous family of plus-end tracking proteins (+TIPs) specifically accumulate at the plus-ends of microtubules, and this location strategically placing them in a position to control microtubule dynamics, growth, and the cross-talk between microtubules and the actin cytoskeleton (Akhmanova and Hoogenraad, 2005; Basu and Chang, 2007; Akhmanova and Steinmetz, 2008). Among the +TIPs, cytoplasmic linker associated proteins (CLASPs) are widely conserved in fungi, plants and animals (Galjart,

2005; Bratman and Chang, 2008). Mammalian CLASPs are represented by two closely-related homologs, a ubiquitously expressed CLASP1 and the brain enriched CLASP2 (Akhmanova et al., 2001). CLASPs accumulate asymmetrically toward the leading edges of migrating fibroblasts suggesting that CLASPs are required for cell polarity and persistent motility (Akhmanova et al., 2005; Wittmann and Waterman-Storer, 2005). In addition, CLASP2 has been shown to mediate asymmetric microtubule nucleation at the Golgi apparatus and are crucial for establishing the continuity and morphology of the Golgi apparatus (Efimov et al., 2007; Miller et al., 2009).

Relatively little is known about the role of CLASP in the mammalian nervous system. Genetic evidence placed Orbit/MAST, the *Drosophila* ortholog of CLASP, as acting downstream from Slit to induce growth cone repulsion and CLASP mutants were shown to exhibit deficits in axon growth and pathfinding (Lee et al., 2004). Here, we characterize the role of CLASP2 in neuronal development, specifically during axon and dendrite formation, synaptogenesis and functional plasticity. We found CLASP2 protein levels increased steadily during neuronal development and were enriched in growth cones of developing neurites of primary mouse hippocampal neurons. CLASP2 shRNA-expressing neurons displayed a significant decrease in dendritic branching and neurite length. Conversely, overexpression of CLASP2 in primary neurons caused formation of multiple axons, enhanced dendritic arborization and Golgi condensation, implicating CLASP2 in neuronal morphogenesis. In addition, we found that overexpression of CLASP2 increased both spontaneous release of neurotransmitters and surface levels of GluA1 receptors at excitatory synapses, suggesting that CLASP2 regulates synaptic

function. Quantification of synaptic proteins showed that overexpression of CLASP2 caused a selective increase in presynaptic proteins involved in the synaptic vesicle fusion machinery suggesting that this increase may contribute to the CLASP2-mediated presynaptic transmission phenotype.

3.2 Results

3.2.1 CLASP2 Expression During Neural Development

Previous experiments have shown that CLASP1 is expressed in all tissues, whereas CLASP2 is specifically enriched in the brain (Akhmanova et al., 2001). To examine the localization of CLASP2 during neuronal development, we characterized the endogenous distribution of CLASP2 in hippocampal neuronal cultures by immunofluorescence microscopy. Staining with CLASP2, SMI-312 (a pan-axonal neurofilament marker) and β -tubulin detected CLASP2 expression along the length of all processes including intense labeling of growth cones at the leading tip 4-5 DIV (Figure 3.1A-B). This result supports previous evidence of CLASP2 as a +TIP and is consistent with a role for CLASP2 in growth cone dynamics within neurons (Akhmanova and Steinmetz, 2008; Hur et al., 2011). Additional staining for α -tubulin demonstrates that CLASP2 is also highly expressed in astrocytes, suggesting that CLASP2 also plays a role in the microtubule dynamics of glia (Fig. 3.1C).

To examine the role of CLASP2 in vivo, we probed mouse brain homogenates at different postnatal days for CLASP2, dendritic (MAP2), and axonal (SMI-312) markers (Fig. 3.1D). CLASP2 expression was detected at postnatal day 1-2 (P1-2) and strikingly increased by 4.5-fold at P5 before stabilizing in the adult brain. The present results also

show that MAP2 was synthesized at the earliest time point examined at P1 and that MAP2 protein levels remained similar throughout development. Conversely, protein expression of the axonal protein marker SMI-312 markedly increased into adulthood.

Lentiviral infection of primary cortical neurons was used to determine the effects of CLASP2 overexpression or knockdown on neurite development and maintenance. In primary cortical neurons treated with control GFP, CLASP2 protein levels are detected as early as 3 DIV and steadily increase from 7 to 14 DIV (Fig. 3.1E). Lentiviral-induced human CLASP2 overexpression increased CLASP2 levels 2 to 3.5 fold higher at 7-11 DIV as compared to endogenous levels. By 14 DIV, the levels of overexpressed CLASP2 were comparable to control levels (at 108%). Conversely, we found that CLASP2 shRNA efficiently decreased CLASP2 protein expression as early as 3 DIV and resulted in a significant 90% knockdown by 7 DIV. We also investigated the distribution of overexpressed CLASP2 in primary hippocampal neurons. When CLASP2 is overexpressed in neurons, CLASP2 was found to accumulate along the whole length of microtubules, colocalizing with both axonal and dendritic markers (data not shown). These results indicate that overexpression did not produce aberrant localization of CLASP2 when compared to endogenous expression. We conclude that CLASP2 protein levels gradually increase during neuronal development and that CLASP2 is specifically enriched at microtubule growing tips during neurite polarization and outgrowth.

3.2.2 CLASP2 Regulates Polarization and Axon Growth

To investigate the role of CLASP2 on axon polarization and dendritic branching, we compared primary hippocampal neurons infected at 1 DIV with control shRNA, human

CLASP2, or CLASP2 shRNA by immunofluorescence. At 2 DIV, quantitative analysis showed that overexpression of human CLASP2 resulted in a significant 20% increase in axon length (Figure 3.2A-B). The shRNA-mediated knockdown of CLASP2 decreased axon length by 20% compared to control-infected neurons. To determine whether the decrease in axon length resulted specifically from CLASP2 knockdown, we coexpressed CLASP2 shRNA with human CLASP2 cDNA which rescued the CLASP2 shRNA phenotype (Figure 3.2A-B).

In addition, we found that 38% of neurons overexpressing human CLASP2 had multiple SMI-312 positive axons when compared to control neurons that predominantly extend a single primary axon at 2 DIV (Figure 3.2C). This increase was further pronounced at 9 DIV when 55% of CLASP2 overexpressing neurons exhibited more than one SMI-positive axon (data not shown). Conversely, CLASP2 shRNA knockdown did not affect the number of polarized axon-bearing neurons. Coexpression of CLASP2 shRNA with human CLASP2 cDNA was similar to control-infected neurons.

3.2.3 CLASP2 Regulates Dendritic Growth and Branching

Next, we examined the time course of dendrite development from neurons infected with control shRNA, human CLASP2 or CLASP2 shRNA. We found that overexpression of human CLASP2 significantly increased the total number of MAP2-positive processes at 5 DIV, with extensive dendrite outgrowth in both primary and secondary dendritic branching (Figure 3.3A). To examine the complexity of the dendritic arbor and the overall pattern of arborization, we used Sholl analysis to examine global changes in neuronal morphology (Figure 3.3B). Sholl analysis revealed that overexpression of

human CLASP2 shifted the distribution upward and to the right as compared to control neurons indicating both an increase in number and length of the neurites (Figure 3.3C-D). Conversely, the shRNA knockdown of CLASP2 greatly reduced dendritic growth. To confirm the specificity of the observed effects, the CLASP2 knockdown phenotype was rescued by overexpressing human CLASP2. Overexpression of human CLASP2 fully reversed the negative effects of CLASP2 shRNA on total neurite length but not the number of MAP2-positive processes (Figure 3.3C-D). In summary, these results suggest that CLASP2 has an important role in axon polarization, neurite growth, and dendritic branching.

3.2.4 CLASP2 Controls Neuronal Golgi Morphology

Previous experiments have shown that CLASP2 localizes to the Golgi in both fibroblast and epithelial cells and is crucial for establishing continuity and proper morphology of the Golgi complex (Akhmanova et al., 2001; Efimov et al., 2007); however, little is known about the role of CLASP2 on the Golgi complex in neurons. To examine CLASP2 distribution in the Golgi of hippocampal neurons, we double-labeled for CLASP2 and the Golgi marker GM130 and found that endogenous CLASP2 localization overlapped with GM130 (Figure 3.4A).

In mammalian cells, CLASP2 is required for the nucleation of microtubules originating from the Golgi apparatus in a centrosome-independent manner (Efimov et al., 2007). In addition, Golgi-derived CLASP-dependent microtubules control proper morphology of the Golgi complex which is essential for cell polarization and motility in retinal pigment epithelial cells (Miller et al., 2009). To determine whether CLASP2

regulates morphology of the Golgi complex in neurons, we examined cultured hippocampal neurons at 4 DIV that were infected with control shRNA, human CLASP2 or CLASP2 shRNA expressing lentivirus. In the control condition, the Golgi in about 65% of all neurons appear condensed and ‘stacked’ near the nucleus while the other 35% appear elongated with a continuous ‘ribbon’ structure extending into the dendritic process (Figure 3.4B-C). We found that overexpression of human CLASP2 led to 80% of the Golgi assuming a ‘stacked’ conformation rather than Golgi deployment into dendrites (Figure 3.4C). CLASP2 shRNA knockdown did not affect the percentage of ribbon and stacked Golgi phenotype compared to control. Coexpression of CLASP2 shRNA with human CLASP2 cDNA was similar to control-infected neurons.

At 4 DIV, we also found that the Golgi is highly fragmented in CLASP2 knockdown neurons (Figure 3.4B, D), indicative of impaired membrane fusion. CLASP2 knockdown neurons contained a significant 1.9-fold increase in the number of fragments compared to control neurons. Overexpression of human CLASP2 fully reversed the fragmented effects of CLASP2 shRNA on the Golgi. Together, these data suggests that CLASP2 control the morphology and organization of the Golgi complex in hippocampal neurons.

3.2.5 CLASP2-Mediated Golgi Morphology Correlates with Dendritogenesis

Since Golgi morphology has been implicated in different aspects of neuronal polarity and dendritic development (Hanus and Ehlers, 2008), we examined whether changes in CLASP2-mediated Golgi morphology coincides with dendritic outgrowth and branching. We examined cultured hippocampal neurons that were infected with control GFP or

CLASP2 expressing lentivirus and double-labeled with MAP2 and GM130 antibodies.

We found that the increase in branching due to CLASP2 overexpression was restricted to neurons with a stacked Golgi phenotype (Figure 3.5). These data suggest that the effects of CLASP2 on Golgi morphology has an important role in maintaining dendritic development and branching.

3.2.6 CLASP2 Regulates Spontaneous Excitatory Synaptic Transmission

To determine whether the morphological changes in neuronal growth and branching lead to functional alterations in synaptic transmission, we performed whole-cell recordings to monitor the frequency and amplitude of spontaneous miniature events from hippocampal neurons at 14-17 DIV following infection with control shRNA, human CLASP2 or CLASP2 shRNA expressing lentivirus. Neurons overexpressing human CLASP2 showed a 4.6-fold increase in miniature event frequency in excitatory synapses compared to control neurons, suggesting that CLASP2 alters excitatory presynaptic neurotransmitter release machinery (Figure 3.6A-B). In addition, we found a small but significant 1.3-fold increase in miniature event amplitude between CLASP2 and control neurons, suggesting that CLASP2 overexpression also has a smaller effect on postsynaptic receptors (Figure 3.6A,C). Interestingly, we found no changes in frequency and amplitude in mIPSCs suggesting the effects of CLASP2 are specific and restricted to the development and function of excitatory synapses (Figure 3.6D-F).

We further examined the effects of CLASP2 shRNA knockdown on mEPSCs and found a 1.5-fold decrease in miniature event frequency in excitatory synapses compared to control neurons suggesting a change in the presynaptic release apparatus (Figure 3.6A-

C). No changes in the amplitude of mEPSCs were observed in CLASP2-mediated knockdown neurons. We next tested whether overexpression of human CLASP2 rescued the effects of CLASP2 shRNA on mEPSCs. Overexpression of human CLASP2 fully restored the miniature event frequency in excitatory synapses.

3.2.7 CLASP2 Affects on Synapse Morphology and Protein Levels

The electrophysiological results raise the possibility that the number of vesicles docked at the active zone is increased in CLASP2 overexpressing hippocampal neurons. To test this, we examined the ultrastructure of cultured neurons infected with control GFP or human CLASP2 expressing lentivirus by electron microscopy at 14 DIV (Figure 3.7A and Table 3.1). Analysis of control synapses revealed presynaptic nerve terminals with clustered synaptic vesicles at the active zone and a filamentous postsynaptic density. Synapses of CLASP2-overexpressing neurons exhibited no significant change in the number of synaptic vesicles that are either docked at the active zone or in close proximity, indicative of the readily releasable pool of synaptic vesicles. However, we observed a significant 28% increase in presynaptic terminal circumference in neurons overexpressing human CLASP2, which may be a consequence of increased vesicle fusion with the plasma membrane and could be a cause for the functional effect in spontaneous synaptic transmission.

We next examined whether overexpression of CLASP2 alters the number and size of synapses. We performed immunofluorescence labeling using antibodies against the presynaptic protein synapsin and the postsynaptic marker PSD95 on hippocampal neurons infected with control shRNA, human CLASP2 or CLASP2 shRNA at 14 DIV

(Figure 3.7B). We measured the number and the size of synapses defined by the colocalization of synapsin and PSD95 and found that CLASP2 overexpression led to a 2.5-fold increase in the number of synapses and a 25% increase in synapse area (Figure 3.7C-D). Conversely, the shRNA-mediated knockdown of CLASP2 decreased the number of synapses by 25% compared to control-infected neurons, while the synapse area remained the same. Overexpression of human CLASP2 cDNA rescued the CLASP2 shRNA phenotype. Together, these data suggest that CLASP2 regulates synaptic morphology leading to functional alterations in synaptic transmission.

To examine whether changes in synaptic protein composition contribute to the CLASP2-mediated synaptic phenotype, we measured synaptic protein levels in cultured neurons overexpressing CLASP2 from 5 to 13 DIV. Quantitative immunoblotting uncovered pronounced changes in a subset of presynaptic proteins during the formation of synapses and clustering of synaptic vesicles at 9 DIV (Figure 3.7E) (Basarsky et al., 1994; Kavalali et al., 1999; Mozhayeva et al., 2002). This included a selective 15% increase in the levels of the presynaptic vesicular protein synapsin in CLASP2-overexpressed neurons. In addition, we found an increase in synaptobrevin (33%) and SNAP25 (27%) but not syntaxin, presynaptic proteins essential for the synaptic vesicle fusion machinery. Overexpression of CLASP2 did not affect postsynaptic proteins such as PSD95 and excitatory glutamate receptor GluA1 expression (Figure 3.7E-F). The early increase in the subset of presynaptic proteins suggests that overexpression of CLASP2 causes early synaptic remodeling and/or synaptogenesis. CLASP2 knockdown selectively decreased synapsin, syntaxin and PSD95 levels which was rescued by overexpressed

human CLASP2. We found no changes in β -tubulin levels in any of the groups examined. These results suggest that CLASP2 specifically regulates synaptic proteins, possibly through stabilization of the cytoskeleton and subsequently regulating synaptic activity.

The increased miniature EPSC amplitude induced by CLASP2 overexpression (Figure 3.6C) strongly suggests alterations in postsynaptic receptors and a role for CLASP2 in the trafficking of receptors to synapses. We therefore examined GluA1 receptor subunit expression at the cell surface as assessed by biotinylation (Figure 3.7F). All surface proteins in neurons were biotinylated, washed, lysed and precipitated with immobilized neutravidin-agarose beads and probed with a GluA1 receptor antibody by Western blotting. We found a 50% increase in the levels of surface GluA1 receptor subunits in CLASP2 overexpressing neurons compared to controls, indicating that the regulated expression and surface insertion of receptors could account for the increase in mEPSC amplitude induced by CLASP2 overexpression (Figure 3.7F).

3.2.8 CLASP2 is Required for PI3K-Induced Axon Elongation

Previous findings indicate that phosphatidylinositol 3-kinase (PI3K) signaling through glycogen synthase kinase 3 β (GSK3 β) is an important mediator for CLASP2 function (Akhmanova et al., 2001; Wittmann and Waterman-Storer, 2005; Kumar et al., 2009; Watanabe et al., 2009; Al-Bassam et al., 2010). Also, PI3K-GSK3 β signaling underlies axon elongation and guidance (Kim et al., 2011). To determine whether CLASP2 is important for PI3K-induced axon elongation, we treated neurons with LY 294002, a specific inhibitor for PI3K. As expected, overexpression of human CLASP2 resulted in a significant 49% increase in axon length (Figure 3.8A-B). The PI3K inhibitor decreased

axon length by 17% compared to control-infected neurons. Overexpression of human CLASP2 in the presence of PI3K inhibitor completely rescued the axon growth defect. These data suggests that CLASP2 is required for PI3K-induced axon polarization.

3.3 Discussion

In the present study, we show that the microtubule plus-end binding protein CLASP2 is an important regulator of neuron polarity and synaptic function. We found endogenous CLASP2 protein expression steadily increased during neuronal development and was present in both axonal and somato-dendritic compartments (Figure 3.1). CLASP2 downregulation in primary neurons impairs axon elongation and dendritic branching which could be rescued by co-expression with human CLASP2. Conversely, overexpression of CLASP2 induced the growth of multiple axons, enhanced dendritic branching and ultimately lead to functional alterations in synaptic structure and function (Figures 3.2-7).

CLASP2 was initially identified as a binding partner of the cytoplasmic linker protein of 170 kDa (CLIP-170) in motile fibroblasts and previously has been shown to be an important regulator in cell polarity by stabilizing microtubules at their plus ends (Akhmanova et al., 2001; Galjart, 2005). The asymmetric distribution of CLASP in regulating cellular polarity was shown to be mediated by PI3K signaling through GSK3 β . The spatially activated PI3K signaling is conveyed downstream through localized inhibition of GSK3 β activity which enhances CLASP2 binding to microtubules (Akhmanova et al., 2001; Wittmann and Waterman-Storer, 2005; Kumar et al., 2009; Watanabe et al., 2009; Al-Bassam et al., 2010). Interestingly, these two spatially coupled

kinases have previously been shown to control axon growth via regulation of the +TIP adenomatous polyposis coli (APC) (Zhou et al., 2004). Recent studies also show that CLASP2 is enriched in growth cones and supports axon regeneration by stabilizing the growing ends of axonal microtubules downstream of GSK3 β (Hur et al., 2011). In line with other +TIPs such as APC (Zhou et al., 2004) and CLIPs (Neukirchen and Bradke, 2011), our data demonstrates that overexpression of CLASP2 in primary hippocampal neurons promotes axon elongation and induces growth of multiple axons per neuron. Also, we show that PI3K-driven axon elongation depends on microtubule dynamics of CLASP2.

In addition to increasing axon outgrowth during neuronal polarization, CLASP2 overexpression induced dendritic development. Overexpression of CLASP2 significantly increased dendritic length and the total number of MAP2-positive processes at 5 DIV with extensive dendrite outgrowth in both primary and secondary dendritic branching (Figure 3.3). These results strongly suggest that CLASP2 plays an active role in regulating the initial stabilization of both axons and dendrites; however the cellular and molecular mechanisms underlying their specific targeting to the growing plus-ends of neurites remain elusive. The differential regulation of +TIP interactions with microtubule ends and the composition of the microtubule cytoskeleton can influence whether a process becomes an axon or a dendrite either as a result of specific motor-based loading or regional control of post-translational modifications (Akhmanova and Steinmetz, 2008). For instance, axon-specific microtubules are uniformly oriented with plus-ends pointing outward, efficiently recruiting kinesin-1 motor-driven transport, whereas microtubule

orientations of mixed polarity in dendrites facilitate dynein motor entry (Kapitein and Hoogenraad, 2011). Axonal and dendritic microtubule arrays also differ in their patterns of post-translational modification. For example, acetylated and detyrosinated microtubules are enriched in axons and selectively recruit kinesin-1 motor proteins (Witte and Bradke, 2008; Konishi and Setou, 2009). Since CLASP2 is regulated by the PI3K-GSK3 β signaling pathway, it is possible that phosphorylation is a molecular switch capable of inducing rapid changes in the microtubule dynamic between axons and dendrites.

In non-neuronal cells, there is a substantial Golgi-associated pool of CLASPs and previous results indicate that CLASP2 promotes microtubule nucleation from the trans-Golgi network leading to asymmetry of microtubule arrays in polarized cells (Efimov et al., 2007). In addition, Golgi-derived CLASP-dependent microtubules are crucial for establishing continuity and proper morphology of the Golgi complex which is essential for cell polarization and motility (Miller et al., 2009). Microtubules nucleated at the Golgi are preferentially oriented towards the leading edge and direct polarized trafficking in motile cells similar to the microtubule-dependent trafficking required during axon specification (Hoogenraad et al., 2001; Witte et al., 2008; Miller et al., 2009). In neurons, the Golgi apparatus has also been implicated in neuronal polarity where the position of the Golgi and the adjoined centrosome correlates with newly emerging axons (Zmuda and Rivas, 1998; de Anda et al., 2005; de Anda et al., 2010). In addition, specialized Golgi outposts exclusively localize at dendritic branchpoints and have been shown to regulate extension and retraction of dendritic branching (Horton et al., 2005; Ye et al.,

2007; Hanus and Ehlers, 2008). Here, we found that CLASP2 colocalizes with the Golgi marker GM130 in primary neurons and that increasing CLASP2 expression leads to increased Golgi condensation (Figure 3.4). We also found CLASP2 overexpression led to increased neuritic branching only in neurons with stacked as opposed to ribbon Golgi morphology (Figure 3.5), suggesting that CLASP2 mediates specific changes in the Golgi that stabilize the cytoskeleton to promote branching.

Microtubules act as the main cytoskeletal tracks for transport of materials to and from the synapse (Conde and Caceres, 2009; Hoogenraad and Bradke, 2009; Goellner and Aberle, 2012). However, little is known about the role of the cytoskeletal machinery, specifically +TIPs on synapse formation and function in mammals. Previous experiments indicate that dynamic EB3 positive microtubule comets can enter dendritic spines and are required for controlling levels of F-actin, spine morphology, and synaptic transmission (Jaworski et al., 2009). Our results indicate that CLASP2 has a functional role in spontaneous neurotransmission (Figure 3.6). The shRNA knockdown of CLASP2 reduced miniature event frequency in excitatory synapses, while overexpression of CLASP2 caused an increase in both miniature event frequency and amplitude specifically in excitatory synapses, suggesting that CLASP2 regulates both presynaptic neurotransmitter release machinery and postsynaptic receptor trafficking. The current changes in spontaneous neurotransmission could be due to CLASP2 effects on axon and dendritic outgrowth, exclusively targeting excitatory neurons which have been shown to vary greatly in their somatic, dendritic and axonal morphologies compared to inhibitory neurons (Markram et al., 2004). Interestingly, we found that CLASP2 induced

ultrastructural changes in asymmetric excitatory synapses that support the presynaptic changes we observed electrophysiologically (Figure 3.7). Quantitative electron microscopy revealed a selective increase in presynaptic terminal circumference that may be a consequence of increased vesicle fusion with the plasma membrane. In line with the ultrastructural data, the size and number of synapses as assessed by synapsin-PSD95 colocalization was significantly enhanced in neurons overexpressing CLASP2. We surveyed several synaptic proteins to determine whether CLASP2 has selective effects on the composition of the synapse. We found that CLASP2 overexpression caused pronounced increases in pre- (synapsin, synaptobrevin, and SNAP25) but not post- (PSD95, GluR1) synaptic protein expression (Figure 3.7). Recent studies demonstrate that while action potential-evoked or spontaneous neurotransmitter release may utilize the same molecular machinery, they rely on distinct molecular interactions for normal function (Ramirez and Kavalali, 2011). For example, structure-function analyses of neuronal SNARE proteins (syntaxin, synaptobrevin and SNAP25) revealed key differences that give rise to spontaneous versus evoked fusion (Ramirez and Kavalali, 2011). For example, loss of SNAP25 or synaptobrevin largely abolishes calcium-dependent evoked release but leaves spontaneous fusion release intact (Schoch et al., 2001; Washbourne et al., 2002; Bronk et al., 2007). Therefore, the CLASP2-mediated increase in synapsin, synaptobrevin, and SNAP25 may provide possible mechanistic detail of the functional increase in evoked mEPSCs as alterations in expression levels of these proteins have been shown to cause calcium-dependent evoked neurotransmitter

release (Lu et al., 1992; Rosahl et al., 1995; Schoch et al., 2001; Washbourne et al., 2002; Bronk et al., 2007).

At the postsynaptic membrane, we found that CLASP2 plays an important role in glutamate receptor trafficking, including an increase in surface levels of GluA1 in CLASP2 overexpressing neurons. This raises the possibility that CLASP2 functions as a factor controlling the delivery of synaptic components to synaptic terminals (Figure 3.7). Previously, +TIPs have been shown to play important roles in positioning neurotransmitter receptors and ion channels. APC and end-binding protein1 (EB1) have been shown to be involved in assembly and stabilization of $\alpha 3$ nicotinic acetylcholine receptor at the postsynaptic side of cholinergic synapses by anchoring microtubules (Temburni et al., 2004). EB1 was also shown to target voltage-gated potassium (Kv1) channels to axons (Gu et al., 2006). In principal, localized remodeling of the cytoskeleton through +TIPs could achieve the spatial remodeling required for synapse-specific and activity-dependent synaptic plasticity. It is possible that binding of CLASP2 to microtubules or to other end-binding proteins is important for the phenotypes we observed, but further studies will be necessary to investigate this possibility.

In summary, our results suggest that the control of microtubule organization by CLASP2 may represent a mechanism for regulated growth cone motility as well as synapse formation and plasticity. We find that increasing CLASP2 expression leads to accelerated and enhanced neuron and synaptic development. Although the cellular and molecular mechanism remains to be determined, CLASP2 has a number of specific binding domains that allow for protein interactions at the Golgi, cytoskeleton and the

growing tips of neurites. The enhanced neuronal development may therefore arise due to altered Golgi function, increased trafficking along microtubules or increased vesicle fusion due to stabilization of the cytoskeleton. The specific CLASP2 domains responsible for these functional changes will be important to address in the future.

Figure 3.1

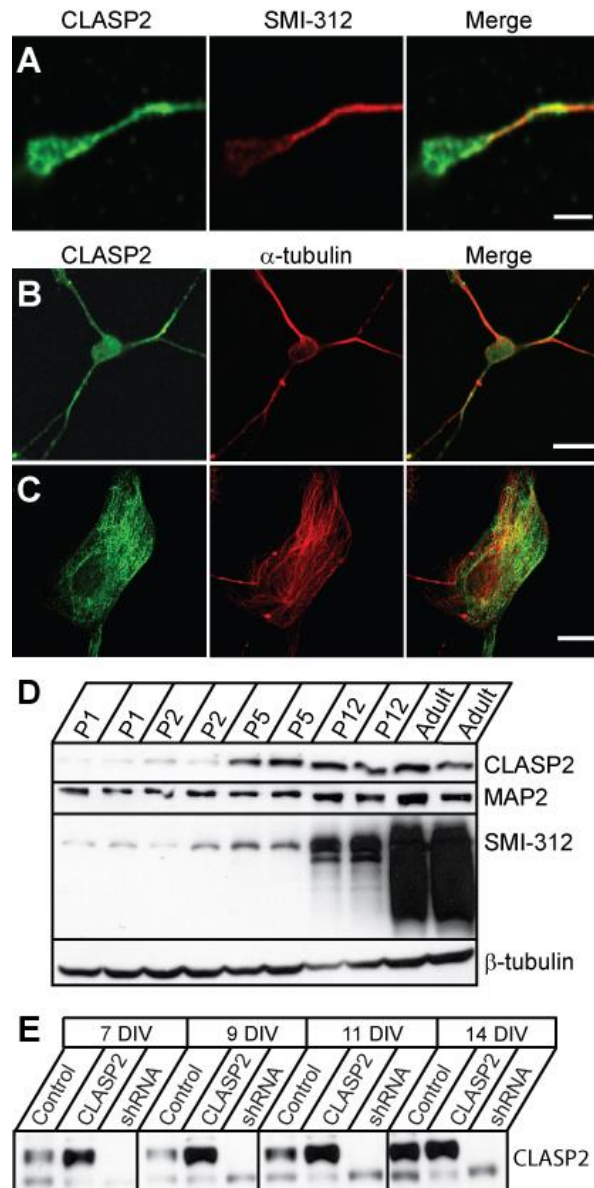


Figure 3.1: Localization and Expression of CLASP2 in the Developing Neuron

A, Representative images of endogenous CLASP2 demonstrating enrichment at the growth cone of a mouse, hippocampal axon at 4-5 DIV. Image is double labeled with anti-CLASP2 (green) and anti-SMI-312 (red) antibodies. Representative images of a hippocampal neuron (**B**) and a glial cell (**C**) at 4 –5 DIV following double labeling with anti-CLASP2(green) and anti- β -tubulin(red) antibodies. Scale bars: **A**, 2.5 μ m; **B**, 16 μ m; **C**, 15 μ m. **D**, Protein expression levels of CLASP2, MAP2, SMI-312, and β -tubulin during postnatal development examined by immunoblotting of total mouse brain lysate at the indicated ages (Adult = 3 months). **E**, Expression levels of CLASP2 was examined by immunoblotting of total lysate from primary mouse cortical neurons DIV 7-14. Neurons were infected with control, human CLASP2, or CLASP2shRNA lentivirus.

Josefa Sullivan performed the ICC used in Figure 3.1A-C

Greg Dillon collected lysates and performed the western blot for Figure 3.1 D-E

Figure 3.2

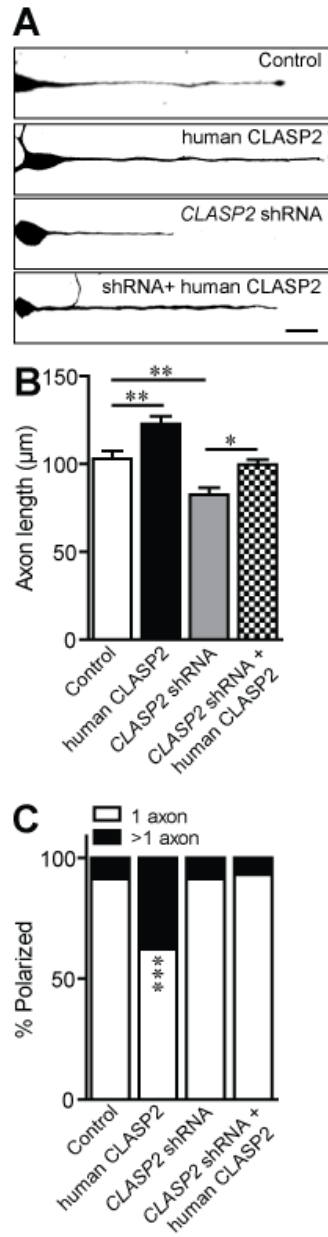


Figure 3.2: CLASP2 Increases Axon Length and Induces the Formation of Multiple Axons

A, Hippocampal neurons infected at 1 DIV with control, human CLASP2, CLASP2 shRNA or CLASP2 shRNA coexpressing human CLASP2 were fixed at 2 DIV and stained with SMI-312 (axonal marker). Scale bar=20 μm . **B**, Quantitative analysis showed that human CLASP2 significantly increased axon length at 2 DIV (n=49 neurons for each group; * $p<0.05$, ** $p<0.001$). **C**, Hippocampal neurons infected were fixed at 4 DIV and stained with SMI-132. Neurons infected with human CLASP2 demonstrated multiple axons compared to control and CLASP2 shRNA (n=62 neurons for each group; *** $p<0.0001$). Neuronal polarity phenotypes were categorized into two groups: single axon (white bar) and multiple axons (black bar).

Josefa M. Sullivan and Christine E. Stuart performed the ICC and analyzed the pictures used in Figure 3.2

Figure 3.3

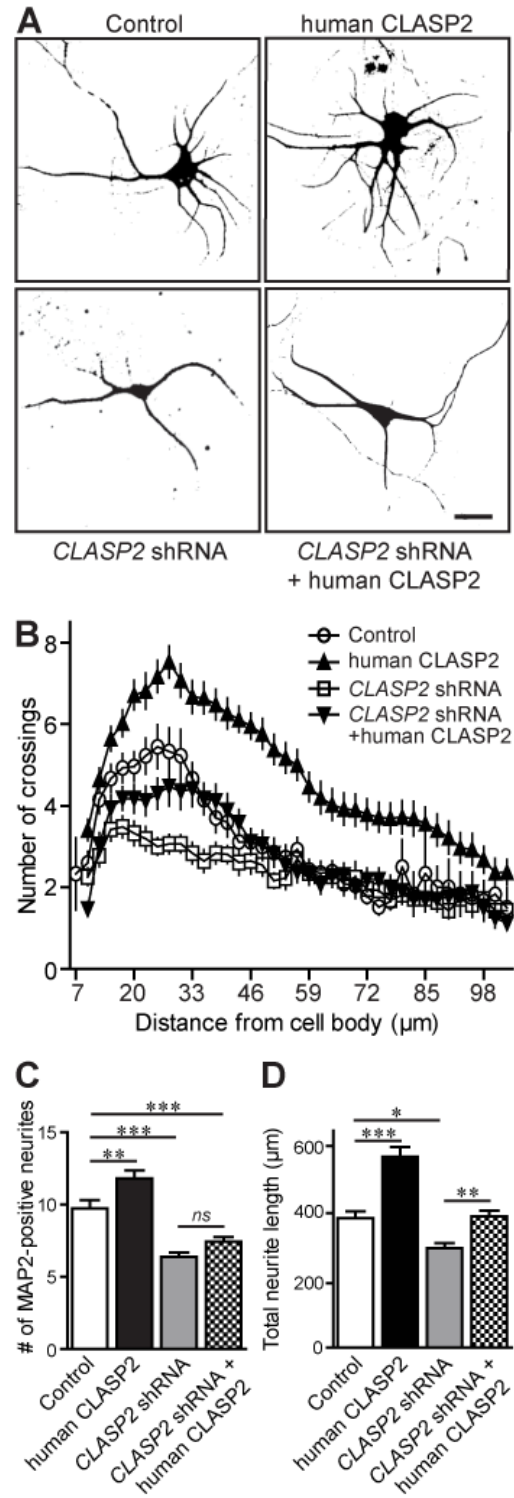


Figure 3.3: CLASP2 Regulates Dendritic Growth and Branching

A, Hippocampal neurons infected at 1 DIV with control, human CLASP2, CLASP2 shRNA or CLASP2 shRNA coexpressing human CLASP2 were fixed at 5 DIV and stained with MAP2 (dendritic marker). Scale bar=20 μm . **B**, Sholl analysis based on the number of dendritic crossings distributed over the distance from the cell body (n=17 neurons for each group). **C**, CLASP2 significantly increased the total length of all neurites (n=32 for each group; ** p<0.01, *** p<0.001, ns=not significant) and **D**, the length of the longest dendrite (n=19 for each group; * p<0.05 ** p<0.01, *** p<0.001).

Josefa M. Sullivan, Christine E. Stuart, and Greg Dillon performed the ICC and analyzed the pictures used in Figure 3.3.

Figure 3.4

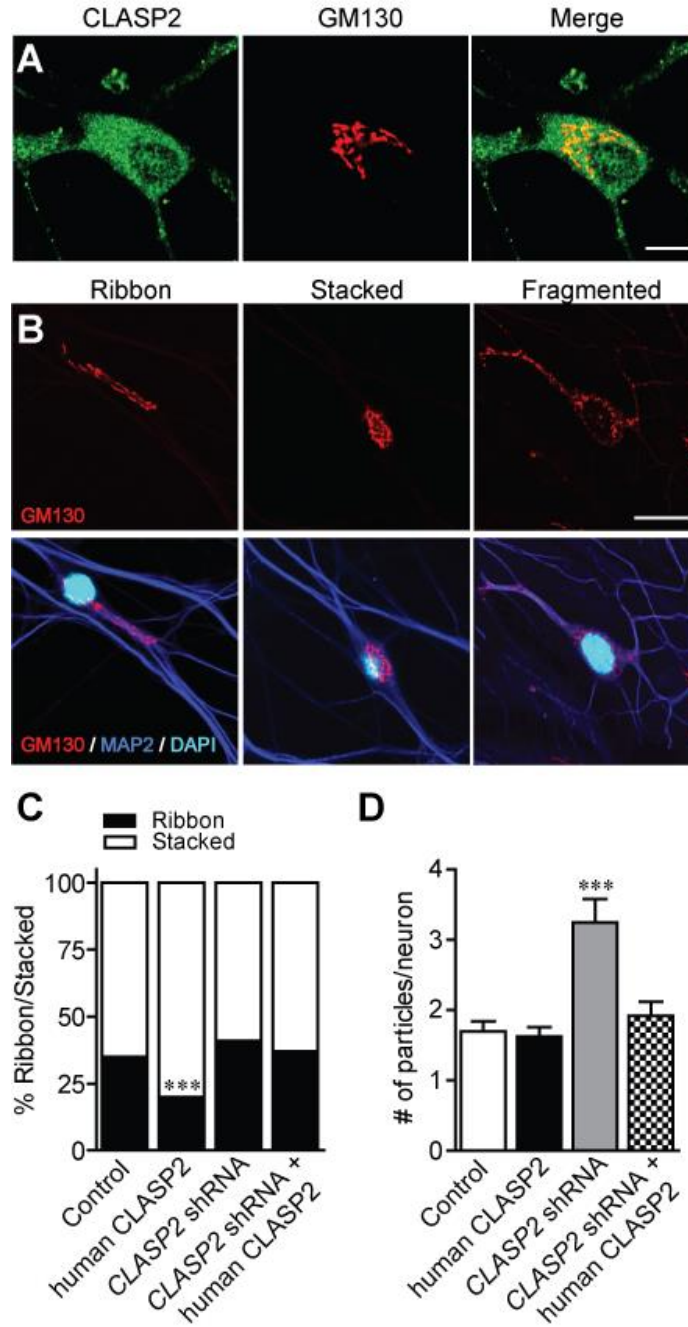


Figure 3.4: CLASP2 Regulates Golgi Morphology in Neurons

A, Representative images of anti-CLASP2 (green) and anti-GM130 antibodies (red) showing colocalization of endogenous CLASP2 with Golgi complex in a hippocampal neuron at 5 DIV. **B**, Neurons treated at 1 DIV with control, human CLASP2 or CLASP2 shRNA lentivirus were stained for GM130 (red), MAP2 (cyan) and DAPI (blue) to assess ribbon, stacked and fragmented Golgi morphology in hippocampal neurons at 5 DIV. Scale bar in **A**=1.5 μm , **B**=10 μm . **C**, CLASP2 led to a significant increase in the percentage of neurons with a stacked Golgi phenotype compared with those with a ribbon-shaped Golgi (n=100 for each group; *** p<0.0001). **D**, The Golgi is highly fragmented in CLASP2 knockdown neurons (n=100 for each group; *** p<0.0001).

Josefa M. Sullivan and Greg Dillon performed the ICC and analyzed the pictures used in Figure 3.4.

Figure 3.5

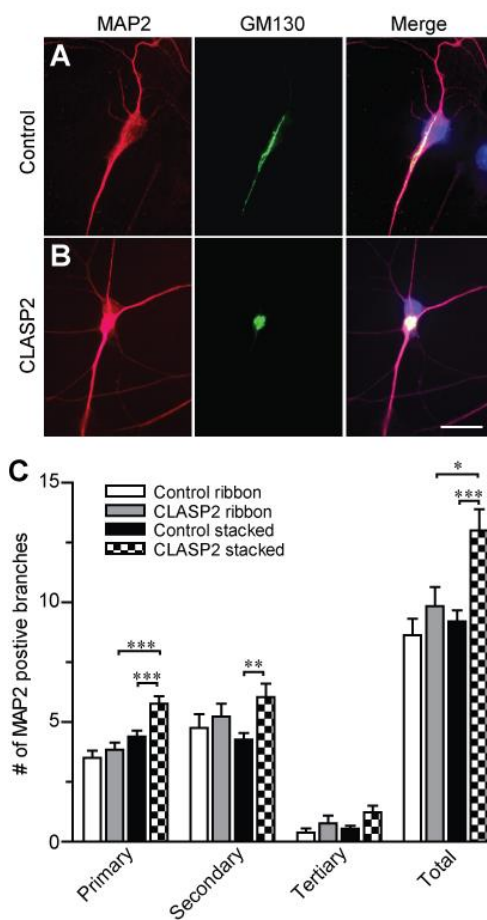


Figure 3.5: CLASP2 Increases Dendritic Branching in Neurons with Stacked but Not Ribbon Golgi Phenotypes

A-B, Primary hippocampal neurons infected at 1 DIV with control or CLASP2 were fixed at 4 DIV and immunostained for MAP2 (red) and GM130 (green). Scale bar=23 μ m. **C**, All primary, secondary, tertiary and total number of MAP2 positive branches were counted and separated by treatment and Golgi phenotype. (n>13 for each group; * p=0.029, ** p=0.004, *** p<0.0009).

Josefa M. Sullivan, performed the ICC and analyzed the pictures used in Figure 3.5.

Figure 3.6

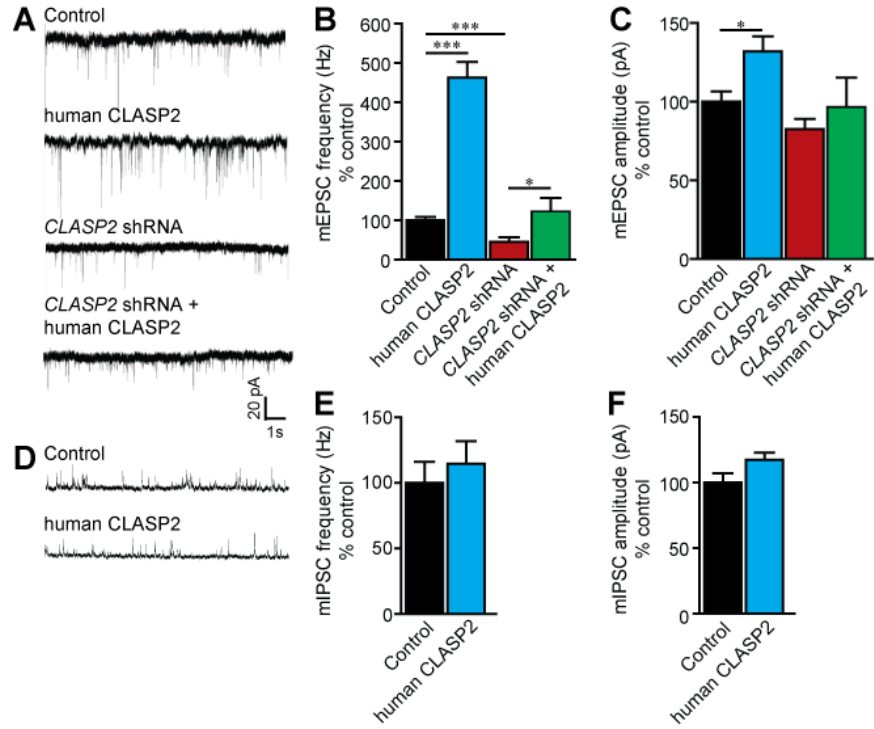


Figure 3.6: CLASP2 Increases Spontaneous Synaptic Activity at Excitatory but Not Inhibitory Synapses

A, Sample traces showing miniature excitatory postsynaptic currents (mEPSC) of control, human CLASP2, CLASP2 shRNA or CLASP2 shRNA coexpressing human CLASP2 at 14-17 DIV. **B**, Bar graph of mEPSC frequency revealed a significant 4.6-fold increase in miniature frequency in neurons infected with human CLASP2 compared to control (n>14 for each group; * p<0.05, *** p<0.0001). **C**, Bar graph of mEPSC amplitude demonstrating a significant increase in mEPSC amplitude in neurons infected with human CLASP2 (n>14 for each group; * p<0.05). **D**, Sample traces showing miniature inhibitory postsynaptic currents (mIPSC) of control and overexpressed human CLASP2. **E**, No changes in mIPSC frequency were detected in neurons infected with human CLASP2 compared to control (n>10 for each group). **F**, Bar graph of mIPSC amplitude showed no changes in miniature amplitude in neurons infected with human CLASP2 (n>10 for each group)

Greg Dillon and JP Gilbert performed electrophysiological recordings and analyzed the data used for Figure 3.6.

Figure 3.7

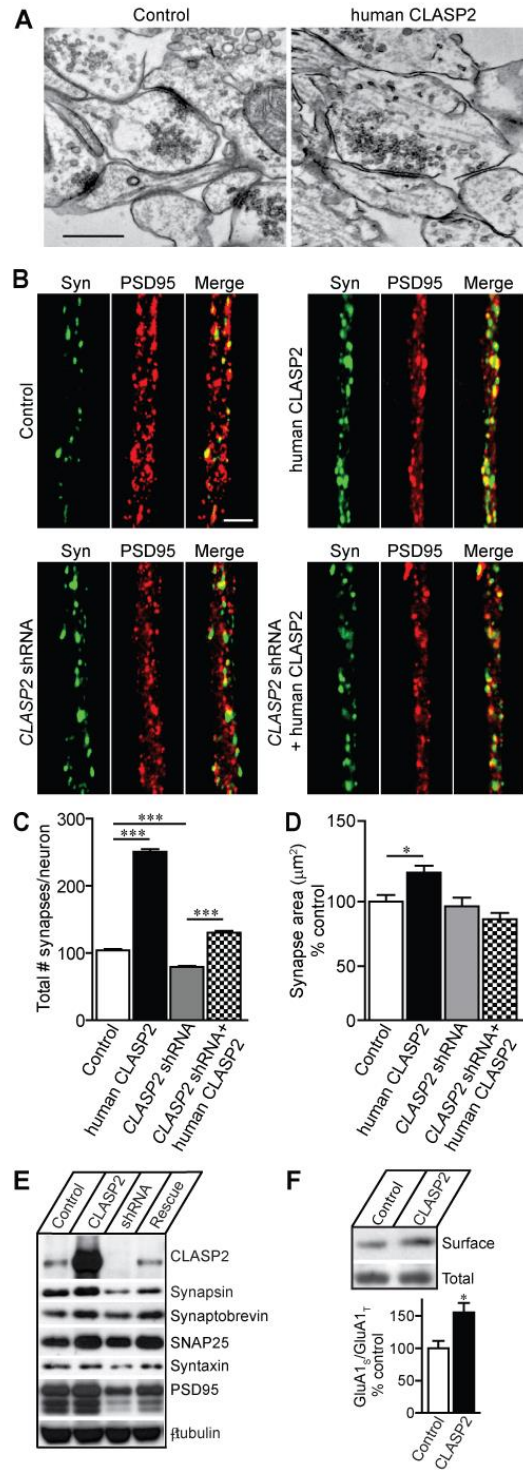


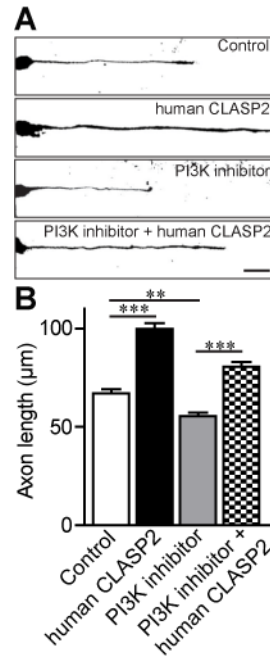
Figure 3.7: CLASP2 Regulates Synaptic Structure and Synaptic Protein Levels

A, Ultrastructural analysis by electron microscopy of synaptic structure in hippocampal neuronal cultures infected with control and overexpressed human CLASP2 at 14 DIV. Representative images of asymmetric excitatory synapses of control and CLASP2 infected neurons. Scale bar=500 nm. **B**, Hippocampal neuronal processes infected with control, human CLASP2, CLASP2 shRNA or CLASP2 shRNA coexpressing human CLASP2 at 14 DIV stained with synapsin (Syn, green) and PSD95 (red). Scale bar=4 μ m. **C-D**, CLASP2 increases overall synapse number and area of colocalization of synapsin and PSD95 in neuronal processes at 14 DIV (* $p < 0.05$, *** $p < 0.0001$). **E**, Western blotting of CLASP2, various synaptic markers and β -tubulin in response to control, human CLASP2, CLASP2 shRNA or CLASP2 shRNA coexpressing human CLASP2 (rescue) in cortical neurons. **F**, We detected a significant increase of surface (S) compared to total (T) endogenous GluA1 receptor subunit in cultured cortical neurons that overexpressed CLASP2 at 14 DIV using a biotinylation assay (left, immunoblot; right, quantification). Total GluA1 levels were determined from input lysates whereas surface GluA1 was determined after elution from neutravidin precipitation (* $p = 0.04$).

Josefa M. Sullivan performed the ICC and analyzed the pictures for Figure 3.7B-D.

Greg Dillon analyzed the electron microscopy pictures used for Figure 3.7A and Table 3.1. and performed the western blot for Figure 3.7E.

Angela Ho performed the biotinylation assay used for Figure 3.7F.

Figure 3.8**Figure 3.8: CLASP2 is Required for PI3K-Induced Axon Elongation**

A, Hippocampal neurons infected at 1 DIV with control, human CLASP2 or treated with PI3K inhibitor LY 294002 were fixed at 2 DIV and stained with SMI-312 (axonal marker). Scale bar=20 µm. **B**, Quantitative analysis showed that overexpressed human CLASP2 significantly increased axon length at 2 DIV and rescued the axonal growth defect in neurons treated with LY 294002 (n=47 neurons for each group; ** p<0.01, *** p<0.001).

Josefa M. Sullivan performed the ICC and analyzed the pictures for Figure 3.8

Table 3.1: Quantitative Ultrastructural Analysis of Asymmetric Neuronal Synapses

Parameter	Control	CLASP2	<i>p</i> value
Presynaptic terminal area (μm^2)	2.13 \pm 0.23	2.82 \pm 0.29	<i>p</i> = 0.074
Presynaptic terminal circumference (μm)	2.61 \pm 0.15	3.34 \pm 0.23	<i>p</i> = 0.012*
Length of Postsynaptic density (μm)	0.33 \pm 0.04	0.42 \pm 0.06	<i>p</i> = 0.187
Docked vesicles per active zone	1.86 \pm 0.36	1.94 \pm 0.37	<i>p</i> = 0.882
Vesicles 150 nm of the active zone	10.07 \pm 0.9	8.64 \pm 0.80	<i>p</i> = 0.241
Vesicles per terminal	57.97 \pm 5.5	48.18 \pm 4.7	<i>p</i> = 0.180
Vesicle density	4.71 \pm 0.89	8.12 \pm 1.60	<i>p</i> = 0.073
<i>All data are presented as means \pm SEM. Control, n = 29; CLASP2, n = 33.</i>			
<i>*Indicates significance</i>			

CHAPTER 4:
PHOSPHORYLATION OF CLASP2 CONTROLS DAB1 SIGNALING
NECESSARY FOR PROPER NEURON MIGRATION

The studies presented in this chapter include contributions from additional post-doctorate, graduate, and undergraduate students. Dr. Tarik Haydar, Dr. Bill Tyler, Dr. Uwe Beffert and Dr. Angela Ho were instrumental in helping to design most of the experiments. Undergraduates John A. Kambouris, Elias Fong, Alicia Dupre, Kirsten Kuhn, and Christine Learned performed immunocytochemistry, acquired fluorescent microscope images, and analyzed the data which has been incorporated into Figures 4.3-4.7. Kerilyn Omuro performed qPCR for Figure 4.2 and measured the length of the apical process for Figure 4.10. Special thanks to Dr. Bill Tyler who performed most of the *in utero* electroporation surgeries used for this chapter.

4.1 Introduction

The complex architecture of the brain requires precise control over the timing of neuron proliferation, differentiation, and migration. The mammalian cortex is distinguished by its six major cell layers each with distinct morphological and functional identities.

Cortical layers normally form in an “inside-out” pattern with early-born neurons forming deeper layers and later-born neurons migrating past them to form more superficial layers of the cortical plate (Rakic 1974). In particular, the Reelin signaling pathway plays a crucial role in correct cortical lamination. Reelin is a large secreted glycoprotein that exerts its function by binding to the lipoprotein receptors ApoER2 and VLDLR and inducing tyrosine phosphorylation of the intracellular adaptor protein Dab1 (Howell et al., 2000; Bock and Herz, 2003). Phosphorylation of Dab1 recruits downstream signaling molecules to promote the cytoskeletal changes necessary for neuronal migration, final positioning, and morphology (D'Arcangelo 2005). Mutations of Reelin, the dual ApoER2/VLDLR receptor, or Dab1 leads to an inversion of the normal inside-out pattern of cortex development (D'Arcangelo et al., 1995; Howell et al., 1997; Trommsdorff et al., 1999). In addition, a number of mutations in cytoskeletal-encoded genes produce deficits in neuron migration and cortical lamination phenotypically similar to Reelin mutants. For example, human mutations in lissencephaly-1, doublecortin, and tubulin, each integral components of the microtubule cytoskeleton, cause severe cortical lamination defects with later born neurons failing to migrate past previously born neurons (Gleeson et al., 1998; Romaniello et al., 2015). The culmination of these genetic studies indicates that several signaling pathways, including the Reelin pathway, converge on downstream

cytoskeletal proteins to affect proper neuronal migration and brain development.

However, little is known about the relationship between Reelin signaling and the control of cytoskeletal dynamics.

CLASPs (cytoplasmic linker associated proteins) belong to a heterogeneous family of plus-end tracking proteins (+TIPs) that specifically accumulate at the growth cone and this localization strategically places them in a position to control neurite growth, directionality, and the crosstalk between microtubules and the actin cytoskeleton.

Previous evidence suggests that CLASPs accumulate asymmetrically towards the leading edges of migrating fibroblasts indicating a role for CLASPs in cell polarity (Akhmanova et al., 2005; Wittmann and Waterman-Storer, 2005). We have demonstrated that CLASP2 protein levels steadily increase throughout neuronal development and are specifically enriched at the growth cones of extending neurites. The short-hairpin RNA (shRNA) mediated knockdown of CLASP2 in primary mouse neurons decreases neurite length, whereas overexpression of human CLASP2 caused the formation of multiple axons, enhanced dendritic branching, and resulted in Golgi condensation (Beffert et al., 2012). These results implicate a role for CLASP2 in neuronal morphogenesis and polarization; however, the *in vivo* function of CLASP2 during brain development is unknown.

Here we demonstrate that CLASP2 is a genetic modifier of the Reelin signaling pathway using microarray gene expression comparison between Reelin, the double ApoER2/VLDLR receptor or Dab1 mutant phenotypes. We found that downregulation of CLASP2 in migrating neurons within the cortical plate leads to mislocalized cells at deeper layers, abnormal spatial positioning of the centrosome-Golgi complex, and

aberrant orientation of the apical dendrite away from the pial surface. In addition, CLASP2 knockdown in the ventricular zone disrupts cell cycle exit and increases the percentage of neural progenitor cells. We identify an interaction between Dab1 and CLASP2 and found that the serine/arginine rich domain of CLASP2, was essential for binding to Dab1. In addition, we found that GSK3 β -mediated phosphorylation of CLASP2 controls Dab1 binding and is required for regulating CLASP2 effects on neuron morphology and migration. Thus, CLASP2 is an essential modifier of the cytoskeleton in response to the Reelin signaling pathway that is necessary for cortical lamination.

4.2 Results

4.2.1 CLASP2 Expression is Developmentally Regulated and Associated with the Reelin Signaling Pathway.

In an effort to identify novel genes downstream of Reelin signaling, we took advantage of genetic mouse models available for the Reelin pathway. We examined expression of mRNA transcripts by microarray between adult brain cortices from mice deficient in Reelin, the double ApoER2/VLDLR receptor mutant, or Dab1, and compared Affymetrix gene expression profiles against age-matched, wild-type mice. Importantly, all three of these mouse models present an identical phenotype that includes severe neuronal migration defects (D'Arcangelo et al., 1995; Howell et al., 1997; Trommsdorff et al., 1999). We then used systems analysis (Ingenuity Systems) to define a large biological network of genes perturbed above a threshold of 1.5 fold in response to deficient Reelin signaling. Our initial screen identified 832 genes up-regulated and 628 genes down-regulated that were common to all three mouse models (Figure 4.1A). Ingenuity Pathway

Analysis identified a set of genes forming a network functionally related to cytoskeleton organization, microtubule dynamics, development/proliferation of neurons, and cell migration (Figure 4.1B). In addition, this network was enriched in genes previously implicated in neuronal migration and intellectual disability phenotypes. One of the handful of cytoskeletal candidate gene identified is the microtubule plus-end tracking protein, CLASP2. Specifically, CLASP2 mRNA expression is increased in all three Reelin mutant phenotypes whereas we did not find any changes in CLASP1 mRNA expression (Figure 4.1B). Consistent with the microarray data, CLASP2 protein levels were 2.8-fold higher in Dab1 knockout mice (Figure 4.1C). These finding suggests that Reelin signaling exerts transcriptional control over CLASP2 mRNA levels and in addition, this lead to translational changes in CLASP2 protein expression. Together these results establish the first molecular link that CLASP2 functions downstream of extracellular Reelin signaling.

4.2.2 Differential Expression of CLASP2 Isoforms During Mouse Cortical Development.

CLASPs represent a unique family of microtubule-associated proteins conserved across yeast, plants, insects and mammals (Lee et al., 2004; Bratman and Chang, 2008; Ambrose et al., 2007). CLASP2 is predominantly expressed in the nervous system in two distinct isoforms, CLASP2 α and CLASP2 γ (Akhmanova et al., 2001). These CLASP2 isoforms share all known protein interaction domains differing only at the N-terminus where the longer CLASP2 α contains an additional dis1/TOG domain previously shown to regulate mitotic spindle assembly, actin binding, and tubulin polymerization (Figure 4.2A)

(Tsvetkov and Popov, 2007; Patel and Heald, 2012). To examine CLASP2 α and CLASP2 γ expression levels during brain development, we performed quantitative PCR on mouse, cortical brain lysates across a range of developmental timepoints. We found that CLASP2 α mRNA is elevated at embryonic stages as early as embryonic day 12.5 (E12.5) while CLASP2 γ mRNA remain relatively stable throughout development relative to the adult (Figure 4.2B). In addition, *in situ* hybridization analysis using an antisense probe to the CLASP2 α mRNA revealed CLASP2 α is preferentially expressed in the ventricular zone (VZ) and intermediate zone (IZ) of the developing cortex at E16.5 (Figure 4.2C). An antisense probe to the CLASP2 γ mRNA revealed that CLASP2 γ is highly expressed across the entire cortex (Figure 4.2C). These results suggest that CLASP2 α and γ isoforms are differentially regulated during cortical development.

4.2.3 CLASP2 is Necessary for Proper Neuron Migration During Corticogenesis.

During brain development, the Reelin signaling pathway is necessary for the formation of laminated structures. In the current study we have shown that Reelin signaling regulates CLASP2 expression. To further investigate the role of CLASP2 in neuronal migration, we introduced previously characterized GFP-CLASP2 shRNA constructs (Beffert et al., 2012) into E14.5 mouse embryos by *in utero* electroporation. For quantitative analysis, the distribution of GFP-positive cells were analyzed for cortical position at E16.5, P0 and P14. At E16.5, the majority of GFP-positive neurons in control brains were mainly found in the VZ and IZ (Figure 4.3A). However, there were obvious differences in spatial distribution in CLASP2-mediated knockdown neurons with a greater percentage of transfected cells located in the VZ compared to control (Figure 4.3A). At P0, most of the

control GFP-positive neurons had migrated into the cortical plate region whereas cells electroporated with CLASP2 shRNA remained in the IZ with a smaller percentage of neurons in the upper cortical plate (upCP; Figure 4.3B). By P14, we found ~100% of control neurons have migrated within the upCP to their final positions at layer II/III; however, CLASP2 knockdown neurons were found in the lower cortical plate (loCP) suggesting that CLASP2 downregulation caused a delay in neuronal migration but did not permanently restrict cells to the IZ (Figure 4.4A).

We next analyzed the molecular profile at P14, a stage at which neuronal migration is complete. As expected, we found that the majority of control GFP-positive neurons electroporated at E14.5 were located in layers II/III and expressed the characteristic CDP (CCAAT displacement protein) molecular marker (data not shown). Interestingly, we found that CLASP2 knockdown neurons also expressed CDP marker suggesting that the mislocalized neurons in the loCP were not reprogrammed prior to migration to reside at deeper cortical positions (Figure 4.4B). We next sought to determine the effect of CLASP2 on the post-migratory differentiation *in vivo*. In the upCP of the *in utero* electroporated brains, the CLASP2 knockdown neurons had significantly more primary processes as compared to controls (Figure 4.4C-D). The phenotype was not exclusive to upper-layer neurons, CLASP2 down regulation also impaired the number of primary processes in the mislocalized neurons in the loCP suggesting that the effect of CLASP2 on neuron morphology was cell autonomous and not the result of mislocalization within the cortical plate.

To determine whether CLASP2 overexpression alters neuronal migration, we performed *in utero* electroporation at E14.5 with a control or CLASP2 α full-length expression vector. At P0, overexpression of CLASP2 α caused an increase in the number of GFP-positive neurons in the IZ and a smaller percentage of neurons which had entered the upCP compared to control (Figure 4.5), a phenotype similar to that seen following CLASP2 knockdown. Together these results suggest that CLASP2 expression is tightly regulated and is critical to ensure proper neuronal migration during cortical lamination.

4.2.4 CLASP2 is Required for the Extension and Orientation of the Leading Process of Migrating Neurons

Since CLASP2 has been shown to regulate neurite length and dendritic arborization in mouse primary neurons (Beffert et al., 2012), we reasoned that CLASP2 might similarly affect the morphology of migrating neurons. Migrating neurons are highly polarized in the direction of their movement and this is achieved through the correct orientation and remodeling of a leading process which acts to guide cell movement. We therefore measured the length and orientation of the leading process in control and CLASP2 knockdown neurons electroporated at E14.5 and analyzed at P0. Our results demonstrate that CLASP2 knockdown neurons retracted their leading processes causing a 48% decrease in the length of the leading process when compared to layer-matched controls (Figure 4.5A). In addition, we examined the orientation of the thickest leading process relative to the pial surface to determine each cells likely migratory path. CLASP2 knockdown caused an increase in the angle of the leading process in relation to the pial surface (Figure 4.6B). Specifically, 85% of migrating GFP-positive control neurons had a

leading process that was oriented between 0-10 degrees to the pia (Figure 4.6C). In contrast, only 13% of CLASP2 knockdown neurons kept this normal, apical orientation. In fact, we found nearly 65% of CLASP2 knockdown neurons had a leading process that was oriented between 11-90 degrees and 22% of which had their leading process inverted between 91-180 degrees. Alterations of the leading process in CLASP2 knockdown neurons were not due to disruptions of the radial morphology of nestin-positive radial glial cell fibers (Figure 4.8A-B), suggesting that CLASP2 plays an intrinsic role in regulating both the length and orientation of the leading process of migrating cortical projection neurons.

4.2.5 CLASP2 Controls the Spatial Positioning of the Centrosome and Golgi Complex.

To examine whether nucleus-centrosome coupling is disrupted by CLASP2 knockdown, we electroporated E14.5 embryos with control or CLASP2 shRNA and analyzed the distance between the nucleus and centrosome in migrating neurons within the cortical plate at P0. Nearly 80% of the control GFP-positive neurons displayed one or a pair of closely juxtaposed centrioles, that were immunostained with pericentrin, positioned at the apical side of the nucleus toward the leading process. In contrast, nearly 60% of CLASP2 knockdown neurons had pericentrin immunostaining adjacent to the nucleus (Figure 4.7A). In addition, control cells had a substantial distance between the centrosome and nucleus ($7.9 \pm 0.78 \mu\text{m}$), while the CLASP2 knockdown neurons had the centrosome very close to the nucleus ($3.9 \pm 0.74 \mu\text{m}$) (Figure 4.7A).

Since live cell imaging indicates that movement of the centrosome and the Golgi apparatus into the leading neurite can precede cell movement in the developing brain (Yanagida et al., 2012; Sakakibara et al., 2013) and that localization of the centrosome/Golgi complex is a key step in selecting migratory direction (Yanagida et al., 2012), we examined the positioning and shape of the Golgi apparatus. Embryos were electroporated at E14.5 with control or CLASP2 shRNA and immunostained with the Golgi marker GM130 at P0. We found that the majority of GM130 immunostaining in control GFP-positive neurons was localized in the leading process whereas there was differences in spatial positioning of GM130 immunostaining distributed near the cell body, in CLASP2 knockdown neurons (Figure 4.7C). In addition, we found that while control GFP-positive neurons favored a Golgi-ribbon phenotype, CLASP2 knockdown neurons favored a Golgi-stacked phenotype (Figure 4.7D). These observations suggest that CLASP2 plays an important role in spatial positioning of the centrosome and Golgi complex into the leading process that is necessary for proper nucleokinesis of migrating neurons.

4.2.6 CLASP2 is Necessary for Regulating Proliferative Cells in the Ventricular Zone

To investigate whether the migratory defects following CLASP2 knockdown could be attributed to perturbations in specific populations of neural progenitors, we electroporated E14.5 with control or CLASP2 shRNA plasmids and labeled apical and basal progenitors with antibodies against transcriptional factors Sox2 and Tbr2, respectively. Sox2⁺ progenitors, primarily consist of multi-potent radial glial cells and short-neural precursors

(SNPs) located in the VZ (peak at bin areas 1-2; Figure 4.9A) (Anthony et al., 2004; Malatesta et al., 2003; Stancik et al., 2010). In addition, radial glial cells are capable of generating a second, transient neural progenitor population, the basal (or intermediate) Tbr⁺ progenitor cells, which reside predominantly in the subventricular zone (peak at bin areas 2-4) and whose divisions are mostly neurogenic (Figure 4.9B) (Haubensak et al., 2004). We found a significant increase in the percentage of apical Sox2⁺ and basal Tbr2⁺ progenitor cells following CLASP2 knockdown indicating that CLASP2 is likely affecting terminal cell division and differentiation (Figure 4.9A and 4.9B).

4.2.7 CLASP2 Regulates Progenitor Cell Cycle Dynamics.

Because CLASP2 knockdown caused an increase in the percentage of progenitor cells, we postulated that CLASP2 could be directly controlling cell division in the developing cortex. To test this possibility, we electroporated at E14.5 and labeled cells in the M-phase of the cell cycle with an antibody against phospho-Histone H3 (PH3) at E16.5. Indeed, there was a greater percentage of GFP-positive CLASP2 knockdown neurons co-localized with PH3. These results indicate that CLASP2 could be prolonging the cell cycle or preventing terminal differentiation thereby maintaining progenitors in a proliferative state (Figure 4.10A).

In addition, CLASP2 knockdown neurons showed defects in the mitotic spindle orientation of glial progenitor cells. Pericentrin staining of dividing PH3⁺ progenitors showed that CLASP2 knockdown resulted in an increase in the angle of the mitotic spindle relative to the ventricular surface and higher distribution of cells with a planar/vertical cleavage plane (commonly associated with “symmetric” cell divisions

where one progenitor generates two proliferative daughter cells; Figure 4.10C) (Chen and McConnell, 1995).

We also evaluated the interkinetic nuclear migration of radial glia and SNPs which consists of a slow G1 phase migration in the basal direction and a fast G2 phase migration in the apical direction, both of which occur during a single cell cycle (Matsuzaki and Shitamukai, 2015). Since interkinetic nuclear migration arises from the restriction of mitosis to the apical surface where the centrosome attaches, the position of the nucleus relative to pericentrin staining was measured. We found that CLASP2 knockdown resulted in significantly shorter apical processes (Figure 4.10D) indicating that the increase in the number of PH3⁺ mitotic cells following CLASP2 knockdown correlated with a higher percentage of progenitors at the apical ventricular surface.

4.2.8 CLASP2 Knockdown Delays Differentiation.

To determine whether the effects of CLASP2 on cell division were due to changes in cell fate or cell cycle dynamics, we electroporated at E14.5 and pulse labeled by EdU injection into pregnant dams at E15.5. We then analyzed brain sections at E16.5 by double staining with EdU and Ki67 antibodies. Since Ki67 labels a nuclear transcriptional factor expressed from S phase through M phase, EdU and Ki67 double-positive cells represent progenitors that remain in the cell cycle, whereas EdU-positive/Ki67-negative cells represent progenitors which have exited the cell cycle in the 24 hour period following EdU injection. CLASP2 knockdown resulted in an increase in the percentage of electroporated cells that were positive for EdU (Figure 4.11C) and Ki67 (Figure 4.11D) located in the VZ (bin area 1). We also found that the fraction of

EdU⁺/Ki67⁻ is significantly lower in CLASP2 knockout cells suggesting that CLASP2 knockdown disrupts cell migration by delaying terminal division (Figure 4.11F).

4.2.9 GSK3 β Phosphorylation of CLASP2 Regulates Binding to Dab1.

The molecular mechanism by which Reelin signaling regulates CLASP2 expression and function is unknown. We hypothesize that the CLASP2-mediated effects on neuronal development are dependent on an interaction between Dab1 and CLASP2 and/or activated through Dab1-dependent phosphorylation signaling pathways. To investigate whether CLASP2 interacts with Dab1, we co-transfected Dab1 with GFP-CLASP1 or GFP-CLASP2 α in HEK293T cells and performed immunoprecipitation assays. Both CLASP1 and CLASP2 co-immunoprecipitated with Dab1 (Figure 4.12B). In particular, the N-terminal portion of CLASP2 (1-820 amino acids) selectively co-immunoprecipitated with Dab1 (Figure 4.12B). To further characterize the CLASP2-Dab1 interaction, we generated five additional GFP-CLASP2 fragments that contained the first TOG1 domain (1-270 amino acids), TOG2 domain (271-573 amino acids), positively-charged serine/arginine rich region (S/R rich, 574-820 amino acids), TOG3 domain (821-1200 amino acids) or the C-terminal CLIP domain (1200-1515 amino acids) (Figure 4.12A). We co-transfected Dab1 with each of the GFP-CLASP2 fragments in HEK293T cells and immunoprecipitated with GFP. We observed that the S/R rich domain of CLASP2 specifically co-immunoprecipitated with Dab1 (Figure 4.12C). Interestingly, embedded in the S/R rich region are nine serine residues constituting GSK3 β phosphorylation consensus motifs which have previously been shown to disrupt the electrostatic bonds between CLASP2 and microtubules preventing plus-end tracking

(Watanabe and Kaibuchi 2009; Kumar and Wittmann, 2012). To determine whether GSK3 β -mediated phosphorylation of CLASP2 affects Dab1 binding, we produced GFP-CLASP2 phospho-mutants that mimic a constitutively active phosphorylated state where eight serine residues in the S/R domain of CLASP2 were replaced with aspartate (GFP-CLASP2-8S/D) or a non-phosphorylatable CLASP2 mutant (GFP-CLASP2-9S/A) where all nine serine residues were replaced with alanines. When HEK293T cells were co-transfected with Dab1 and GFP-CLASP2 phospho-mutants, we found that both GFP-CLASP2 wild type and phospho-resistant GFP-CLASP2-9S/A co-immunoprecipitated with Dab1 whereas the phospho-mimetic GFP-CLASP2-8S/D greatly reduces its binding to Dab1. These results indicate that phosphorylation of CLASP2 can alter Dab1 binding affinity (Figure 4.13A-B). We also tested whether the presence of GSK3 β could alter CLASP2-Dab1 binding by co-transfecting GFP-CLASP2, Dab1 and a constitutively active GSK3 β in HEK293T cells. GSK3 β expression completely disrupted the CLASP2-Dab1 interaction (Figure 4.13C). Since Reelin exerts its function by binding to the lipoprotein receptors ApoER2 and VLDLR and inducing tyrosine phosphorylation of the intracellular adaptor protein Dab1 by src family kinases (Howell et al., 2000; Bock and Herz, 2003), we wanted to determine whether src-mediated phosphorylation of Dab1 could affect its binding to CLASP2. Surprisingly, the addition of src had no effect on the CLASP-Dab1 interaction indicating that the phosphorylation state of Dab1 is not relevant to its association with CLASP2 (Figure 4.13D).

4.2.10 GSK3 β Phosphorylation of CLASP2 Controls Cell Motility and Neurite

Extension

To determine whether GSK3 β phosphorylation of CLASP2 affects its function, we compared aggregates of primary cortical neurons infected at day of plating with control shRNA, CLASP2 shRNA, and CLASP2 shRNA rescued with human CLASP2 wild type, phospho-resistant CLASP2-9S/A, or phospho-mimetic CLASP2-8S/D lentivirus. Cortical neurons isolated from newborn pups were dissociated and allowed to form aggregates by incubating in a polypropylene tube before plating on matrigel-coated coverglass. Cell migration was assessed by measuring the area of migration away from the initial aggregates at day of plating using live imaging over a 48 hour period (Figure 4.14A). The shRNA-mediated knockdown of CLASP2 decreased cell migration compared to control (Figure 4.14B). In addition, both CLASP2 wild type and phospho-resistant CLASP2-9S/A rescued the CLASP2 shRNA phenotype whereas phospho-mimetic CLASP2-8S/D had no effect indicating that GSK3 β -mediated CLASP2 phosphorylation alters cell motility (Figure 4.14C-D).

Since neuron movement requires extension of a leading process to provide traction forces and influence directionality, we also evaluated whether GSK3 β phosphorylation of CLASP2 affects neurite extension. We compared primary cortical neurons co-infected at day of plating with control shRNA, CLASP2 shRNA, and CLASP2 shRNA rescued with human CLASP2 wild type, phospho-resistant CLASP2-9S/A, or phospho-mimetic CLASP2-8S/D mutants for axon growth. At 2 days *in vitro*, quantitative analysis showed that CLASP2 knockdown resulted in a 27% decrease in

axon length as indicated by tau immunofluorescence (Figure 4.15A-B). Both CLASP2 wild type and phospho-resistant CLASP2-9S/A rescued the CLASP2 shRNA phenotype whereas phospho-mimetic CLASP2-8S/D had no effect (Figure 4.15A-B). These results suggest that GSK3 β phosphorylation of CLASP2 plays an important role controlling cell motility and neurite extension.

4.3 Discussion

Normal brain function is dependent on the correct positioning and connectivity of neurons established during development. In particular, the Reelin pathway plays a crucial role in cortical lamination and mutations in genes associated with Reelin signaling lead to profound defects in neuronal positioning during brain development in both mice and humans. However, the molecular mechanisms by which Reelin controls neuronal morphology and movement are poorly understood. We have used a systems analysis approach to identify genes perturbed in the Reelin signaling pathway and identified microtubule stabilizing CLIP-associated protein 2 (CLASP2) as a key cytoskeletal modifier of Reelin mutant phenotypes; however, currently, little is known about the role of CLASP2 in the developing brain. In the present study, we have characterized the role of CLASP2 during cortical development by *in utero* electroporation of shRNA plasmids and found that silencing CLASP2 in the ventricular zone disrupts cell cycle exit and increases the percentage of both apical and basal progenitors. In addition, we show that down-regulation of CLASP2 in migrating neurons of the cortical plate leads to mislocalized cells at deeper cortical layers, abnormal positioning of the centrosome-Golgi complex, and aberrant length/orientation of the leading process. Moreover, rescue

experiments *in vitro* indicate that GSK3 β -mediated phosphorylation of CLASP2 controls Dab1 binding and is required for regulating CLASP2 effects on neuron morphology and migration.

During brain development, Reelin signaling is necessary for the formation of laminated brain structures, such as the cerebral cortex, hippocampus, and cerebellum (Curran and D'Arcangelo, 1998; Lambert de Rouvroit and Goffinet, 1998). Several cellular processes involved in neuron migration have been attributed to Reelin signaling including: cell translocation (Franco et al., 2011; Sekine et al., 2012), detachment from radial glia fibers (Cooper, 2008), and extension of the leading process (O'Dell et al., 2015). However, the molecular mechanisms connecting Reelin to each of these processes is unclear. The current results provide the first evidence that expression of the +TIP, CLASP2 is regulated by Reelin signaling. CLASP2 mRNA expression was significantly increased in mice deficient for either Reelin, the double ApoER2/VLDLR receptor mutant, or in the knockout of the adaptor protein Dab1 (Figure 4.1B). Interestingly, these mouse models all show similar histological and behavioral phenotypes, suggesting common downstream effectors (Olsen, 2014). In addition, our current data demonstrates that CLASP2 binds directly to Dab1 (Figure 4.12B) and that this binding is regulated by GSK3 β phosphorylation of CLASP2 (Figure 4.13C). Therefore, CLASP2 represents a cytoskeletal effector of the Reelin pathway crucial for normal cortex development.

CLASPs belong to a heterogeneous family of +TIPs which regulate microtubule stability during both interphase and mitosis (Galjart, 2005). In the present study, *in utero* electroporation of CLASP2 shRNA at E14.5 resulted in significant defects in cortical

lamination at both embryonic (E16.5, P0; Figure 4.3) and adult time points (P14, Figure 4.4). Interestingly at P14, neurons electroporated with CLASP2 shRNA demonstrated an un-polarized morphology indicated by the loss of a detectable, apical dendrite and with an overall increase in the number of primary processes regardless of their final cortical position (Figure 4.4E). These results suggest a permanent arrest in the migration of a subset of cortical neurons that is dependent on CLASP2 function. Therefore, rather than slowing the speed of migration, CLASP2 may control intrinsic polarity signals by regulating stability of the cytoskeleton.

Migrating neurons in the cortical plate extend a leading process that is responsible for sampling the microenvironment and provides an anchor point during saltatory movement (Marin et al., 2010). CLASP2 localization at the growth cone places it in a strategic position to regulate neurite outgrowth and the crosstalk between extracellular cues and intracellular polarity signals. Our results demonstrate that in neurons migrating through the cortical plate, CLASP2 regulates both the length (Figure 4.6A) and orientation of the leading process (Figure 4.6 B-C). Compared to controls, migrating neurons electroporated with CLASP2 shRNA had significantly shorter leading processes and the orientation of these neurites was often directed away from the pial surface. The CLASP2 α isoform contains a total of three TOG-like domains which bind soluble tubulin dimers and also interact with the dynamic, actin cytoskeleton at the leading edge (Al-Bassam et al., 2010; Tsvetkov et al., 2007). Therefore, CLASP2 may work to supply extending neurites with a concentration of soluble tubulin, preventing catastrophe events and neurite retraction. Interestingly, pharmacological agents such as nocodazole, which

destabilize the microtubule network have also been shown to shorten the leading process of cortical interneurons during their migration and although these cells show no deficits in migration speed, they frequently change their trajectories and colonize smaller cortical areas (Baudoin et al., 2008). Therefore, CLASP2 may regulate neuron migration by stabilizing the leading process in the correct orientation in order to guide directional movement.

During migration, movement of the microtubule organizing centers (MTOCs, Golgi/centrosome complex) into the leading process provides the traction forces necessary for somal translocation (Marin et al., 2012). In addition, effective extension of the leading process requires polarized secretory trafficking from the Golgi in order to supply new membrane materials to the polymerizing tip (Yadav and Linstedt, 2011). Consequently, efficient cell movement requires both longitudinal microtubules linking the leading edge with MTOCs and a microtubule cage linking the nucleus with the centrosome (Tsai and Gleeson 2005; Vallee et al., 2009). Our results show that electroporation of CLASP2 shRNA caused mislocalization of the centrosome and Golgi away from the leading process closer to the nucleus (Figure 4.7). In addition, CLASP2 knockdown resulted in a loss of Golgi ribbon morphology (Figure 4.7D). Previously, CLASP-dependent nucleation of microtubules at the Golgi has been shown to be required for directional cargo trafficking and the construction of asymmetric microtubule arrays (Miller et al., 2009; Efimov et al., 2007). Therefore, the loss of a polarized Golgi ribbon following CLASP2 knockdown likely prevents directed trafficking to the leading process in migrating neurons. Together, these results suggest that CLASP2 stabilization of

microtubules regulates the positioning of the Golgi and centrosome during cell movement. Further work will be needed to determine whether CLASP2 regulation of Golgi morphology directly influences leading process length and orientation.

CLASP2 is represented by two main isoforms CLASP2 α and CLASP2 γ which differ only at the N-terminus where CLASP2 α contains a 233 amino acid dis1/TOG domain insertion. The current study provides the first evidence demonstrating that expression of the longer CLASP2 α isoform peaks during neurogenesis (Figure 4.2B). In addition, *in situ* hybridization of E16.5 cortical sections indicates an increase in CLASP2 α mRNA in the proliferative ventricular and subventricular zone when compared to post-mitotic neurons of the cortical plate (Figure 4.2C). Together, these data suggest that CLASP2 isoforms may be differentially expressed during the cell cycle and that CLASP2 α may play an important role in cell division. To support this data, we knocked down CLASP2 expression in neural progenitors through *in utero* electroporation of CLASP2 shRNA plasmids at E14.5 and examined the transfected progenitor populations 48 and 72 hours later. Our results show a significant increase in the percentage of apical (Sox2⁺) and basal (Tbr2⁺) progenitors in the CLASP2 shRNA condition when compared to age-matched controls (Figure 4.9). In addition, CLASP2 shRNA caused an increase in the percentage of cells positive for cell division marker PH3 (Figure 4.10) and resulted in a decrease in the percentage of electroporated cells which exited from the cell cycle over a 24 hour period following EdU injection (Figure 4.11). Knockdown of CLASP2 may be increasing the percentage of neural progenitors during development by delaying the terminal differentiation of radial glia cells into neurons.

Inside the cell, Reelin signaling is propagated by stimulating tyrosine phosphorylation of the adapter protein Dab1 (Howell et al., 1999). Our results provide the first evidence that CLASPs can bind to Dab1 (Figure 4.12B) suggesting a mechanism by which extracellular Reelin could regulate CLASP localization and/or expression. In order to determine the domain responsible for CLASP2-Dab1 binding, we generated truncated GFP-CLASP2 constructs using the Eukaryotic Linear Motif (ELM) resource dividing CLASP2 α into five, distinct domains (Figure 4.12A). In particular, ELM was primarily used to identify regions of lowest stability in order to avoid disrupting conserved domains. Our results demonstrate that Dab1 binds CLASP2 specifically between amino acids 574-820, the S/R rich domain (Figure 4.12C). Previous experiments demonstrate that this S/R rich domain is highly conserved across species and is responsible for CLASP-EB1 binding and consequently plus-end tracking (Mimori-Kiyosue et al., 2005). Specifically, the S/R domain contains two EB1, SXIP (Serine -any amino acid- Isoleucine -Proline) binding motifs which are embedded in a positively-charged serine/arginine rich region. Multi-site phosphorylation by GSK3 β near these motifs has been shown to disrupt the electrostatic bonds formed between CLASP2 and the acidic C-terminal tail of tubulin, preventing association of CLASP with microtubules (Wantanabe and Kaibuchi 2009; Kumar and Wittmann, 2012). Our current results indicate that CLASP2-Dab1 binding is also regulated by phosphorylation of CLASP2 at GSK3 β sites within this central domain. Addition of constitutively active GSK3 β resulted in a significant decrease in CLASP2-Dab1 binding (Figure 4.13C) and mimicking CLASP2 phosphorylation with mutations at known GSK3 target motifs (CLASP2 8S/D) prevented the association of CLASP2 and

Dab1 (Figure 4.13A-B). Together, these results show a novel mechanism by which CLASP2 phosphorylation may regulate its function within the cell through Dab1 binding.

CLASP2 binding to Dab1 is regulated by GSK3 β phosphorylation; however, it is not known if GSK3 β -mediated phosphorylation controls the function of CLASP2 on neural development and migration. Previously, our lab has demonstrated that CLASP2 expression levels control neurite outgrowth and arborization in primary neuron cultures and that this effect is dependent on PI3K activity (Beffert et al., 2012). In addition, our current results suggest a link between the role of CLASP2 in leading process dynamics and proper neuron migration. Therefore, we co-infected primary neuron cultures with CLASP2 shRNA and attempted to rescue the deleterious effects with either wild-type or phospho-mutants of CLASP2. As expected, we found that knockdown of CLASP2 causes reductions in neuron migration (Figure 4.14B) and axon length (Figure 4.15B). Interestingly, these deficits could be rescued by co-infection of CLASP2 α wild-type or the phospho-resistant CLASP2 α 9S/A, but not the phospho-mimetic CLASP2 α 8S/D (Figure 4.14D and Figure 4.15A-B) suggesting that GSK3 β phosphorylation of CLASP2 is an important regulator for neuron morphology and migration.

In contrast to most other kinases, GSK3 β activity is high in non-stimulated cells and is inhibited at the leading edge of migrating astrocytes and in the growth cone of extending neurites (Etienne-Manneville and Hall, 2003; Zhou et al., 2004). Previous experiments have demonstrated that activated GSK3 β can cause cortical migration defects, abnormal centrosome positioning, and destabilization of microtubules at the leading process (Asada and Sanada, 2010) all phenotypes similar to those resulting from

Reelin signaling mutants. Furthermore, Reelin signaling has been shown to directly inhibit GSK3 β activity through PI3K and Akt signaling mechanisms (Beffert et al., 2002). Therefore, we propose a model where the localization of CLASP2 at the leading process is regulated by GSK3 β inactivation by Reelin and that CLASP2 enrichment at the leading edge is necessary to stabilize the leading process for correct neuron migration and morphology (Figure 4.16).

Together, these results represent the first demonstration of CLASP2 function in the developing mammalian brain. In the cerebral cortex, defects in neuronal morphogenesis, cell migration, and synaptogenesis can lead to mental retardation, autism spectrum disorders and epilepsy. Therefore, elucidating the pathways which integrate, extracellular cues with cytoskeleton reorganization are essential to understand correct cortical architecture and connectivity.

Figure 4.1

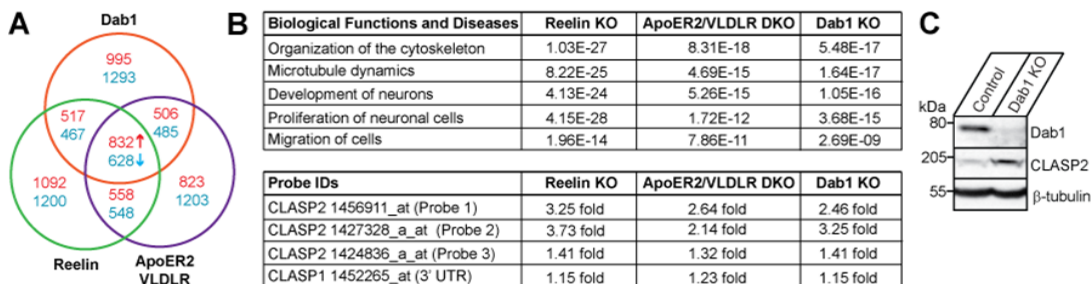


Figure 4.1: CLASP2 Expression is Regulated by the Reelin Signaling Pathway

(A) We examined expression of mRNA transcripts by microarray between adult brain cortices from mice deficient in Reelin, the double ApoER2/VLDLR receptor mutant, or Dab1, and compared Affymetrix gene expression profiles against age-matched, wild-type mice (n= 3 brain samples for each condition). Our initial screen identified 832 genes up-regulated and 628 genes down-regulated that were common to all three mouse models above a threshold of 1.5 fold.

(B) Ingenuity Pathway Analysis identified several gene networks that were impaired across Reelin, the double ApoER2/VLDLR receptor or Dab1 knockout mouse models. CLASP2 mRNA expression is increased in all three Reelin mutant phenotypes whereas we did not find any changes in CLASP1 mRNA expression.

(C) Consistent with the microarray data, CLASP2 protein levels were 2.8-fold higher in Dab1 knockout mice.

Figure 4.2

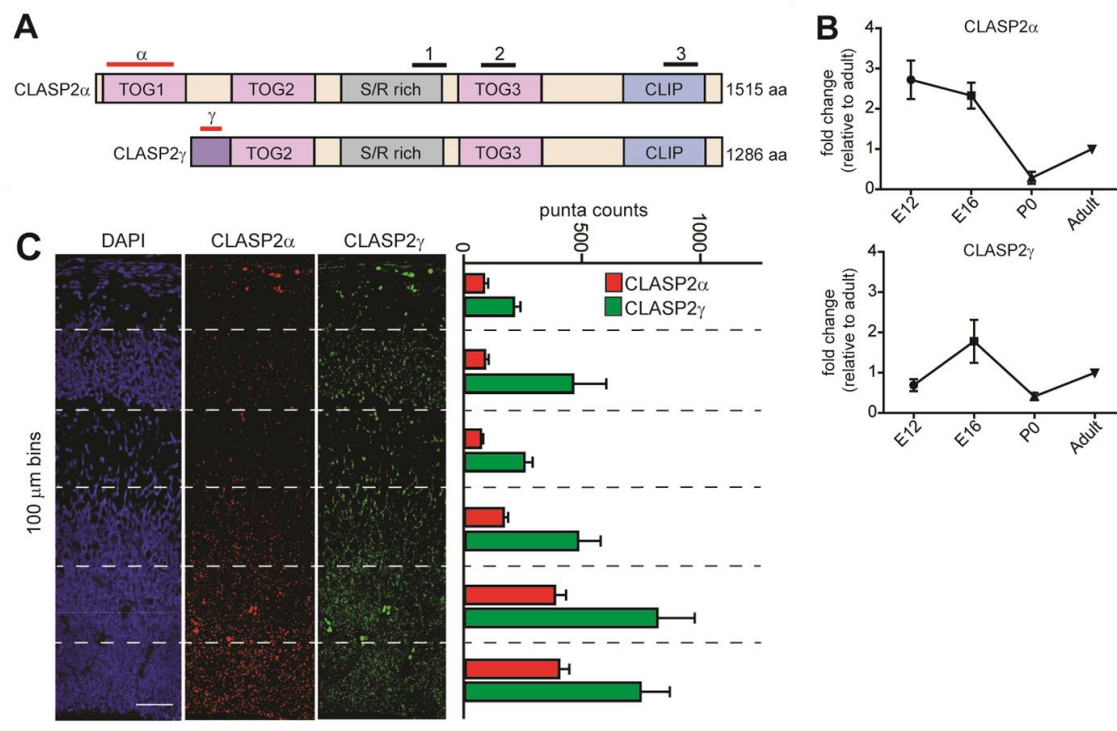


Figure 4.2: Differential Expression of CLASP2 Isoforms during Mouse Cortical Development

(A) Schematic representation of known protein binding domains for human CLASP2 α and γ . Location of the probes used for qPCR, *in situ* hybridization (marked in red) and the three probe IDs for microarray (black) are indicated. Mapping analysis of the CLASP2 protein reveals an N-terminal tumor overexpressed gene (TOG) domains, a repetitive middle region rich in serine, arginine, and proline residues (S/R rich) and a C-terminal region CLIP-170 domain

(B) Fold change of CLASP2 isoforms relative to adult as measured by qPCR from dissociated wild type cortical lysates taken at E12.5, E16.5, P0 and adult. CLASP2 α expression peaks during embryonic stages while the expression of CLASP2 γ remains stable (n=5 brains for each time point)

(C) Representative images of the cortex showing *in situ* hybridization for CLASP2 α and γ isoforms at E16.5. Fluorescent puncta were counted at every 100 μm bins from the ventricle to the pial surface. CLASP2 α expression was highest in the first 200 μm which represents the proliferative ventricular and subventricular zones (n=6 brain sections for each group). Scale bar represents 50 μm .

Figure 4.3

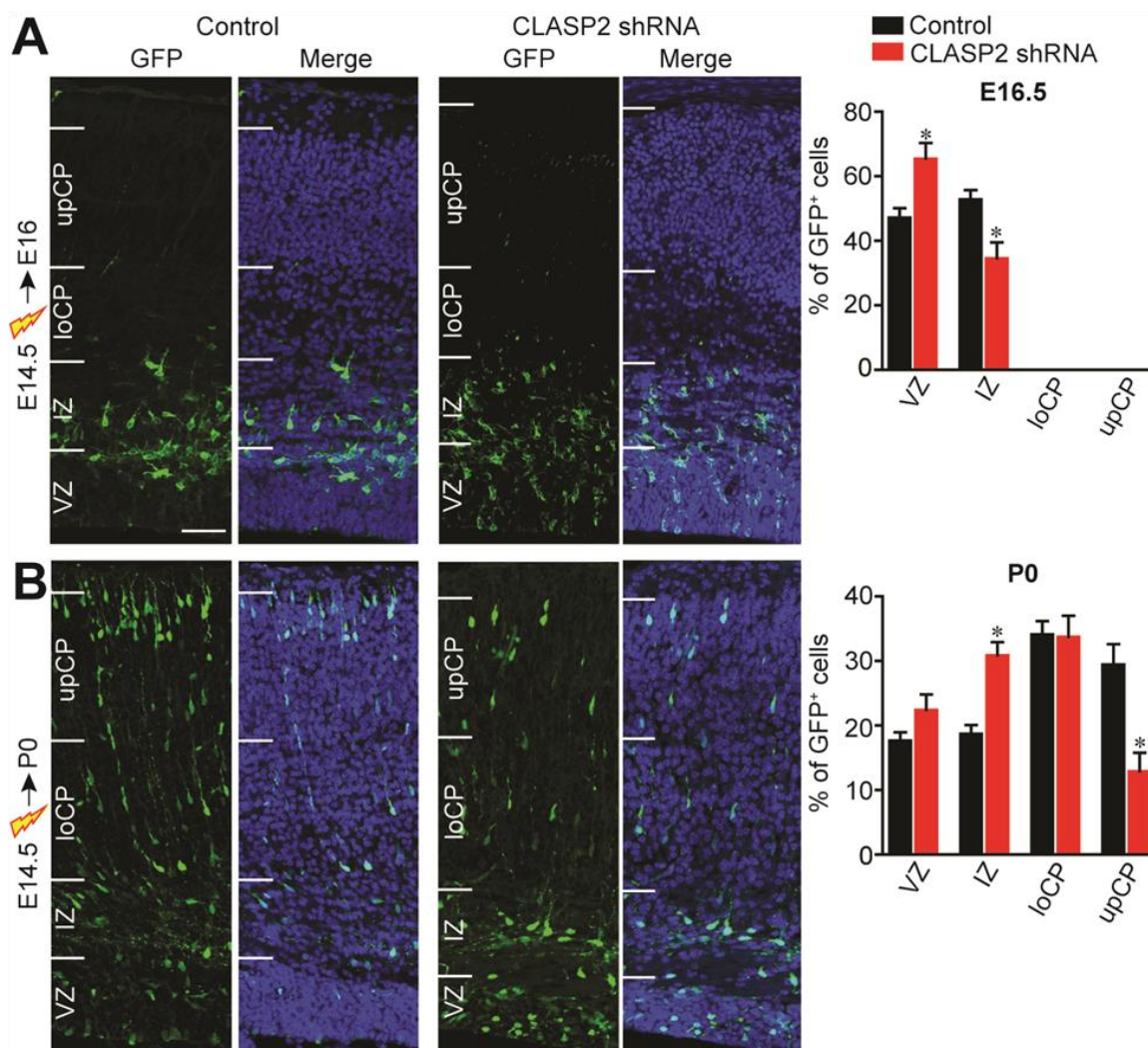


Figure 4.3: CLASP2 is Necessary for Radial Migration of Cortical Projection Neurons

Mouse embryos were electroporated at E14.5 with scrambled control or CLASP2 shRNA. Coronal sections of the cortex were visualized for transfected GFP-positive neurons (green) and cell nuclei (Hoechst 33342, blue) at E16.5 (**A**) and P0 (**B**). White lines indicate the demarcations for different cortical areas (VZ=Ventricular Zone, IZ = Intermediate Zone, loCP = lower cortical plate, upCP = upper cortical plate). The percentage of total transfected cells in each zone are expressed as the mean \pm SEM.

Scale bar represents 50 μ m

(A) At E16.5, CLASP2 shRNA showed higher percentage of cells arrested in the ventricular zone (VZ: $p < 0.001$, IZ: $p < 0.001$; Control n=8 brains, CLASP2 shRNA n=7 brains)

(B) At P0, a higher percentage of control GFP-positive cells have reached the final position in the upper cortical plate (upCP) when compared to CLASP2 shRNA (upCP: $p=0.018$, IZ $p=0.008$; Control n=3 brains; CLASP2 shRNA n=3 brains).

Figure 4.4

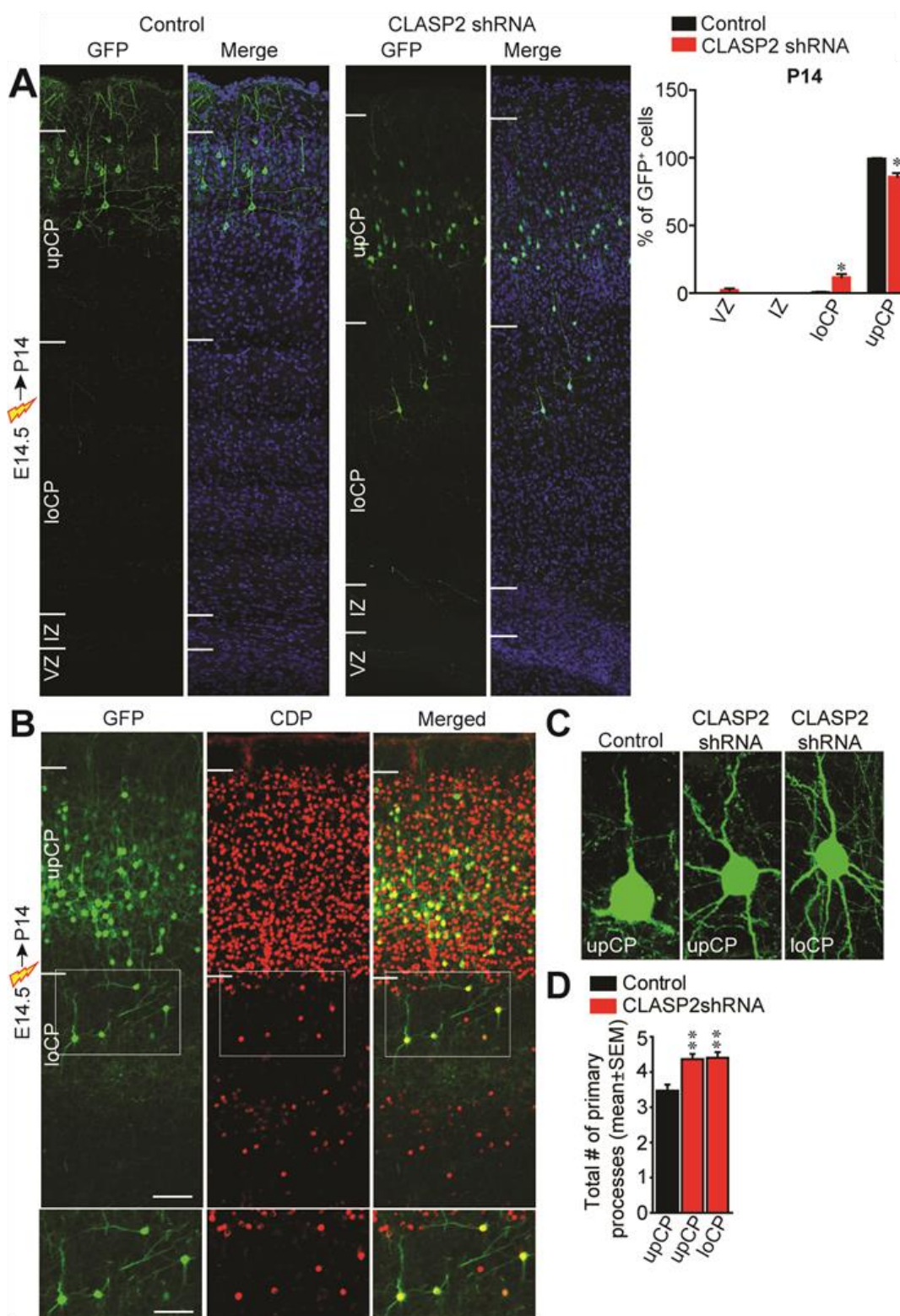


Figure 4.4: CLASP2 Knockdown Affects Neuron Morphology But Not Cell Fate

Mouse embryos were electroporated at E14.5 with scrambled control or CLASP2 shRNA. Coronal sections of the cortex were visualized for transfected GFP-positive neurons (green) and cell nuclei (Hoechst 33342, blue) at P14 (A). White lines indicate the demarcations for different cortical areas (VZ=Ventricular Zone, IZ = Intermediate Zone, loCP = lower cortical plate, upCP = upper cortical plate). The percentage of total transfected cells in each zone are expressed as the mean \pm SEM.

Scale bar represents 50 μ m

(A) CLASP2 knockdown caused a permanent arrest in the migration of \sim 10% of CLASP2 shRNA electroporated neurons at the lower cortical plate (upCP $p=0.004$, loCP $p=0.005$; Control $n=4$ brains, shRNA $n=6$ brains).

(B) Brain sections were immunostained with the layers II/III marker CDP. Mislocalized cells electroporated with CLASP2 shRNA still expressed the layers II/III marker CDP.

(C-D) The number of processes originating from the cell soma was quantified for transfected cells across multiple sections. Knockdown of CLASP2 caused an increase in the number of primary neurites independent of cortical layer (Control $n=53$ cells; CLASP2 shRNA upCP: $p<0.001$, $n=60$ cells, loCP: $p<0.001$, $n=39$ cells).

Figure 4.5

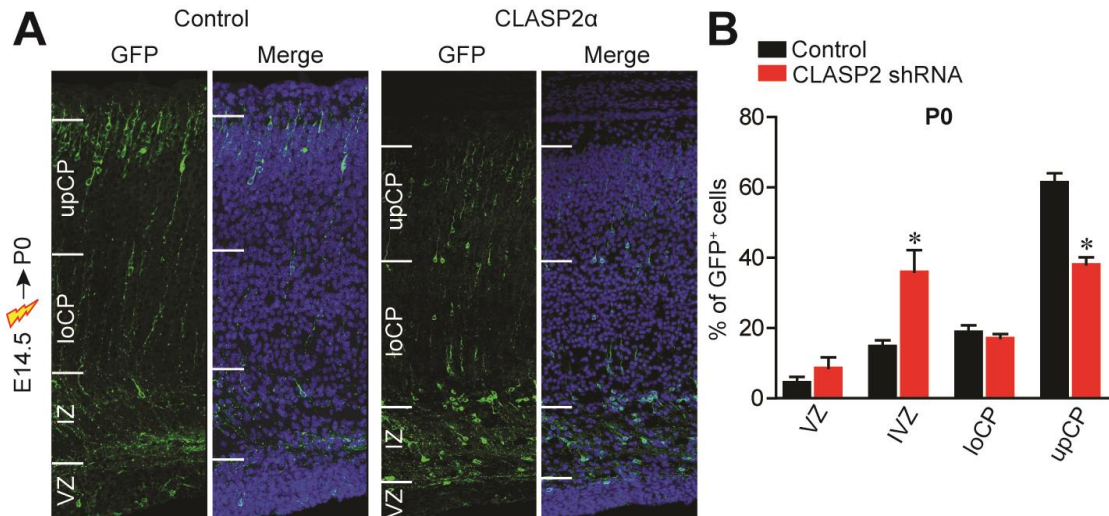


Figure 4.5: Overexpression of CLASP2 α Perturbs Neuron Migration

(A) Mouse embryos were electroporated at E14.5 with control or GFP-CLASP2 α .

Coronal sections of the cortex were visualized for transfected GFP-positive neurons (green) and cell nuclei (Hoechst 33342, blue) at P0 (A). White lines indicate the demarcations for different cortical areas (VZ=Ventricular Zone, IZ = Intermediate Zone, loCP = lower cortical plate, upCP = upper cortical plate). The percentage of total transfected cells in each zone are expressed as the mean \pm SEM.

(B) At P0, CLASP2 α overexpression caused a higher percentage of cells to be arrested in the intermediate zone (IZ: $p < 0.015$, upCP: $p < 0.001$; Control n=4 brains, CLASP2 shRNA n=4 brains)

Figure 4.6

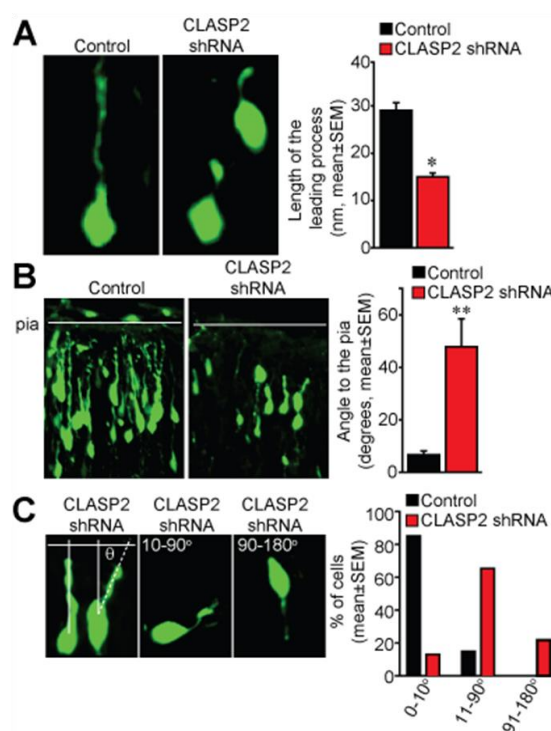


Figure 4.6: CLASP2 Affects Leading Process Extension and Orientation.

Mouse embryos were electroporated at E14.5 with scrambled control or CLASP2 shRNA and the brains were visualized at P0. The morphology of the leading process was examined only for transfected neurons which had entered the cortical plate.

(A) CLASP2 shRNA decreased the length of the leading process (Control n=96 cells; CLASP2 shRNA n=65 cells; $p<0.001$).

(B-C) Sample images representing the angle of the leading process in relation to the pial surface. The angle was measured by using the closest connecting line from the cell soma to the pia. CLASP2 shRNA caused an increase in the angle of the leading process in relation to the pia (Control n=20 cells; CLASP2 shRNA n=23 cells; $p<0.001$).

Figure 4.7

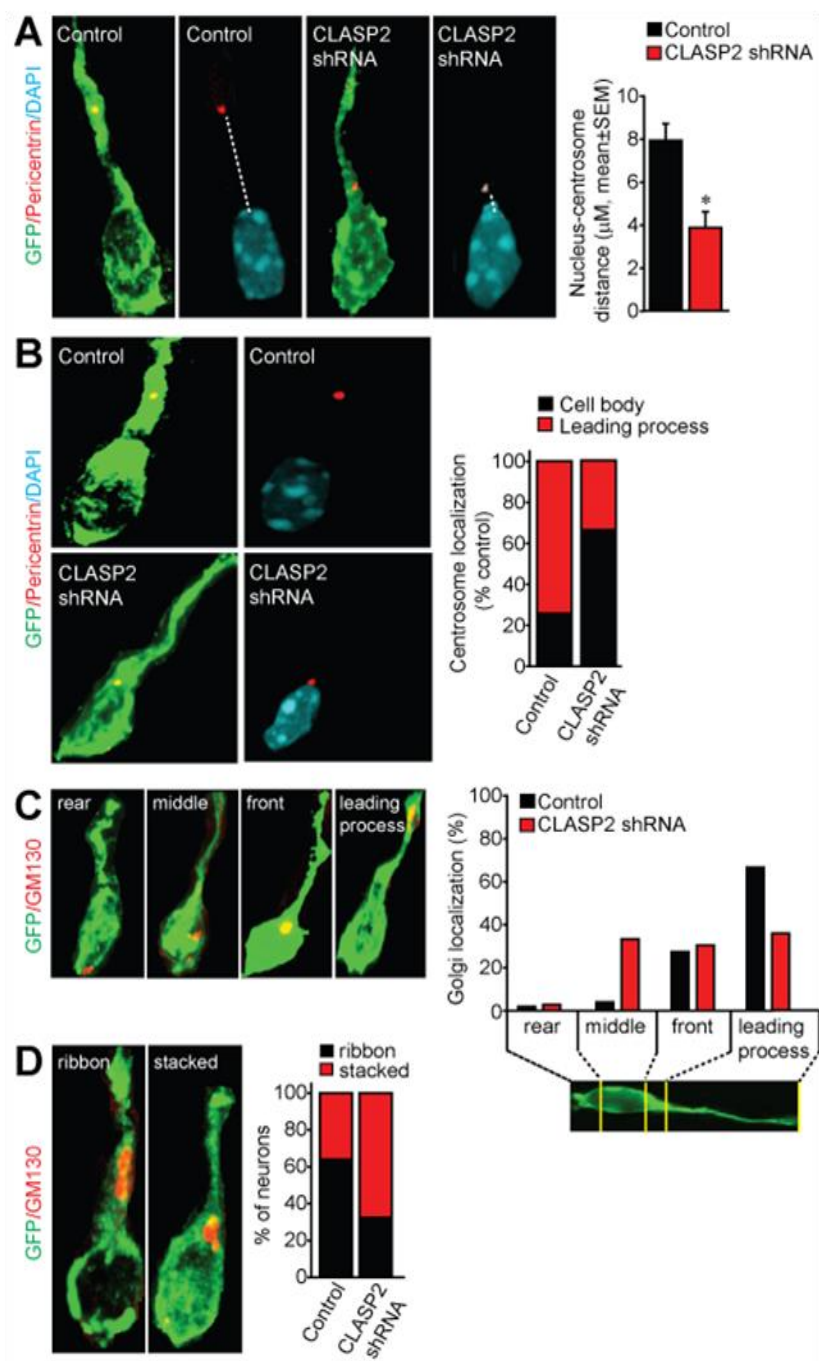


Figure 4.7: CLASP2 Knockdown Leads to Aberrant Localization of the Golgi/Centrosome Complex.

Mouse embryos were electroporated at E14.5 with scrambled or CLASP2 shRNA and the brains were visualized at P0.

(A-B) Representative images show transfected GFP-positive neurons (green) and centrosome staining (Pericentrin-red). Within migrating neurons, CLASP2 shRNA resulted in a shorter distance between the centrosome and nucleus (Control n=43 cells, CLASP2 shRNA n=53 cells; $p<0.001$).

(B-C) The localization of the Golgi/centrosome was examined only for transfected GFP-positive neurons which had entered the cortical plate and was verified by creating 3-D reconstructions of intact, transfected neurons from confocal Z-stacks at 0.5 μm steps. Knockdown of CLASP2 resulted in an aberrant mislocalization of the Golgi and centrosome away from the leading process adjacent to the nucleus (Golgi: Control n=51 cells, CLASP2 shRNA n=36 cells; Centrosome: Control n=43 cells, CLASP2 shRNA n=53 cells).

(D) CLASP2 knockdown resulted in a reduction of Golgi (GM130) polarity as indicated by more circular, condensed Golgi phenotype.

Figure 4.8

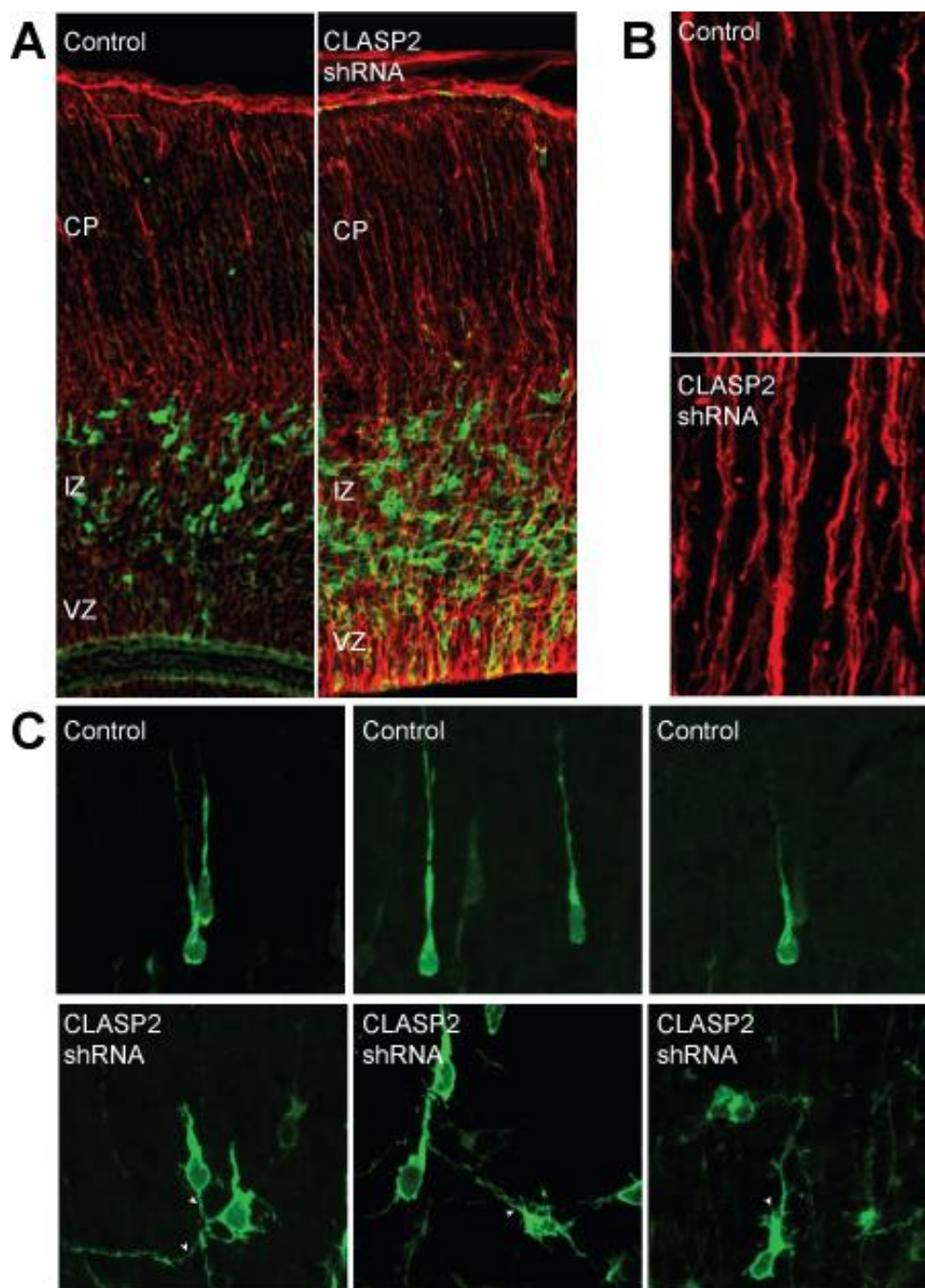


Figure 4.8: CLASP2 Expression Does Not Alter the Radial Glia Scaffold.

Mouse embryos were electroporated at E14.5 with scrambled control or CLASP2 shRNA and the brains were visualized at E16.5.

(A) Representative images at E.16.5 of scrambled control or CLASP2 shRNA plasmids showing transfected cells (green) and ascending radial glia fibers immunostained against Nestin (red).

(B) High magnification image in the cortical plate of control and CLASP2 shRNA brains immunostained with Nestin demonstrating intact radial fibers orientated towards the pial surface.

(C) Representative images of transfected control and CLASP2 shRNA neurons entering the cortical plate indicating the aberrant polarization of CLASP2 shRNA electroporated cells.

Figure 4.9

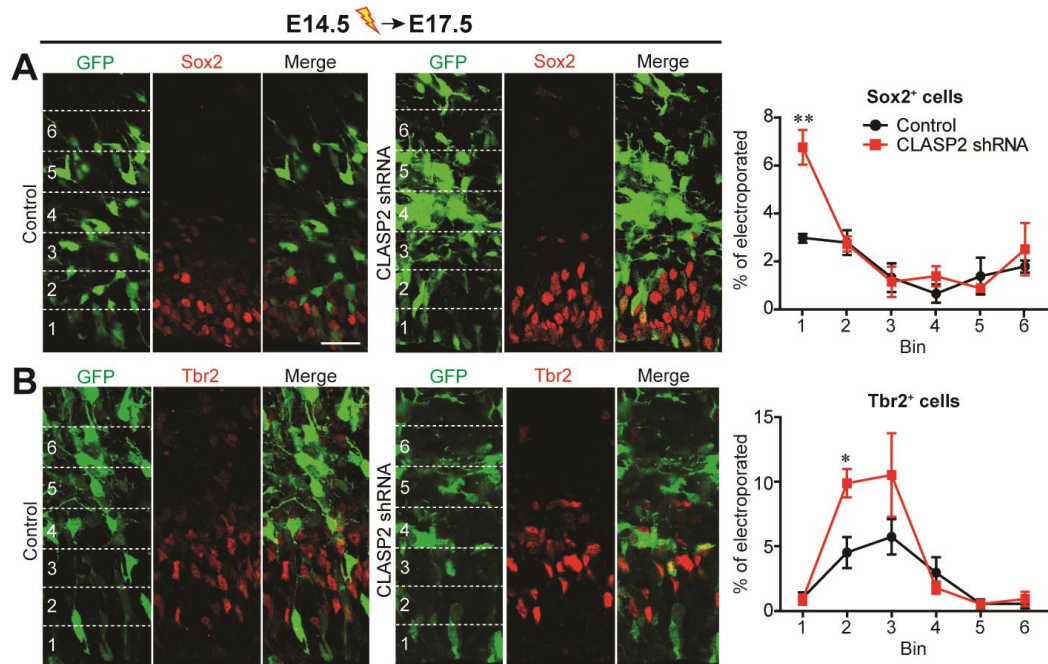


Figure 4.9: CLASP2 Regulates the Percentage of Proliferative Cells

Mouse embryos were electroporated at E14.5 with scrambled control or CLASP2 shRNA and analyzed at E17.5. Apical and basal progenitors were labeled with antibodies against the transcription factors Sox2 and Tbr2, respectively. The percentage of transfected cells positive for Sox2 or Tbr2 was calculated from the total number of electroporated cells.

(A) CLASP2 shRNA caused an increase in the percentage of Sox2-positive transfected cells within the first 20 μm from the ventricle surface ($p=0.008$).

(B) CLASP2 shRNA caused an increase in the percentage of Tbr2-positive transfected cells at 20-40 μm from the ventricle ($p=0.0166$).

Figure 4.10

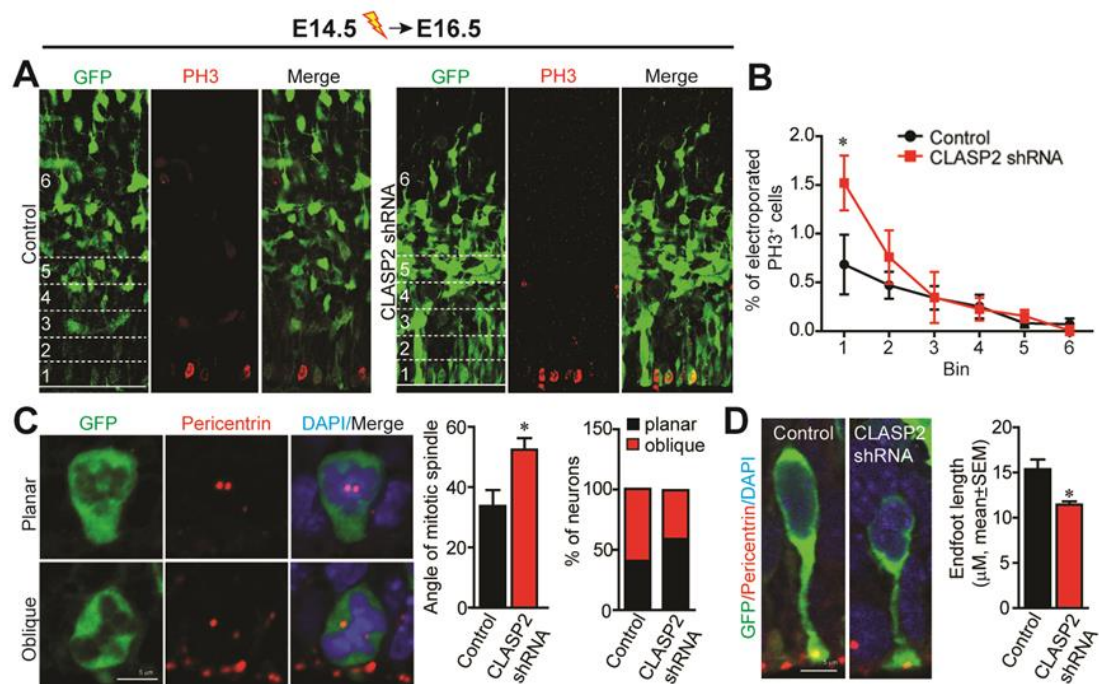


Figure 4.10: CLASP2 may Regulate Progenitor Cell Differentiation by Altering the Angle of the Cleavage Plane

Mouse embryos were electroporated at E14.5 with scrambled control or CLASP2 shRNA and analyzed at E16.5.

(A-B) Representative images showing transfected GFP-positive neurons (green) and the mitotic marker PH3 (red). CLASP2 knockdown resulted in more dividing cells at the ventricular surface compared to control (Control n=5 brains, CLASP2 shRNA n=6 brains; $p=0.0193$).

(C) Representative images indicating the cleavage plane of dividing cells following double-labeling for PH3 (not shown) and the centrosome marker pericentrin (red). Dividing cells electroporated with CLASP2 shRNA had greater angle of the mitotic spindle correlating with a higher percentage of planar divisions (control n=22 cells, CLASP2 shRNA n=52 cells; $p=0.009$). Scale bar represents 5 μm

(D) Control cells had longer apical processes when compared to CLASP2 shRNA (control n=294 cells, CLASP2 shRNA n=298 cells; $p=0.0358$). Scale bar represents 5 μm

Figure 4.11

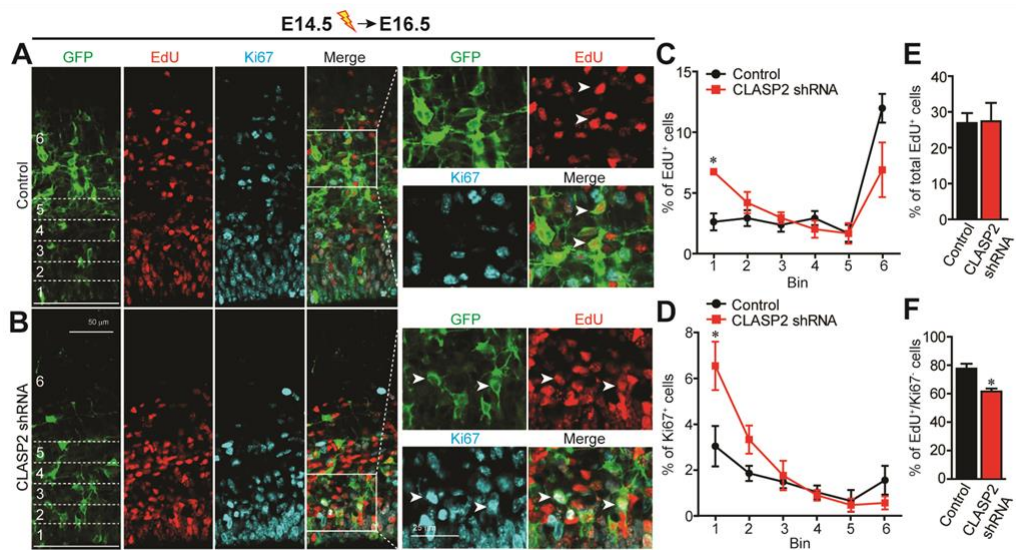


Figure 4.11: CLASP2 Knockdown Delays Differentiation of Progenitors

Mouse embryos were electroporated at E14.5 with scrambled or CLASP2 shRNA. The pregnant dam were injected with Edu 24 hours following electroporation and embryos were analyzed at E16.5.

(A-B) Representative images show transfected GFP-positive neurons (green), Edu (red), and the active cell cycle marker, Ki67 (light blue). All percentages were calculated based on the total number of electroporated cells (control n=4 brains, CLASP2 shRNA n=3 brains). Scale bar represents 50 μ m

(C) CLASP2 knockdown resulted in an increase in the percentage of Edu⁺ cells remaining within 20 μ m on the ventricle ($p=0.004$).

(D) CLASP2 shRNA increased the percentage of electroporated cells in the active cell cycle adjacent to the ventricular surface ($p=0.047$).

(E) There was no effect of CLASP2 shRNA on the total number of Edu⁺ cells

(F) CLASP2 shRNA caused a decrease in the number of Edu⁺ cells exiting the cell cycle over a 24 hour period ($p=0.016$).

Figure 4.12

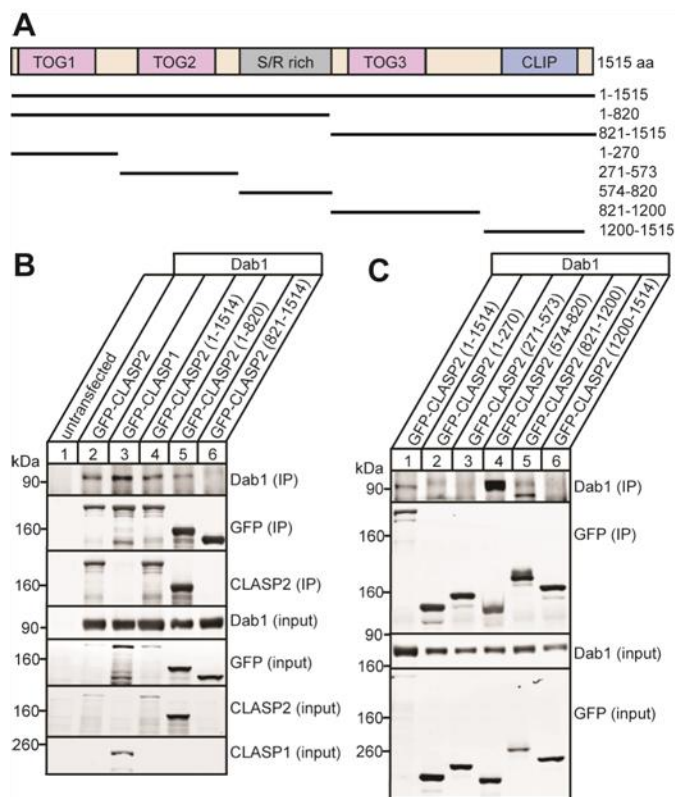


Figure 4.12: CLASP2 Binds to Dab1 at the S/R Domain of CLASP2.

HEK293T cells were co-transfected with Dab1 and GFP-CLASP plasmids. Cell lysates were collected 48 hours post-transfection and immunoprecipitated with a GFP antibody.

(A) Schematic of CLASP2 α indicating known protein binding regions

(B) Both CLASP1 and CLASP2 bind to Dab1. The binding region for Dab1 is within the first 820 amino acids of CLASP2.

(C) CLASP2 specifically binds to Dab1 at the S/R rich domain (574-820 amino acids).

Figure 4.13

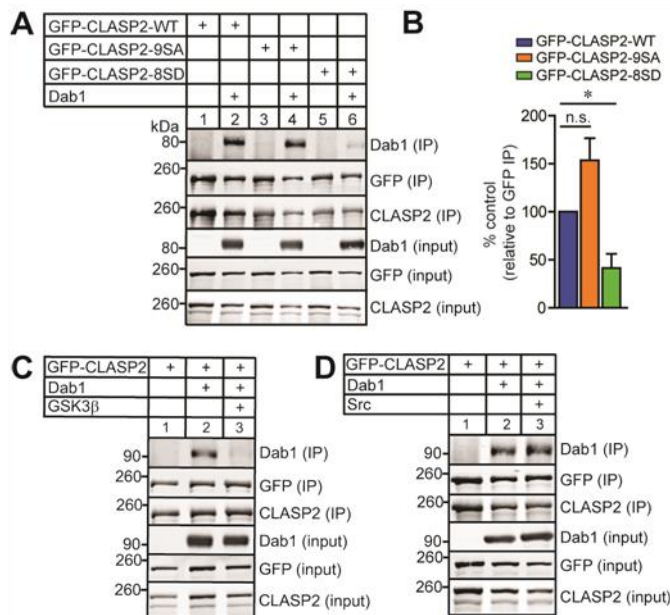


Figure 4.13: GSK3 β Phosphorylation of CLASP2 Regulates its Binding to Dab1

HEK293T cells were co-transfected GFP-CLASP2 α wild type (WT) or phospho-mutants (9S/A or 8S/D) and Dab1. Cell lysates were collected 48 hours post-transfection and immunoprecipitated with a GFP antibody.

(A-B) The phospho-mimetic CLASP2 α 8S/D showed less binding to Dab1 when compared to CLASP2 α WT or the phospho-resistant CLASP2 α 9S/A mutant. These results were quantified as relative to the immunoprecipitated level of GFP (n=3 independent experiments)

(C) Addition of constitutively active GSK3 β plasmid abolishes CLASP2 binding with Dab1 (n=2 independent experiments).

(D) Phosphorylation of Dab1 with constitutively active Src did not affect CLASP2 binding (n=3 independent experiments).

Figure 4.14

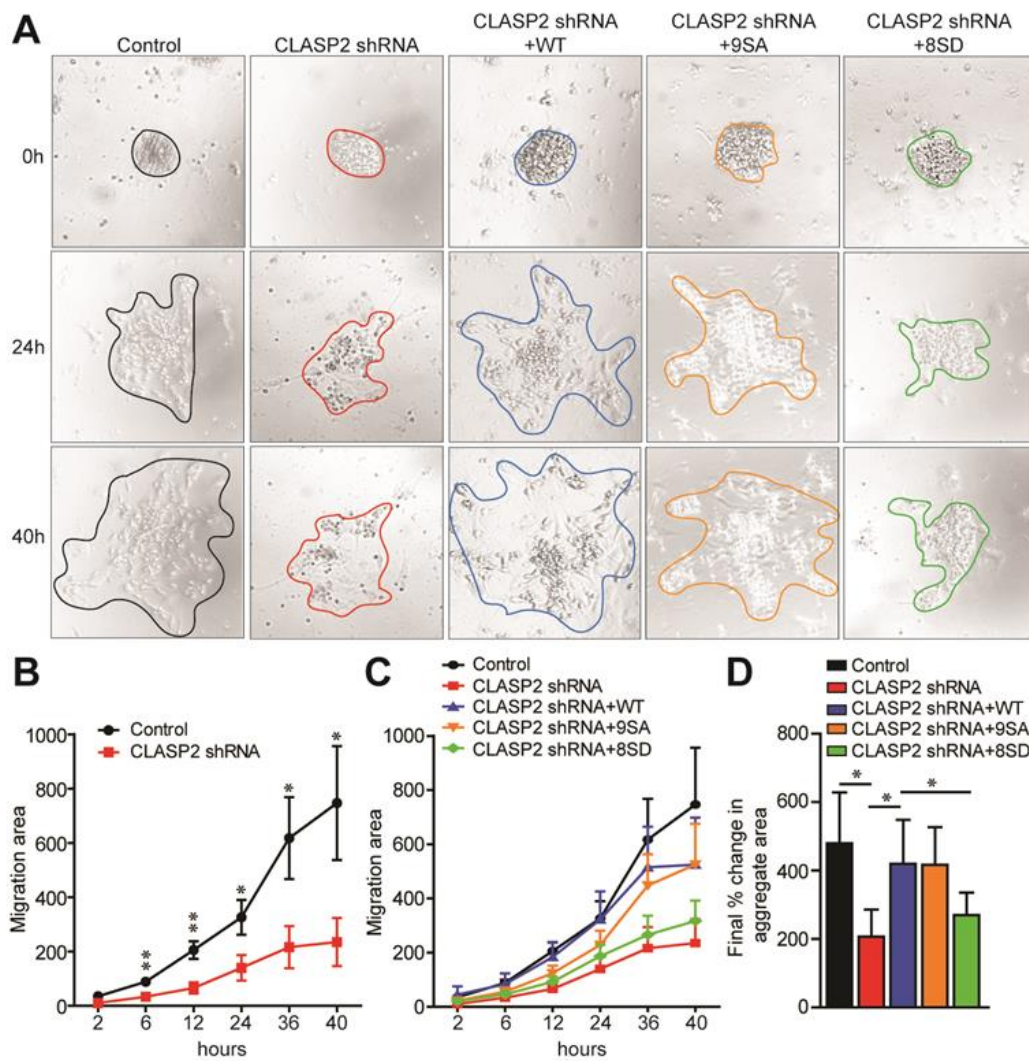


Figure 4.14: GSK3 β Phosphorylation of CLASP2 Regulates Cell Motility.

Primary neuron cultures were co-infected with CLASP2 shRNA or CLASP2 shRNA with CLASP2 α WT, CLASP2 α 9S/A, or CLASP2 α 8S/D phosphomutants.

(A) Cell migration was assessed by measuring the area of migration away from the initial aggregates over a 48 hour period.

(B) CLASP2 shRNA caused a decrease in migration area when compared to control (Control n=8; CLASP2 shRNA n=8; p=0.032).

(C-D) Phospho-mimetic CLASP2 α 8S/D was unable to rescue the deleterious effects of CLASP2 shRNA on cell motility compared to CLASP2 WT and 9S/A phosphomutant (CLASP2 α n=5, CLASP2 α 9S/A n=9, CLASP2 α 8S/D n=13; p=0.047).

Figure 4.15

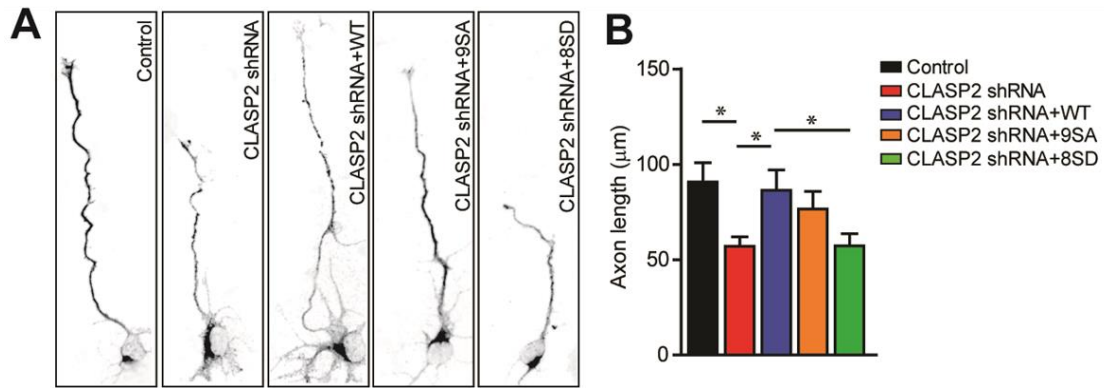


Figure 4.15: GSK3 β Phosphorylation of CLASP2 Regulates Neurite Extension.

Primary neuron cultures were co-infected at the day of plating with control, CLASP2 shRNA or CLASP2 shRNA with CLASP2 α WT, CLASP2 α 9S/A, or CLASP2 α 8S/D, collected 48 hours later, and immunostained against tau axonal marker.

(A) Representative images of hippocampal neurons stained with Tau

(B) CLASP2 shRNA caused a decrease in axon length when compared to control (control n=19 cells CLASP2 shRNA n=28 cells; $p=0.014$). Phospho-mimetic CLASP2 α 8S/D was unable to rescue the deleterious effects of CLASP2 shRNA on neurite extension

(CLASP2 α WT n=21 cells, CLASP2 α 9S/A n=17 cells, CLASP2 α 8S/D n=33 cells; $p=0.011$)

Figure 4.16

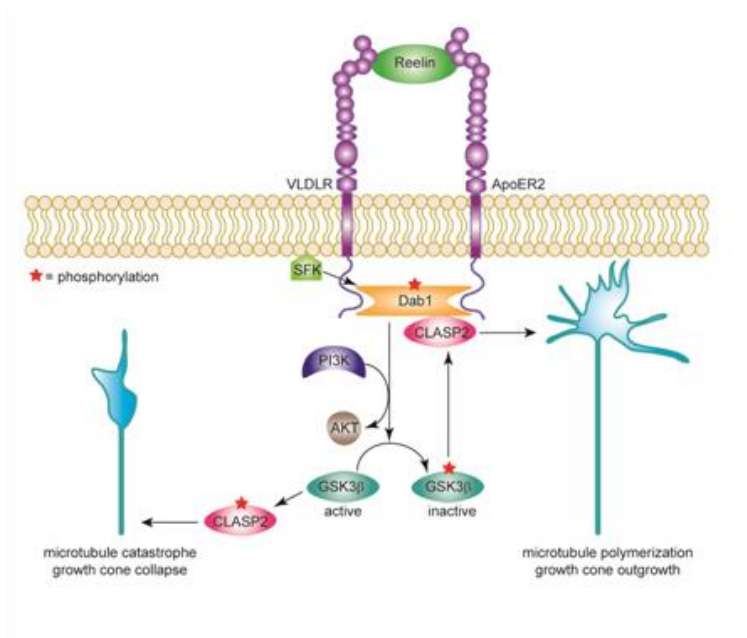


Figure 4.16: The GSK3 β -mediated phosphorylation of CLASP2 controls Dab1 binding and is required for regulating CLASP2 effects on neuron morphology and migration

Reelin exerts its function by binding to the lipoprotein receptors apolipoprotein E receptor 2 (ApoER2) and very-low-density-lipoprotein receptor (VLDLR) and inducing tyrosine phosphorylation of the intracellular adaptor protein disabled-1 (Dab1). Reelin signaling has been shown to directly inhibit GSK3 β activity through PI3K and Akt signaling mechanisms. In the current study, we demonstrate that CLASP2 binds to Dab1 and that this binding is regulated by GSK3 β phosphorylation. We propose a model where the localization of CLASP2 at the leading process is regulated by GSK3 β inactivation through extracellular Reelin and that CLASP2 enrichment at the leading edge is necessary to stabilize the leading process for correct neuron migration and morphology.

CHAPTER 5: GENERAL DISCUSSION

5.1: Major Findings

Microtubules are cytoskeletal filaments that are fundamental to many essential cellular processes including cell division, intracellular trafficking, and movement. Neurons, in particular are highly polarized cells with specialized compartments for receiving and sending information. In order to achieve polarity, neurons must be able to dynamically regulate the microtubule network during development. Microtubule plus-end tracking proteins (+TIPs) represent a specialized class of microtubule binding proteins that are enriched at the growing tip of polymerizing microtubules. This localization places +TIPs in a strategic position to control microtubule dynamics in response to extracellular cues; however, little is known about the role of +TIPs during brain development. In this dissertation, I investigated the role of the +TIP, CLASP2 in neural development.

In Chapter 3, I have shown that the expression of CLASP2 steadily increases throughout neuronal development and is necessary for correct polarization and morphogenesis. In primary mouse neurons, the shRNA-mediated knockdown of CLASP2 decreased neurite length, whereas overexpression of CLASP2 caused the formation of multiple axons, enhanced dendritic branching, and Golgi condensation. To determine whether the morphological changes in neurite growth and branching leads to functional alterations in synaptic transmission, I performed whole-cell recordings to monitor the frequency and amplitude of spontaneous miniature events. My results demonstrated that CLASP2 expression levels correlate with synaptic activity at excitatory but not inhibitory synapses. In addition, quantitative immunoblotting revealed that CLASP2 overexpression

caused a pronounced increase in a subset of pre-synaptic proteins at early developmental time points in vitro. In summary, the results from Chapter 3 demonstrate that increased CLASP2 expression leads to accelerated neurite growth, enhanced synaptic development, and activity; however, the role of CLASP2 during brain development was unknown.

Because we have demonstrated a role for CLASP2 in neuron polarization and morphology, we hypothesize that CLASPs could also serve an important role in neurogenesis and cortical lamination. CLASPs belong to a heterogeneous family of +TIPs which regulate microtubule stability during both mitosis and interphase. During cell division, CLASPs are enriched at the kinetochores and are necessary for kinetochore-microtubule attachment as well as chromosome alignment/segregation (Logarinho et al., 2012; Mathe et al., 2003; Cheeseman et al., 2005; Hannak and Heald, 2006). Previous experiments in non-neuronal cells have indicated that CLASP2 knockdown prolongs the cell cycle (Maiato et al., 2005); therefore CLASP may also affect terminal differentiation of neuronal progenitors during development. We demonstrate in Chapter 3 that CLASP2 localizes to the growing tip of post-mitotic neurons and it is necessary for neurite extension. During development, migrating neurons in the cortical plate extend a leading process that is responsible for sampling the microenvironment and provides an anchor point during saltatory movement (Marin et al., 2010). CLASP2 localization at the growth cone places it in a strategic position to regulate neurite outgrowth and the crosstalk between extracellular cues and intracellular polarity signals. Therefore, we hypothesize that CLASP2 may regulate leading process dynamics affecting neuron migration through the cortical plate.

During brain development, the Reelin signaling pathway is necessary for the formation of laminated structures, such as the cerebral cortex, hippocampus, and cerebellum. In addition, several cellular processes involved in neuron migration have been attributed to Reelin signaling including cell translocation, detachment from radial glia fibers, and extension of the leading process (Olsen, 2014); however, the molecular mechanisms underlying how Reelin regulates these cellular processes is unclear. In Chapter 4, I provide the first evidence that CLASP2 is a genetic modifier of the Reelin signaling pathway by comparing microarray gene expression between Reelin, the double ApoER2/VLDLR receptor, or Dab1 mutant. In addition, we have characterized the role of CLASP2 during cortical development by *in utero* electroporation of shRNA plasmids and found that silencing CLASP2 in migrating neurons leads to mislocalized cells at deeper cortical layers, abnormal positioning of the centrosome-Golgi complex, and aberrant length/orientation of the leading process. Moreover, we found that GSK3 β -mediated phosphorylation of CLASP2 controls Dab1 binding and is required for regulating CLASP2 effects on neuron morphology and migration. This dissertation provides the first steps in gaining insight into how Reelin signaling affects cytoskeletal reorganization in order to regulate fundamental features of neuronal migration, positioning, and morphogenesis.

5.2: The Effects of CLASP2 on Cortical Circuits

In Chapter 4 we found that CLASP2 knockdown leads to a defect in neuron migration and positioning that persisted within the adult brain; however, there are several outstanding questions that would be important to address in the future. Is the effect of

CLASP2 on migration specific for layer II/III cortical neurons? Do mislocalized neurons function normally and make proper synaptic connections and do mislocalized neurons contribute to the proper cortical circuits?

To extend our current findings we can investigate whether the aberrant migration phenotype following CLASP2 knockdown is exclusive to neurons of layers II/III. The mammalian cerebral cortex forms in an “inside-out” pattern with early-born neurons forming deeper layers and later-born neurons migrating past to reside in more outer/superficial layers of the cortical plate (Ayala et al., 2007). Therefore, neuron birth date can reliably predict final cortical position. We can conduct *in utero* electroporation on embryos at an earlier developmental time point (E12.5 and E13.5) thus knocking down CLASP2 expression in neurons destined for deeper cortical layers (layer V-VI). These results would demonstrate whether CLASP2 is necessary for the migration of neurons independent of cortical layer.

During development, cortical interneurons migrate tangentially from the ganglionic eminence into the cortex. To determine whether the effects of CLASP2 knockdown on migration are specific to cortical projection neurons, we can conduct *in utero* electroporation experiments driving control and CLASP2 constructs into the medial ganglion eminence. By changing the orientation of the electrical field, we will transfect progenitors at E14.5 and analyze brain sections at P14 for changes in neuron migration, laminar organization, and molecular markers of different cell types. I expect CLASP2 knockdown will result in deficits in the dispersal of interneurons into the cortex. These

studies will expand our understanding on the role of CLASP2 in the different types of migratory behavior necessary for proper brain development.

To determine whether CLASP2 plays a role in axonal growth and guidance *in vivo*, we can assess for changes in efferent axons from layer II/III pyramidal neurons. In order to examine axon connectivity, a crystal of the retrograde carbocyanine dye (DiI) can be administered from the tip of a micropipette into the hemisphere opposite the electroporation site. DiI is a non-toxic, fluorescent lipophilic compound which can diffuse along plasma membranes in lightly fixed tissue. Neurons which show co-staining for both GFP and DiI indicate the retrograde movement of the tracer from the contralateral hemisphere along the axon to the cell body of the electroporated neuron. I expect that CLASP2 shRNA will cause severe defects in axon growth preventing correct path-finding. In contrast, CLASP2 overexpression may lead to ectopic midline crossings through the corpus callosum or to subcerebral targets.

In order to extend our previous findings we plan to investigate the effects of CLASP2 on neural activity *in vivo*. Therefore, we will knockdown or increase CLASP2 protein expression in the developing cortex or hippocampus by *in utero* electroporation at E14.5. Appropriate brain regions will be dissected at P15 and cut into coronal slices. GFP-labeled cells will be identified by fluorescent microscopy.

a) For cortical sections, GFP-labeled cells and their appropriate pyramidal, layer-matched controls will undergo patch clamp recording for spontaneous miniature activity. Results from this study will determine whether CLASP2 effects the intrinsic excitability of cortical neurons.

b) In the hippocampus, field recordings will be performed to examine whether CLASP2 affects properties of long-term potentiation (LTP) and/or depression (LTD). Synaptic responses will be evoked by stimulating Schaffer collaterals and then recording field excitatory postsynaptic potentials (fEPSPs) in the stratum radiatum of the CA1 region. Results from these studies will determine if CLASP2 effects on cortical lamination significantly affects the formation of cortical/hippocampal circuits.

I expect that CLASP2 will affect spontaneous activity at the single cell level due to changes in neurite branching, synapse number, and alterations in the presynaptic transmitter release. In addition, CLASP2 may affect the processes of LTP/LTD through the mislocalization of cells following incorrect migration. Alternatively, it is possible that the in utero electroporation of CLASP2 plasmids will not affect LTP or LTD because of the transfection efficacy or the small percentage of mislocalized cells.

5.3: The Effects of CLASP2 on Mitosis versus Migration

We found that CLASP2 knockdown can delay the cell cycle exit of neural progenitors and cause abnormal growth and orientation of the leading process in migrating neurons. These two functions of CLASP2 are likely to be independent of each other and largely related to binding events at the mitotic spindle and growth cone, respectively. Therefore, future experiments are needed to elucidate the role of CLASP2 during different phases of cortical development.

To determine whether the abnormal migration of CLASP2 shRNA cells results indirectly from the defects observed in VZ progenitors, or reflects a distinct, cell autonomous function of CLASP2 in neurons we could silence CLASP2 specifically in

post-mitotic neurons. To do this, we could use a construct that expresses the CLASP2 shRNA in a Cre-dependent manner (Floxed stop-CLASP2 shRNA) and perform in utero electroporation on Nex-Cre mice, which express Cre only in post-mitotic cortical neurons (Goebbels et al., 2006). Results from this experiment would demonstrate whether CLASP2 effects on the leading process or cell cycle exit result in the permanent defects in cortical lamination following CLASP2 knockdown.

5.4: CLASP2 Regulation of the Golgi Complex

In neurons, CLASP2 is enriched at two main cellular compartments: the Golgi and the growth cone (Beffert et al., 2012). CLASP2 localization at the Golgi is required for the nucleation of Golgi-derived microtubules, most of which are directed towards the leading edge and are biochemically dissimilar from centrosomal microtubule arrays (Efimov et al., 2007). In addition, our results show that CLASP2 regulates the morphology of both the Golgi and the leading process; however, it is unclear whether CLASP regulation of Golgi-derived microtubules controls polarization, neurite outgrowth, and subsequent migration of neurons.

CLASP2 localizes to the Golgi complex through direct binding between the C-terminal domain of CLASP2 and the Golgin protein, GCC185. Therefore, in utero electroporation of GCC185 shRNA could be used to prevent CLASP2 enrichment at the Golgi. In addition, plasmids overexpressing the C-terminal fragment of CLASP2 could be used to competitively compete with endogenous, full-length CLASP2 for GCC185 binding thereby preventing Golgi localization. The results from these studies would

determine if CLASP2 localization at the Golgi or the growth cone is affecting leading process morphology and dynamics.

5.5: Conclusions and Significance

The results presented in this dissertation represent the first demonstration of CLASP2 function in the developing mammalian brain. Subsequently, future studies are necessary to dissect the role of CLASP2 during different phases of neuron development from mitosis to migration and finally morphogenesis. In the cerebral cortex, defects in neuronal morphogenesis, migration and synaptogenesis can lead to mental retardation, autism spectrum disorders and epilepsy. Therefore, elucidating the pathways which integrate, extracellular cues with cytoskeleton reorganization are essential to understand correct cortical architecture and connectivity.

BIBLIOGRAPHY

- Ahmad, F.J., C.J. Echeverri, R.B. Vallee, and P.W. Baas (1998) "Cytoplasmic dynein and dynactin are required for the transport of microtubules into the axon." Journal of Cell Biology **140**(2): 391-401.
- Aist, J. R., C.J. Bayles, W. Tao, and M.W. Berns (1991) "Direct experimental evidence for the existence, structural basis and function of astral forces during anaphase B in vivo." Journal of Cell Science **100**: 279-88.
- Akhmanova, A. and C.C. Hoogenraad (2005) "Microtubule plus-end-tracking proteins: mechanisms and functions." Current Opinions in Cell Biology **17**(1):47-54.
- Akhmanova A. and M.O. Steinmetz (2008) "Tracking the ends: a dynamic protein network controls the fate of microtubule tips." Nature Reviews. Molecular Cell Biology **9**(4):309-22.
- Akhmanova, A. and M.O. Steinmetz (2010) "Microtubule +TIPs at a glance." The Journal of Cell Science. **123**(20):3415-9.
- Akhmanova A., C.C. Hoogenraad, K. Drabek, T. Stepanova, B. Dortland, T. Verkerk, W. Vermeulen, B.M. Burgering, C.I. De Zeeuw, F. Grosveld, and N. Galjart (2001) "Clasps are CLIP-115 and -170 associating proteins involved in the regional regulation of microtubule dynamics in motile fibroblasts." Cell **104**(6):923-35.
- Akhmanova A., A.L. Mausset-Bonnefont, W. van Cappellen, N. Keijzer, C.C. Hoogenraad, T. Stepanova, K. Drabek, J. van der Wees, M. Mommaas, J. Onderwater, H. van der Meulen, M.E. Tanenbaum, R.H. Medema, J. Hoogerbrugge, J. Vreeburg, E.J. Uringa, J.A. Grootegoed, F. Grosveld, and N. Galjart (2005) "The microtubule plus-end-tracking protein CLIP-170 associates with the spermatid manchette and is essential for spermatogenesis." Genes & Development **19**(20):2501-15.
- Al-Bassam, J. and F. Chang (2011) "Regulation of microtubule dynamics by TOG-domain proteins XMAP215/Dis1 and CLASP." Trends in Cell Biology **21**(10):604-14.
- Al-Bassam J., H. Kim, G. Brouhard, A. van Oijen, S.C. Harrison, and F. Chang (2010) "CLASP promotes microtubule rescue by recruiting tubulin dimers to the microtubule." Developmental Cell **19**(2):245-58.
- Ambrose, J.C., T. Shoji, A.M. Kotzer, J.A. Pighin, and G.O. Wasteneys (2007) " The Arabidopsis CLASP gene encodes a microtubule-associated protein involved in cell expansion and division." Plant Cell **19**(9): 2763-75.

- Angevine, J.B. Jr. and R.L. Sidman RL(1961) "Autoradiographic study of cell migration during histogenesis of cerebral cortex in the mouse." Nature **25**(192):766-8.
- Anthony, T.E., C. Klein, G. Fishell, and N. Heintz (2004) "Radial glia serve as neuronal progenitors in all regions of the central nervous system." Neuron **41**(6): 881-90.
- Asada, N. and K. Sanada (2010) "LKB1-mediated spatial control of GSK3beta and adenomatous polyposis coli contributes to centrosomal forward movement and neuronal migration in the developing neocortex." Journal of Neuroscience **30**(26): 8852-65.
- Ayala, R., T. Shu and L.H. Tsai (2007) "Trekking across the brain: the journey of neuronal migration" Cell **128**(1): 29-43.
- Bai, J., R.L. Ramos, J.B. Ackman, A.M. Thomas, R.V. Lee, and J.J. LoTurco (2003) "RNAi reveals doublecortin is required for radial migration in rat neocortex." Nature Neuroscience **6**(12):1277-83.
- Basarsky T.A., V. Parpura, and P.G. Haydon (1994) "Hippocampal synaptogenesis in cell culture: developmental time course of synapse formation, calcium influx, and synaptic protein distribution." The Journal of Neuroscience **14**(11):6402-11.
- Baas, P.W., A. Karabay, and L. Qiang (2005) "Microtubules cut and run." Trends in Cell Biology **15**(10):518-24.
- Basu, R. and F. Chang (2007) "Shaping the actin cytoskeleton using microtubule tips." Current Opinions in Cell Biology **19**(1):88-94.
- Baudoin, J.P., C. Alvarez, P. Gaspar, and C. Méтин (2008) "Nocodazole-induced changes in microtubule dynamics impair the morphology and directionality of migrating medial ganglionic eminence cells." Developmental Neuroscience **30**(1-3): 132-43.
- Beffert, U., E.J. Weeber, G. Morfini, J. Ko, S.T. Brady, L.H. Tsai, J.D. Sweatt, and J. Herz (2004) "Reelin and cyclin-dependent kinase 5-dependent signals in regulating neuronal migration and synaptic transmission." The Journal of Neuroscience **24**(8): 1897-906.
- Beffert, U., G.M. Dillon, J.M. Sullivan, C.E. Stuart, J.P. Gilbert, J.A. Kambouris, and A. Ho (2012) "Microtubule plus-end tracking protein CLASP2 regulates neuronal polarity and synaptic function." Journal of Neuroscience **32**(40): 13906-16.
- Bellion, A., J.P. Baudoin, C. Alvarez, M. Bornens, and C. Méтин (2005) "Nucleokinesis in tangentially migrating neurons comprises two alternating phases: forward migration of the Golgi/centrosome associated with centrosome splitting and myosin contraction at the rear" Journal of Neuroscience **25**(24): 5691-9.

- Belgard T.G., A.C. Marques, P.L. Oliver, H.O. Abaan, T.M. Sirey, A. Hoerder-Suabedissen, F. García-Moreno, Z. Molnár, E.H. Margulies, and C.P. Ponting (2011) "A Transcriptomic Atlas of Mouse Neocortical Layers" Neuron **71**(4):605-16.
- Bielas, S.L. and J.G. Gleeson (2004) "Cytoskeletal-associated proteins in the migration of cortical neurons." Journal of Neuroscience **58**(1): 149-59.
- Bisel, B., Y. Wang, J.H. Wei, Y. Xiang, D. Tang, M. Miron-Mendoza, S. Yoshimura, N. Nakamura, and J. Semann (2008) "ERK regulates Golgi and centrosome orientation towards the leading edge through GRASP65." The Journal of Cell Biology. **182**(5):837-43.
- Bock, H.H. and J. Herz (2003) "Reelin activates SRC family tyrosine kinases in neurons." Current Biology **13**(1):18-26.
- Bouquet, C., S. Soares, Y. von Boxberg, M. Ravaille-Veron, F. Propst, and F. Nothias (2004) "Microtubule-associated protein 1B controls directionality of growth cone migration and axonal branching in regeneration of adult dorsal root ganglia neurons." The Journal of Neuroscience **24**(32):7204-13.
- Bradke F. and C.G. Dotti (2000) "Establishment of neuronal polarity: lessons from cultured hippocampal neurons." Current Opinions in Neurobiology **10**(5):574-81.
- Bratman S.V. and F. Chang (2008) "Mechanisms for maintaining microtubule bundles." Trends in Cell Biology **18**(12):580-6.
- Bronk P., F. Deak, M.C. Wilson, X. Liu, T.C. Südhof, and E.T. Kavalali (2007) "Differential effects of SNAP-25 deletion on Ca²⁺ -dependent and Ca²⁺ -independent neurotransmission." Journal of Neurophysiology **98**(2):794-806.
- Brouhard, G.J. and L.M. Rice (2014) "The contribution of $\alpha\beta$ -tubulin curvature to microtubule dynamics." The Journal of Cell Biology **207**(3):323-34.
- Buck, K.B. and J.Q. Zheng (2002) "Growth cone turning induced by direct local modification of microtubule dynamics." The Journal of Neuroscience **22**(21):9358-67.
- Bultje, R.S., D.R. Castaneda-Castellanos, L.Y. Jan, Y.N. Jan, A.R. Kriegstein, and S.H. Shi (2009) "Mammalian Par3 regulates progenitor cell asymmetric division via notch signaling in the developing neocortex." Neuron **63**(2):189-202.
- Carminati, J. L. and T. Stearns (1997) "Microtubules orient the mitotic spindle in yeast through dynein-dependent interactions with the cell cortex." Journal of Cell Biology **138**: 629-41.

- Chai, X., E. Förster, S. Zhao, H.H. Bock, and M. Frotscher (2009) "Reelin stabilizes the actin cytoskeleton of neuronal processes by inducing n-cofilin phosphorylation at serine3." Journal of Neuroscience **29**(1): 288-99.
- Cheeseman, I.M., I. Macleod, J.R. Yates 3rd, K. Oegema, and A. Desai (2005) "The CENP-F-like proteins HCP-1 and HCP-2 target CLASP to kinetochores to mediate chromosome segregation." Current Biology **15**(8):771-7.
- Chenn, A. and S.K. McConnell (1995) "Cleavage orientation and the asymmetric inheritance of Notch1 immunoreactivity in mammalian neurogenesis." Cell **82**(4): 631-41.
- Chen, J.F., Y. Zhang, J. Wilde, K.C. Hansen, F. Lai, and L. Niswander (2014) "Microcephaly disease gene Wdr62 regulates mitotic progression of embryonic neural stem cells and brain size." Nature Communication **5**:3885.
- Conde C. and A. Caceres (2009) "Microtubule assembly, organization and dynamics in axons and dendrites." Nature Reviews. Neuroscience **10**(5):319-32.
- Cooper, J.A. (2008) "A mechanism for inside-out lamination in the neocortex" Trends in Neuroscience **31**(3): 113-9.
- Craig A.M. and G. Banker (1994) "Neuronal polarity." Annual Review of Neuroscience **17**:267-310.
- Creppe, C., L. Malinouskaya, M.L. Volvert, M. Gillard, P. Close, O. Malaise, S. Laguesse, I. Cornez, S. Rahmouni, S. Ormenese, S. Belachew, B. Malgrage, J. P. Chapelle, U. Siebenlist, G. Moonen, A. Chariot, and L. Nguyen (2009) "Elongator controls the migration and differentiation of cortical neurons through acetylation of alpha-tubulin." Cell **136**(3):551-64.
- Curran, T. and G. D'Arcangelo (1998) "Role of reelin in the control of brain development." Brain Research Review **26**(2-3): 285-94.
- D'Arcangelo, G., G.G. Miao, S.C. Chen, H.D. Soares, J.I. Morgan, and T. Curran (1995) "A protein related to extracellular matrix proteins deleted in the mouse mutant reeler." Nature. **374**(6524): 719-23.
- D'Arcangelo G (2005) "The reeler mouse: anatomy of a mutant." International Reviews on Neurobiology **71**:383-417.
- Das T., B. Payer, M. Cayouette, and W.A. Harris (2003) "In vivo time-lapse imaging of cell divisions during neurogenesis in the developing zebrafish retina." Neuron **37**(4): 597-609.

- Das R.M. and K.G. Storey (2012) "Mitotic spindle orientation can direct cell fate and bias Notch activity in chick neural tube." EMBO Reports **13**(5):448-54.
- de Anda F.C., K. Meletis, X. Ge, D. Rei, and L.H. Tsai (2010) "Centrosome motility is essential for initial axon formation in the neocortex." The Journal of Neuroscience **30**(31):10391-406.
- de Anda F.C., G. Pollarolo, J.S. Da Silva, P.G. Camoletto, F. Feiguin, and C.G. Dotti (2005) "Centrosome localization determines neuronal polarity." Nature **436**(7051):704-8.
- de Anda, F.C., A.L. Rosario, O. Durak, T. Tran, J. Gräff, K. Meletis, D. Rei, T. Soda, R. Madabhushi, D.D. Ginty, A.L. Kolodkin, and L.H. Tsai (2012) "Autism spectrum disorder susceptibility gene TAOK2 affects basal dendrite formation in the neocortex." Nature Neuroscience **15**(7):1022-31.
- Dehmelt, L and S. Halpain (2004) "Actin and microtubules in neurite initiation: are the MAPs the missing link?" The Journal of Neurobiology **58**(1):18-33.
- DeFelipe, J. and I. Fariñas (1992) "The pyramidal neuron of the cerebral cortex: morphological and chemical characteristics of the synaptic inputs." Progress in Neurobiology **39**(6): 563-607.
- De Zio, D., F. Molinari, S. Rizza, L. Gatta, M.T. Ciotti, A.M. Salvatore, S.G. Mathiasen, A.W. Cwetsch, G. Filomeni, G. Rosano, and E. Ferraro (2015) "Apaf1-deficient cortical neurons exhibit defects in axonal outgrowth." Cellular and Molecular Life Sciences **72**(21):4173-91.
- Dong, Z., N. Yang, S.Y. Yeo, A. Chitnis, and S. Guo (2012) "Intralineage directional Notch signaling regulates self-renewal and differentiation of asymmetrically dividing radial glia." Neuron **74**(1):65-78.
- Drabek, K., M. van Ham, T. Stepanova, K. Draegestein, R. van Horssen, C.L. Sayas, A. Akhmanova, T. Ten Hagen, R. Smits, R. Fodde, F. Grosveld, and N. Galjart (2006) "Role of CLASP2 in microtubule stabilization and the regulation of persistent motility." Current Biology **16**(22):2259-64.
- Efimov A., A. Kharitonov, N. Efimova, J. Loncarek, P.M. Miller, N. Andreyeva, P. Gleeson, N. Galjart, A.R. Maia, I.X. McLeod, J.R. Yates, 3rd, H. Maiato, A. Khodjakov, A. Akhmanova, and I. Kaverina (2007) "Asymmetric CLASP-dependent nucleation of noncentrosomal microtubules at the trans-Golgi network." Developmental Cell **12**(6):917-30.
- Eom, T.Y., A. Stanco, J. Guo, G. Wilkins, D. Deslauriers, J. Yan, C. Monckton, J. Blair, E. Oon, A. Perez, E. Salas, A. Oh, V. Ghukasyan, W.D. Snider, J.L. Rubenstein, and

- E.S. Anton (2014) "Differential regulation of microtubule severing by APC underlies distinct patterns of projection neuron and interneuron migration." Developmental Cell **31**(6):677-89.
- Etienne-Manneville, S. and A. Hall (2003) "Cdc42 regulates GSK-3beta and adenomatous polyposis coli to control cell polarity." Nature **421**(6924):753-6.
- Feng, Y., and C.A. Walsh (2004) "Mitotic spindle regulation by Nde1 controls cerebral cortical size." Neuron **44**(2):279-93.
- Fishell, G. and A.R. Kriegstein (2003) Neurons from radial glia: the consequences of asymmetric inheritance. Current Opinions in Neurobiology **13**: 34–41.
- Fodde, R., J. Kuipres, C. Rosenberg, R. Smts, M. Kielman, C. Gaspar, J.H. van Es, C. Breukel, J. Wiegant, R.H. Giles, and H. Clevers (2001) "Mutations in the APC tumour suppressor gene cause chromosomal instability." Nature Cell Biology **3**(4):433-8.
- Franco, S.J., I. Martinez-Garay, C. Gil-Sanz, S.R. Harkins-Perry, and U. Müller (2011) "Reelin regulates cadherin function via Dab1/Rap1 to control neuronal migration and lamination in the neocortex." Neuron **69**(3): 482-97.
- Gal, J.S., Y.M. Morozov, A.E. Ayoub, M. Chatterjee, P. Rakic, and T.F. Haydar (2006) "Molecular and morphological heterogeneity of neural precursors in the mouse neocortical proliferative zones." Journal of Neuroscience **26**(3):1045-56.
- Galjart N (2005) CLIPs and CLASPs and cellular dynamics. Nature Reviews Molecular and Cellular Biology **6**:487-498.
- Galjart, N. (2010) "Plus-end-tracking proteins and their interactions at the microtubule ends." Current Biology **20**(12):528-37.
- Gilmore E.C. and C.A. Walsh (2013) "Genetic causes of microcephaly and lessons for neuronal development." Wiley Interdisciplinary Reviews. Developmental Biology **2**(4):461-78.
- Gleeson, J.G., K.M. Allen, J.W. Fox, E.D. Lamperti, S. Berkovic, I. Scheffer, E.C. Cooper, W.B. Dobyns, S.R. Minnerath, M.E. Ross, and C.A. Walsh (1998) "Doublecortin, a brain-specific gene mutated in human X-linked lissencephaly and double cortex syndrome, encodes a putative signaling protein." Cell **92**(1):63-72.
- Goebbels, S., I. Bormuth, U. Bode, O. Hermanson, M.H. Schwab, and K.A. Nave (2006) "Genetic targeting of principal neurons in neocortex and hippocampus of NEX-Cre mice." Genesis **44**(12): 611-21.

- Goellner B. and H. Aberle (2012) "The synaptic cytoskeleton in development and disease." Developmental Neurobiology **72**(1):111-25.
- Götz M. and W.B. Huttner (2005) "The cell biology of neurogenesis." Nature Reviews. Molecular Cell Biology **6**(10):777-88.
- González-Billault, C., J.A. Del Rio, J.M. Ureña, E.M. Jiménez-Mateos, M.J. Barallobre, M. Pascual, L. Pujadas, S. Simó, A.L. Torre, R. Gavin, F. Wandosell, E. Soriano, and J. Avila (2005) "A role of MAP1B in Reelin-dependent neuronal migration." Cerebral Cortex **15**(8):1134-45.
- Green, R.A. and K.B. Kaplan (2003) "Chromosome instability in colorectal tumor cells is associated with defects in microtubule plus-end attachments caused by a dominant mutation in APC." The Journal of Cell Biology. **163**(5):949-61.
- Grimaldi, A.D., T. Maki, B.P. Fitton, D. Roth, D. Yampolsky, M.W. Davidson, T. Svitkina, A. Straube, I. Hayashi, and I. Kaverina (2014) "CLASPs are required for proper microtubule localization of end-binding proteins." Developmental Cell **30**(3):343-52.
- Gu C., W. Zhou, M.A. Puthenveedu, M. Xu, Y.N. Jan, and L.Y. Jan (2006) "The microtubule plus-end tracking protein EB1 is required for Kv1 voltage-gated K⁺ channel axonal targeting." Neuron **52**(5):803-16.
- Hannek, E. and R. Heald (2006) "Xorbit/CLASP links dynamic microtubules to chromosomes in the *Xenopus* meiotic spindle." The Journal of Cell Biology **172**(1):19-25.
- Hanus C. and M.D. Ehlers (2008) "Secretory outposts for the local processing of membrane cargo in neuronal dendrites." Traffic **9**(9):1437-45.
- Haubensak, W., A. Attardo, W. Denk, and W.B. Huttner (2004) "Neurons arise in the basal neuroepithelium of the early mammalian telencephalon: a major site of neurogenesis." Proceedings of the National Academy of Sciences of the United States **101**(9): 3196-201.
- Haydar T.F., E. Ang, Jr, and P. Rakic (2003) "Mitotic spindle rotation and mode of cell division in the developing telencephalon." Proceedings of the National Academy of the Sciences of the United States **100**(5): 2890-5.
- Hayden, J.H., S.S. Bower, and C.L. Rieder (1990) "Kinetochores capture astral microtubules during chromosome attachment to the mitotic spindle: direct visualization in live newt lung cells." The Journal of Cell Biology **111**(3):1039-45.

- Hayes, G.L., F.C. Brown, A.K. Haas, R.M. Nottingham, F.A. Barr, and S.R. Pfeffer (2009) "Multiple Rab GTPase binding sites in GCC185 suggest a model for vesicle tethering at the trans-Golgi." Molecular Biology of the Cell **20**(1):209-17.
- Hill, T.L. (1985) "Theoretical problems related to the attachment of microtubules to kinetochores." Proceedings of the National Academy of the Sciences of the United States **82**(13):4404-8.
- Ho A., X. Liu, and T.C. Südhof (2008) "Deletion of Mint proteins decreases amyloid production in transgenic mouse models of Alzheimer's disease." The Journal of Neuroscience **28**(53):14392-400.
- Ho A., W. Morishita, D. Atasoy, X. Liu, K. Tabuchi, R.E. Hammer, R.C. Malenka, and T.C. Südhof (2006) "Genetic analysis of Mint/X11 proteins: essential presynaptic functions of a neuronal adaptor protein family." The Journal of Neuroscience **26**(50):13089-101.
- Holy, T.E. and S. Leibler (1994) "Dynamic instability of microtubules as an efficient way to search in space." Proceedings of the National Academy of the Sciences of the United States **91**(12):5682-5.
- Hong S.E., Y.Y. Shugart, D.T. Huang, S.A. Shahwan, P.E. Grant, J.O. Hourihane, N.D. Martin, and C.A. Walsh (2000) "Autosomal recessive lissencephaly with cerebellar hypoplasia is associated with human RELN mutations." Nature Genetics **26**(1): 93-6.
- Hoogenraad C.C. and F. Bradke (2009) "Control of neuronal polarity and plasticity--a renaissance for microtubules?" Trends in Cell Biology **19**(12):669-76.
- Hoogenraad C.C., A. Akhmanova, S.A. Howell, B.R. Dortland, C.I. De Zeeuw, R. Willemsen, P. Visser, F. Grosveld, and N. Galjart (2001) "Mammalian Golgi-associated Bicaudal-D2 functions in the dynein-dynactin pathway by interacting with these complexes." The EMBO Journal **20**(15):4041-54.
- Horton A.C., B. Racz, E.E. Monson, A.L. Lin, R.J. Weinberg, and M.D. Ehlers (2005) "Polarized secretory trafficking directs cargo for asymmetric dendrite growth and morphogenesis." Neuron **48**(5):757-71.
- Howell, B.W., R. Hawkes, P. Soriano, and J.A. Cooper (1997) "Neuronal position in the developing brain is regulated by mouse disabled-1." Nature **389**(6652):733-7.
- Howell, B.W., L.M. Lanier, R. Frank, F.B. Gertler, and J.A. Cooper (1999) "The disabled 1 phosphotyrosine-binding domain binds to the internalization signals of transmembrane glycoproteins and to phospholipids." Molecular and Cellular Biology **19**(7): 5179-88.

- Howell, B.W., T.M. Herrick, J.D. Hildebrand, Y. Zhang, and J.A. Cooper (2000) "Dab1 tyrosine phosphorylation sites relay positional signals during mouse brain development." Current Biology **10**(15): 877-85.
- Hur E.M., B.D. Saijilafu, S.J. Lee, W.L. Kim, Xu, and F.Q. Zhou (2011) "GSK3 controls axon growth via CLASP-mediated regulation of growth cone microtubules." Genes & Development **25**(18):1968-81.
- Iacopetti P., M. Michelini, I. Stuckmann, B. Oback, E. Aaku-Saraste, and W.B. Huttner (1999) "Expression of the antiproliferative gene TIS21 at the onset of neurogenesis identifies single neuroepithelial cells that switch from proliferative to neuron-generating division." Proceedings of the National Academy of the Sciences of the United States **96**(8):4639-44.
- Jaffe, A.B. and A. Hall (2005) "Rho GTPases: biochemistry and biology" Annual Review of Cell and Developmental Biology **21**:247-69..
- Job, D., O. Valiron, and B. Oakley (2003) "Microtubule nucleation." Current Opinions in Cell Biology **15**(1): 111-7.
- Kapitein L.C. and C.C. Hoogenraad (2011) "Which way to go? Cytoskeletal organization and polarized transport in neurons." Molecular and Cellular Neurosciences **46**(1):9-20.
- Kapitein, L.C. and C.C. Hoogenraad (2015) "Building the neuronal microtubule cytoskeleton." Neuron **87**(3):492-506.
- Kaplan, K.B., A.A. Burds, J.R. Swedlow, S.S. Bekir, P.K. Sorger, and I.S. Näthke (2001) "A role for the Adenomatous Polyposis Coli protein in chromosome segregation." Nature Cell Biology **3**(4):492-32.
- Kappeler, C., Y. Saillour, J.P. Baudoin, F.P. Tuy, C. Alvarez, C. Houbron, P. Gaspar, G. Hamard, J. Chelly, C. Métin, and F. Fracis (2006) "Branching and nucleokinesis defects in migrating interneurons derived from doublecortin knockout mice." Human Molecular Genetics **15**(19):1387-400.
- Kavalali E.T., J. Klingauf, and R.W. Tsien (1999) "Activity-dependent regulation of synaptic clustering in a hippocampal culture system." Proceedings of the National Academy of Sciences of the United States of America **96**(22):12893-900.
- Kerjan, G. and J.G. Gleeson (2007) "Genetic mechanisms underlying abnormal neuronal migration in classical lissencephaly." Trends in Genetics **23**(12):623-30.
- Kim Y.T., E.M. Hur, W.D. Snider, and F.Q. Zhou (2011) "Role of GSK3 Signaling in Neuronal Morphogenesis." Frontiers in Molecular Neuroscience **4**:48.

- Kirschner, M.W. and T. Mitchison (1986) "Microtubule dynamics." Nature **324**(6098):621.
- Koester, M.P., O. Müller, and G.E. Pollerberg (2007) "Adenomatous polyposis coli is differentially distributed in growth cones and modulates their steering." The Journal of Neuroscience **27**(46):12590-600.
- Komarova, Y., G. Lansbergen, N. Galjart, F. Grosveld, G.G. Borisy, and A. Akhmanova (2005) "EB1 and EB3 control CLIP dissociation from the ends of growing microtubules" Molecular Biology of the Cell **16**(11): 5334-45.
- Konishi Y. and M. Setou (2009) "Tubulin tyrosination navigates the kinesin-1 motor domain to axons." Nature Neuroscience **12**(5):559-67.
- Kosodo, Y., K. Röper, W. Haubensak, A.M. Marzesco, D. Corbeil, and W.B. Huttner (2004) "Asymmetric distribution of the apical plasma membrane during neurogenic divisions of mammalian neuroepithelial cells." EMBO **23**(11):2314-24.
- Kriegstein A. and A. Alvarez-Buylla (2009) "The glial nature of embryonic and adult neural stem cells." Annual Review of Neuroscience **32**:149-84.
- Kumar P. and T. Wittmann (2012) "+TIPs: SxIPping along microtubule ends." Trends in Cell Biology **22**(8):418-28.
- Kumar P., K.S. Lyle, S. Gierke, A. Matov, G. Danuser, and T. Wittmann (2009) "GSK3beta phosphorylation modulates CLASP-microtubule association and lamella microtubule attachment." The Journal of Cell Biology **184**(6):895-908.
- Lai T., D. Jabaudon, B.J. Molyneaux, E. Azim, P. Arlotta, J.R.L. Menezes, J.D. Macklis (2008) "SOX5 controls the sequential generation of distinct corticofugal neuron subtypes" Neuron **57**(2):232-47.
- Lambert de Rouvroit, C. and A.M. Goffinet (1998) "The reeler mouse as a model of brain development." Advances in Anatomy, Embryology and Cell Biology **150**: 1-106.
- Lancaster M.A. and J.A. Knoblich (2012) "Spindle orientation in mammalian cerebral cortical development." Current Opinions in Neurobiology **22**(5):737-46.
- Lansbergen, G., I. Grigoriev, Y. Mimori-Kiyosue, T. Ohtsuka, S. Higa, I. Kitajima, J. Demmers, N. Galjart, A.B. Houtsmuller, F. Grosveld, and A. Akhmanova (2006) "CLASPs attach microtubule plus ends to the cell cortex through a complex with LL5beta." Developmental Cell **11**(1): 21-32.

- Lee H., U. Engel, J. Rusch, S. Scherrer, K. Sheard, and D. Van Vactor (2004) "The microtubule plus end tracking protein Orbit/MAST/CLASP acts downstream of the tyrosine kinase Abl in mediating axon guidance." Neuron **42**(6):913-26.
- Levy, J.R. and E.L. Holzbaur (2008) " Dynein drives nuclear rotation during forward progression of motile fibroblasts." Journal Cell Science **121**(Pt19): 3187-95.
- Lin, Y.C., T.C. Chiang, Y.T. Liu, Y.T. Tsai, L.T. Jang and F.J. Lee (2011) "ARL4A acts with GCC185 to modulate Golgi complex organization." Journal of Cell Science **124**(Pt23): 4014-26.
- Liu, J., Z. Wang, K. Jiang, L. Zhang, L. Zhao, S. Hua, F. Yan, Y. Yang, D. Wang, C. Fu, X. Ding, Z. Guo, and X. Yao (2009) " PRC1 cooperates with CLASP1 to organize central spindle plasticity in mitosis." Journal of Biological Chemistry **284**(34): 23059-71.
- Liu, J.S. (2011) "Molecular genetics of neuronal migration disorders." Current Neurology and Neuroscience Reports **11**(2):171-8.
- Logarinho, E., S. Maffini, M. Barisic, A. Marques, A. Toso, P. Meraldi, and H. Maiato (2012) "CLASPs prevent irreversible multipolarity by ensuring spindle-pole resistance to traction forces during chromosome alignment." Nature Cell Biology **14**(13):295-303.
- LoTurco J.J. and J. Bai (2006) "The multipolar stage and disruptions in neuronal migration." Trends in Neuroscience **29**(7): 407-13.
- Lu B., P. Greengard, and M.M. Poo (1992) "Exogenous synapsin I promotes functional maturation of developing neuromuscular synapses." Neuron **8**(3):521-29.
- Maia, A.R., Z. Garcia, L. Kabeche, M. Barisic, S. Maffini, S. Macedo-Ribeiro, I.M. Cheeseman, D.A. Compton, I. Kaverina, and H. Maiato (2012) " Cdk1 and Plk1 mediate a CLASP2 phospho-switch that stabilizes kinetochore-microtubule attachments." The Journal of Cell Biology **199**(2):285-301.
- Maiato, H., C.L. Rieder, W.C. Earnshaw, and C.E. Sunkel (2003) "How do kinetochores CLASP dynamic microtubules?" Cell Cycle **2**(6):511-4.
- Maiato, H., A. Khodjakov, and C.L. Rieder (2005) "Drosophila CLASP is required for the incorporation of microtubule subunits into fluxing kinetochore fibres." Nature Cell Biology **7**(1):42-7.
- Malatesta, P., M.A. Hack, E. Hartfuss, H. Kettenmann, W. Klinkert, F. Kirchhoff, and M. Götz "Neuronal or glial progeny: regional differences in radial glia fate." Neuron **37**(5): 751-64.

- Marin, O. (2012) "Brain development: The neuron family tree remodelled." Nature **490**(7419):185-6.
- Markram H., M. Toledo-Rodriguez, Y. Wang, A. Gupta, G. Silberberg, and C. Wu (2004) "Interneurons of the neocortical inhibitory system." Nature Reviews. Neuroscience **5**(10):793-807.
- Marx, A., W.J. Godinez, V. Tsimashchuk, P. Bankhead, K. Rohr, and U. Engel (2013) "Xenopus cytoplasmic linker-associated protein 1 (XCLASP1) promotes axon elongation and advance of pioneer microtubules." Molecular Biology of the Cell **24**(10): 1544-58.
- Máthé E., Y.H. Inoue, W. Palframan, G. Brown, and D.M. Glover (2003) "Orbit/Mast, the CLASP orthologue of Drosophila, is required for asymmetric stem cell and cystocyte divisions and development of the polarised microtubule network that interconnects oocyte and nurse cells during oogenesis." Development **130**(5):901-15.
- Matsui, T., T. Watanabe, K. Matsuzawa, M. Kakeno, N. Okumura, I. Sugiyama, N. Itoh, and K. Kaibuchi (2015) "PAR3 and aPKC regulate Golgi organization through CLASP2 phosphorylation to generate cell polarity." Molecular Biology of the Cell **26**(4):751-81.
- Matsuzaki F. and A. Shitamukai (2015) "Cell division modes and cleavage planes of neural progenitors during mammalian cortical development." Cold Spring Harbor Perspectives in Biology **7**(9):1101.
- Maurer, S.P., P. Bieling, J. Cope, A. Hoenger, and T. Surrey (2011) "GTPgammaS microtubules mimic the growing microtubule end structure recognized by end-binding proteins (EBs)." Proceedings of the National Academy of Sciences of the United States **108**(10):3988-93.
- Maurer, S.P., F.J. Fourniol, G. Bohner, C.A. Moores, and T. Surrey (2012) "EBs recognize a nucleotide-dependent structural cap at growing microtubule ends." Cell **149**(2):371-82.
- McConnell, S.K. (1988) "Development and decision-making in the mammalian cerebral cortex." Brian Research **472**(1): 1-23.
- McKenney, R.J., M. Vershinin, A. Kunwar, R.B. Vallee, and S.P. Gross (2010) "LIS1 and NudE induce a persistent dynein force-producing state." Cell **141**(2):304-14.
- Miller P.M., A.W. Folkmann, A.R. Maia, N. Efimova, A. Efimov, and I. Kaverina (2009) "Golgi-derived CLASP-dependent microtubules control Golgi organization and polarized trafficking in motile cells." Nature Cell Biology **11**(9):1069-80.

- Mimori-Kyosue, Y., I. Grigoriev, G. Landsbergen, H. Sasaki, C. Matsui, F. Severin, N. Galjart, F. Grosveld, I. Vorobjev, S. Tsukita, and A. Akhmanova (2005) "CLASP1 and CLASP2 bind to EB1 and regulate microtubule plus-end dynamics at the cell cortex." The Journal of Cell Biology **168**(1):141-53.
- Miyata, T., A. Kawaguchi, H. Okano, and M. Ogawa (2001) "Asymmetric inheritance of radial glial fibers by cortical neurons." Neuron **31**: 727-41.
- Molyneaux, B.J., P. Arlotta, J.R. Menezes, and J.D. Macklis (2007) "Neuronal subtype specification in the cerebral cortex." Nature Reviews in Neuroscience **8**(6): 427-37.
- Moon, H.M., Y.H. Youn, H. Pemble, J. Yingling, T. Wittmann, and A. Wynshaw-Boris (2014) "LIS1 controls mitosis and mitotic spindle organization via the LIS1-NDEL1-dynein complex." Human Molecular Genetics **23**(2):449-66.
- Morin, X. and Y. Bellaïche (2011) "Mitotic spindle orientation in asymmetric and symmetric cell divisions during animal development." Developmental Cell **21**(1): 102-19.
- Mozhayeva M.G., Y. Sara, X. Liu, and E.T. Kavalali (2002) "Development of vesicle pools during maturation of hippocampal synapses." The Journal of Neuroscience **22**(3):654-65.
- Nadarajah B., J.E. Brunstrom, J. Grutzendler, R.O. Wong, and A.L. Pearlman (2001) "Two modes of radial migration in early development of the cerebral cortex." Nature Neuroscience **4**(2):143-50.
- Nagano, T., S. Morikubo, and M. Sato (2004) "Filamin A and FILIP (Filamin A-Interacting Protein) regulate cell polarity and motility in neocortical subventricular and intermediate zones during radial migration." Journal of Neuroscience **24**(43):9648-57.
- Neukirchen D. and F. Bradke (2011) "Cytoplasmic linker proteins regulate neuronal polarization through microtubule and growth cone dynamics." The Journal of Neuroscience **31**(4):1528-38.
- Noctor, S. C., A.C. Flint, T.A. Weissman, R.S. Dammerman, and A.R. Kriegstein (2001) Neurons derived from radial glial cells establish radial units in neocortex. Nature **409**, 714-20.
- Noctor, S.C., A.C. Flint, T.A. Weissman, W.S. Wong, B.K. Clinton, A.R. Kriegstein (2002) Dividing precursor cells of the embryonic cortical ventricular zone have morphological and molecular characteristics of radial glia. Journal of Neuroscience **22**: 3161-73.

- Noctor, S.C., V. Martínez-Cerdeño, L. Ivic, and A.R. Kriegstein (2004) "Cortical neurons arise in symmetric and asymmetric division zones and migrate through specific phases." Nature Neuroscience **7**(2):136-44.
- Oakley, B.R. (2000) "Gamma-Tubulin." Current Topics in Developmental Biology **49**: 27-54.
- O'Dell, R.S., D.A. Cameron, W.R. Zipfel, and E.C. Olson (2015) "Reelin Prevents Apical Neurite Retraction during Terminal Translocation and Dendrite Initiation." Journal of Neuroscience **35**(30): 10659-74.
- Olson, E.C. (2014) "Analysis of preplate splitting and early cortical development illuminates the biology of neurological disease." Frontiers in Pediatrics **2**(121).
- Ori-McKenney, K.M., L.Y. Jan, and Y.N. Jan (2012) "Golgi outposts shape dendrite morphology by functioning as sites of acentrosomal microtubule nucleation in neurons." Neuron **76**(5):921-30.
- Ortiz, J., C. Funk, A. Schäfer, and J. Lechner (2009) "Stu1 inversely regulates kinetochore capture and spindle stability." Genes and Development **23**(23): 2778-91.
- Palazzo, A.F., H.L. Joseph, Y.J. Chen, D.L. Dujardin, A.S. Alberts, K.K. Pfister, R.B. Vallee, and G.G. Gundersen (2001) "Cdc42, dynein, and dynactin regulate MTOC reorientation independent of Rho-regulated microtubule stabilization." Current Biology **11**(19): 1536-41.
- Patel, K., E. Nogales, and R. Heald (2012) "Multiple domains of human CLASP contribute to microtubule dynamics and organization in vitro and in *Xenopus* egg extracts." Cytoskeleton (Hoboken) **69**(3): 155-65.
- Petry, S. and R.D. Vale (2015) "Microtubule nucleation at the centrosome and beyond." Nature Cell Biology **17**(9):1089-83.
- Purro, S.A., L. Ciani, M. Hoyos-Flight, E. Stamatakou, E. Somou, and P.C. Salinas (2008) " Wnt regulates axon behavior through changes in microtubule growth directionality: a new role for adenomatous polyposis coli." The Journal of Neuroscience **28**(34):8644-54.
- Rakic, P. (1974) "Neurons in rhesus monkey visual cortex: systematic relation between time of origin and eventual disposition." Science **183**(4123): 425-7.
- Rakic P. (1988) "Specification of cerebral cortical areas." Science **241**, 170–176.

- Ramirez D.M. and E.T. Kavalali (2011) "Differential regulation of spontaneous and evoked neurotransmitter release at central synapses." Current Opinions in Neuobiology **21**(2):275-82.
- Rasband W.S. (1997-2011) ImageJ, US National Institutes of Health, Bethesda, MD, USA, <http://imagej.nih.gov/ij/>.
- Reed, N.A., D. Cai, T.L. Blasius, G.T. Jih, E. Meyhofer, J. Gaertig, and K.J. Verhey (2006) "Microtubule acetylation promotes kinesin-1 binding and transport." Current Biology **16**(21): 2166-72.
- Rice, D.S. and T. Curran (2001) "Role of the reelin signaling pathway in central nervous system development." Annual Review of Neuroscience **24**: 1005-39.
- Rivero, S., J. Cardenas, M. Bornens, and R.M. Rios (2009) "Microtubule nucleation at the cis-side of the Golgi apparatus requires AKAP450 and GM130." European Molecular Biology Organization **28**(8): 1016-28.
- Rogers, S.L., G.C. Rogers, D.J. Sharp, and R.D. Vale (2002) "Drosophila EB1 is important for proper assembly, dynamics, and positioning of the mitotic spindle." The Journal of Cell Biology **158**(5): 873-84.
- Romaniello, R., F. Arrigoni, M.T. Bassi, and R. Borgatti (2015) "Mutations in α - and β -tubulin encoding genes: implications in brain malformations." Brain & Development **37**(3): 273-80.
- Rosahl T.W., D. Spillane, M. Missler, J. Herz, D.K. Selig, J.R. Wolff, R.E. Hammer, R.C. Malenka, and T.C. Südhof (1995) "Essential functions of synapsins I and II in synaptic vesicle regulation." Nature **375**(6531): 488-93.
- Sahara, S. and D.D. O'Leary (2009) "Fgf10 regulates transition period of cortical stem cell differentiation to radial glia controlling generation of neurons and basal progenitors." Neuron **63**(1):48-62.
- Sakakibara, A., R. Ando, T. Sapir, and T. Tanaka (2013) "Microtubule dynamics and neuronal morphogenesis." Open Biology **3**(7).
- Sakakibara, A., T. Sato, R. Ando, N. Noguchi, M. Masaoka, and T. Miyata (2014) "Dynamics of centrosome translocation and microtubule organization in neocortical neurons during distinct modes of polarization." Cerebral Cortex **24**(5):1301-10.
- Samora, C.P., B. Mogessie, L. Conway, J.L. Ross, A. Straube, and A.D. McAinsh (2011) "MAP4 and CLASP1 operate as a safety mechanism to maintain a stable spindle position in mitosis." Nature Cell Biology **13**(9):1040-50.

- Schoch S., F. Deak, A. Königstorfer, M. Mozhayeva, Y. Sara, T.C. Südhof, and E.T. Kavalali (2001) "SNARE function analyzed in synaptobrevin/VAMP knockout mice." Science **294**(5544):1117-22.
- Sekine, K., T. Kawauchi, K. Kubo, T. Honda, J. Herz, M Hattori, T. Kinashi, and K. Nakajima (2012) "Reelin controls neuronal positioning by promoting cell-matrix adhesion via inside-out activation of integrin $\alpha5\beta1$." Neuron **76**(2): 353-69.
- Shim, S.Y., J. Wang, N. Asada, G. Neumayer, H.C. Tran, K. Ishiguro, K. Sanada, Y. Nakatani, and M.D. Nguyen (2008) "Protein 600 is a microtubule/endoplasmic reticulum-associated protein in CNS neurons." The Journal of Neuroscience **28**(14): 3604-14.
- Siegenthaler, J.A., A.M. Ashique, K. Zarbalis, K.P. Patterson, J.H. Hecht, M.A. Kane, A.E. Folias, Y. Choe, S.R. May, T. Kume, J.L. Napoli, A.S. Peterson, and S.J. Pleasure (2009) "Retinoic acid from the meninges regulates cortical neuron generation." Cell **139**(3):597-609.
- Silkworth, W.T., I.K. Nardi, L.M. Scholl, D. Cimini (2009) "Multipolar spindle pole coalescence is a major source of kinetochore mis-attachment and chromosome mis-segregation in cancer cells." PLoS One **4**(8):6564.
- Slep, K.C. (2009) "The role of TOG domains in microtubule plus end dynamics." Biochemical Society Transactions **37**(5):1002-6.
- Stancik, E.K., I. Navarro-Quiroga, R. Sellke, and T.F. Haydar (2010) "Heterogeneity in ventricular zone neural precursors contributes to neuronal fate diversity in the postnatal neocortex." Journal of Neuroscience **30**(20): 7028-36.
- Stiess, M., N. Maghelli, L.C. Kapitein, S. Gomis-Rüth, M. Wilsch-Bräuninger, C.C. Hoogenraad, I.M. Tolić-Nørrelykke, and F. Bradke (2010) "Axon extension occurs independently of centrosomal microtubule nucleation." Science **327**(5966):704-7.
- Stramer, B., S. Moreira, T. Millard, I. Evans, C.Y. Huang, O. Sabet, M. Milner, G. Dunn, P. Martin, and W. Wood (2010) "Clasp-mediated microtubule bundling regulates persistent motility and contact repulsion in *Drosophila* macrophages in vivo." The Journal of Cell Biology **189**(4):681-9.
- Sun, Y., S.K. Goderie, and S. Temple (2005) "Asymmetric distribution of EGFR receptor during mitosis generates diverse CNS progenitor cells." Neuron **45**(6):873-86.
- Tabata., H, and K. Nakajima (2003) "Multipolar migration: the third mode of radial neuronal migration in the developing cerebral cortex." Journal of Neuroscience **23**(31):9996-10001.

- Temburni M.K., M.M. Rosenberg, N. Pathak, R. McConnell, and M.H. Jacob (2004) "Neuronal nicotinic synapse assembly requires the adenomatous polyposis coli tumor suppressor protein." The Journal of Neuroscience **24**(30):6776-84.
- Tirnauer, J.S., J.C. Canman, E.D. Salmon, and T.J. Mitchison (2002) "EB1 targets to kinetochores with attached, polymerizing microtubules." Molecular Biology of the Cell **13**(12):4308-16.
- Tischfield, M.A., G.Y. Cederquist, M.L. Gupta Jr., and E.C. Engle (2011) "Phenotypic spectrum of the tubulin-related disorders and functional implications of disease-causing mutations." Current Opinions in Genetics & Development **21**(3):286-94.
- Trommsdorff, M., M. Gotthardt, T. Hiesberger, J. Shelton, W. Stockinger, J. Nimpf, R.E. Hammer, J.A. Richardson, and J. Herz (1999) "Reeler/disabled-like disruption of neuronal migration in knockdown mice lacking the VLDL receptor and ApoE receptor 2." Cell **97** (7):689-701.
- Tsai, J.W., Y. Chen, A.R. Kriegstein, and R.B. Vallee (2005) "LIS1 RNA interference blocks neural stem cell division, morphogenesis, and motility at multiple stages." Journal of Cell Biology **170**(6):935-45.
- Tsai J.W., K.H. Bremner, and R.B. Vallee (2007) "Dual subcellular roles for LIS1 and dynein in radial neuronal migration in live brain tissue." Nature Neuroscience **10**(8):970-9.
- Tsvetkov, K.S., A. Samsonov, A. Akhmanova, N. Galjart, and S.V. Popov (2007) "Microtubule-binding proteins CLASP1 and CLASP2 interact with actin filaments." Cell Motility and the Cytoskeleton **64**(7): 519-30.
- Vallee, R.B., G.E. Seale, and J.W. Tsai (2009) "Emerging roles for myosin II and cytoplasmic dynein in migrating neurons and growth cones." Trends in Cellular Biology **19**(7): 347-55.
- Walsh, C.A. and E.C. Engle (2010) "Allelic diversity in human developmental neurogenetics: insights into biology and disease." Neuron **68**(2):245-53.
- Wang, X., J.W. Tsai, J.H. Imai, W.N. Lian, R.B. Vallee, and S.H. Shi (2009) "Asymmetric centrosome inheritance maintains neural progenitors in the neocortex." Nature **461**(7266):947-55.
- Washbourne P., P.M. Thompson, M. Carta, E.T. Costa, J.R. Mathews, G. Lopez-Bendito, Z. Molnar, M.W. Becher, C.F. Valenzuela, L.D. Partridge, and M.C. Wilson (2002) "Genetic ablation of the t-SNARE SNAP-25 distinguishes mechanisms of neuroexocytosis." Nature Neuroscience **5**(1):19-26.

- Watanabe T., J. Noritake, M. Kakeno, T. Matsui, T. Harada, S. Wang, N. Itoh, K. Sato, K. Matsuzawa, A. Iwamatsu, N. Galjart, and K. Kaibuchi (2009) "Phosphorylation of CLASP2 by GSK-3beta regulates its interaction with IQGAP1, EB1 and microtubules." Journal of Cell Science **122**(16):2969-79.
- Westermann, S. and K. Weber (2003) "Post-translational modifications regulate microtubule function." Nature Reviews. Molecular Cell Biology **4**(12):938-47.
- Wise S.P. and Jones (1977) "Cells of origin and terminal distribution of descending projections of the rat somatic sensory cortex." Journal of Comparative Neurology **175**(2):129-57.
- Witte H. and F. Bradke (2008) "The role of the cytoskeleton during neuronal polarization." Current Opinions in Neurobiology **18**(5):479-87.
- Witte H., D. Neukirchen, and F. Bradke (2008) "Microtubule stabilization specifies initial neuronal polarization." The Journal of Cell Biology **180**(3):619-32.
- Wittmann T. and C.M. Waterman-Storer (2005) "Spatial regulation of CLASP affinity for microtubules by Rac1 and GSK3beta in migrating epithelial cells." The Journal of Cell Biology **169**(6):929-39.
- Wynshaw-Boris A., S. Hirotsune, and M. Yamada (2010) "The essential role of LIS1, NDEL1 and Aurora-A in polarity formation and microtubule organization during neurogenesis." Cell Adhesion & Migration **4**(2):180-4.
- Yanagida, M., R. Miyoshi, R. Toyokuni, Y. Zhu, and F. Murakami (2012) "Dynamics of the leading process, nucleus, and Golgi apparatus of migrating cortical interneurons in living mouse embryos." Proceedings in the National Academy of Sciences of the United States of America **109**(41):16737-42.
- Ye B., Y. Zhang, W. Song, S.H. Younger, L.Y. Jan, and Y.N. Jan (2007) "Growing dendrites and axons differ in their reliance on the secretory pathway." Cell **130**(4):717-29.
- Zhong, W., J.N. Feder, M.M. Jiang, L.Y. Jan, and Y.N. Jan (1996) "Asymmetric localization of a mammalian numb homolog during mouse cortical neurogenesis." Neuron **17**(1):43-53.
- Zhou F.Q., J. Zhou, S. Dedhar, Y.H. Wu, and W.D. Snider (2004) "NGF-induced axon growth is mediated by localized inactivation of GSK-3beta and functions of the microtubule plus end binding protein APC." Neuron **42**(6):897-912.

Zmuda J.F. and R.J. Rivas (1998) "The Golgi apparatus and the centrosome are localized to the sites of newly emerging axons in cerebellar granule neurons in vitro." Cell Motility and the Cytoskeleton **41**(1):18-38.

CURRICULUM VITAE

